Real-time fMRI connectivity neurofeedback for modulation of the motor system

Yahia Madkhali

BSc. Radiological Sciences, MSc. Medical Imaging

This thesis is submitted in fulfilment of the requirements for the Degree of Doctor of Philosophy

College of Medical, Veterinary and Life Science
School of Psychology and Neuroscience
Glasgow Experimental MRI Centre,
University of Glasgow

October 2021

Abstract

Advances in functional magnetic resonance imaging (fMRI) have enabled an understanding of the neural mechanisms underlying human brain functions such as motor functions. In recent decades fMRI, which is a non-invasive and high-resolution technique, has been used to investigate the functions of the human brain using the blood oxygen level dependent (BOLD) response as an indirect measurement of brain neural activities. Real-time fMRI (rt-fMRI) has been used as neurofeedback to enable individuals to regulate their neural activity to achieve improvements in their health and performance, such as their motor performance.

Neurofeedback can be defined as the measurement of the neural activity of a participant that is presented to them as visual or auditory signals that enable self-regulation of neural activity. Rt-fMRI has also been used to provide feedback about the connectivity between brain regions. Such connectivity neurofeedback can be a more effective feedback strategy than providing feedback from a single region. Recently, connectivity neurofeedback has been explored to examine how functional connectivity of cortical areas and subcortical areas of the brain can be modulated. Enhancing connectivity between cortical and subcortical regions holds promise for the improvement of performance, particularly motor function performance.

The aim of this PhD research was to modulate connectivity neurofeedback by using real-time fMRI neurofeedback (rt-fMRI-NF) between brain regions and to investigate whether any possible enhancement in the activation due to a successful fMRI-NF will translate into changes in behavioural measures.

The thesis research began with experimental work to establish the experimental paradigm. This included work, using fMRI, to develop and test localisers for different motor areas such as primary motor cortex (M1), supplementary motor cortex (SMA), the motor cerebellum and the motor thalamus. The results showed that the execution of actions, such as hand clenching, can be used to functionally activate many motor areas including M1, SMA and the cerebellum. The motor thalamus was localised using a motor thalamus mask that was created offline using the Talairach atlas. All localisers

tested in this research were feasible and able to be used for applications such as rt-fMRI-NF research to define the regions of interest.

The first rt-fMRI connectivity neurofeedback experimental study of this thesis was conducted to determine whether healthy participants can use neurofeedback to enhance the connectivity between M1 and the thalamus using rt-fMRI. It also aimed to investigate whether successful rt-fMRI-NF of M1-thalamus connectivity could translate into changes in behavioural measures. For this purpose, the behavioural tasks were conducted before and after each MRI session. Two behavioural tasks were used in this experiment: Go/No Go and switching tasks. The results of this experiment showed a significant increase in connectivity neurofeedback in the experimental group (M1-thalamus), hence, rt-fMRI-NF is a useful tool to modulate functional connectivity between M1 and the thalamus using motor imagery and it facilitates the learning by participants of new mental strategies to upregulate M1-thalamus connectivity. The behavioural tasks showed a significant reduction in the switching time in the experimental group while Go/No Go task did not show a significant reduction in the reaction time in the experimental group.

The second rt-fMRI connectivity neurofeedback experimental study of this thesis was conducted to investigate the ability of neurofeedback to modulate M1-cerebellum connectivity using motor imagery based rt-fMRI-NF. The results of this research showed enhanced connectivity between M1 and the cerebellum in each participant. However, this enhancement was not statistically significant.

In summary, this PhD thesis extends and validates the usefulness of connectivity neurofeedback using motor imagery based rt-fMRI to modulate the correlation between cortical and subcortical brain regions. Successful modulation using this technique has the potential to lead to an enhancement in motor functions. Thereby, the results of this PhD research may help to advance connectivity neurofeedback for use as a supplementary treatment for many brain disorders such as stroke recovery and Parkinson’s disease.

Table of Contents

List of Tables

List of Figures

Acknowledgement

I would like to express my deepest appreciation to my supervisor, professor Frank Pollick, for his continuous support and encouragement throughout my PhD research. I am very appreciative of his guidance and comments which have helped me to successfully complete this thesis. He continuously provided encouragement and was always willing and enthusiastic in providing assistance in any way he could throughout my research. I would also like to thank my best friend, Dr Salim Al-Wasity, for his support and help throughout the duration of my PhD.

Finally, my deep and sincere gratitude to my wife, Norah, for her continuous and unparalleled love, help and support. This thesis is dedicated to my wife and my children. You have made me stronger, better and more fulfilled than I could have ever imagined.

Author's Declaration

I hereby certify that this research is entirely my own work and has not been taken from the work of others save and to the extent that such work has been cited and acknowledged within the text of my work.

Abbreviations

ANOVA	Analysis of Variance
AO	Action Observation
AOMI	Action Observation And Motor Imagery
B0	External magnetic field
BA	Brodmann Area
BOLD	blood oxygen level dependent
CT	Computed Tomography
CPMG	Carr-Purcell-Meiboom-Gill
CS	Conditioned Signal
EPI	Echo Planar Imaging
FID	Free Induction Decay
FMRI	Functional Magnetic Resonance Imaging
FWHM	Full Width At A Half Maximum
GLM	General Linear Model
GM	Gray Matter
HDR	Hemodynamic Response
^{1}H	Hydrogen Protons
Hz	Hertz
IFG	Inferior Frontal Gyrus
IFG	Inferior Frontal Gyri
IIC	Intensity Inhomogeneities Correction
IPL	Inferior Parietal Lobule
IR	Impulse Response
ISI	Inter-Stimulus Interval
IVI	Internal Visual Imagery
KI	Kinesthetic Imagery
LCD	Liquid Crystal Display
LH	Left Hemisphere
LI	Laterality Index
M0	Net Magnetization
M1	Primary Motor Cortex
ME	Motor Execution
MI	Motor Imagery
mm	Millimetre
mm^3	Cubic Millimetre
MNI	Neurological Institute Template
MRI	Magnetic Resonance Imaging
MVPA	Multivariate Pattern Analysis
NF	Neurofeedback

NMR	Nuclear Magnetic Resonance
I	Nuclear spin
PcG	Precentral Gyrus
PIT	Pavlovian-Instrumental Transfer
PMC	Premotor cortex
PPC	Posterior Parietal Cortex
pre-SMA	Pre-Supplementary Motor Area
rACC	Rostral Anterior Cingulate Cortex
RFX	Random Effect Analysis
ROI	Region Of Interest
s	Second
sACC	Subgenual Anterior Cingulate Cortex
SEM	Standard Error of The Mean
SI	Primary Somatosensory Cortex
SMA	Supplementary Motor Area
SNR	Signal-To-Noise Ratio
SPL	Superior Parietal Lobule
T_1	Longitudinal Relaxation
T_2	Transverse Relaxation
TBV	Turbo-Brainvoyager
TCP/IP	Transmission Control Protocol/Internet Protocol
TMS	Transcranial Magnetic Stimulation
TR	Repetition Time
μ	magnetic Moment
US	Unconditioned Signal
ω_0	Larmor Frequency
VI	Visual Imagery
vlPFC	Bilateral Ventrolateral Prefrontal Cortex
VMIQ-2	Vividness Of Movement Imagery Questionnaires-2nd Version
vmPFC	Ventromedial Prefrontal Cortex
vPMC	Ventral Premotor Cortex
x,y,z	3D Talairach Coordinates
γ	Gyromagnetic ratio
a	Flip angle
vPM	Ventral Premotor Cortex
WM	White Matter
x,y,z	3D Talairach Coordinates

1 Chapter 1: Literature review

1.1 Introduction

For many years, clinicians and researchers have focused on understanding how people are trained to regulate their physiological functions. In the 1960s and 70s, neurofeedback using electroencephalograms (EEG) was developed. EEG neurofeedback is recognised as an accepted method for treating several neurological disorders (Yucha and Gilbert, 2004; Moss and Kirk, 2004). In the 1990s, functional magnetic resonance imaging (fMRI) was developed, which gave researchers the chance to observe how specific anatomical brain regions are activated. This technology allowed researchers to start exploring the possibilities of using real-time fMRI data feedback to train individuals to regulate their localised brain activations. There are two forms of fMRI feedback: biofeedback and neurofeedback.

Biofeedback can be described as a technique which allows individuals to learn how they can change their physiological activities to improve their performance and health (Gilbert and Moss, 2003). The instruments used in biofeedback provide feedback information about the processes of physiology in an individual, assisting the person to increase their awareness of the processes and thus enabling them to control their mind and body. Biofeedback instruments usually measure electrodermal activity, skin temperature, muscle activity, blood pressure, heart rate variability, heart rate, blood flow, and brain electrical activity. When biofeedback is used in conjunction with other behavioural therapies, it can result in effective treatment of psychological and medical disorders including headache, hypertension and attentional disorders (Yucha and Montgomery, 2008).

1.2 Neurofeedback

In neurofeedback, a visual stimulus is presented on a screen to reinforce or train the brain. Neurofeedback can therefore be described as a type of biofeedback which influences the functions of the brain. It has been used experimentally for more than 50 years. Studies with animals show that rats and other non-human primates can control the firing of single cells within the motor cortex (Koralek et al., 2012). The EEG is currently the most used neurofeedback technique, and

involves an individual trying to control the electrical activity of his or her brain in real time (Gruzelier et al., 2014). When a participant is being trained on neurofeedback, they aim to control their brain activity, based on a feedback signal which represents the activity of a network or brain region of interest.

Although neurofeedback was originally based on cortical signals measured with EEGs, developments in methodology have allowed neurofeedback to be provided based on brain signals (cortical and subcortical) acquired from functional magnetic resonance imaging (fMRI) (Thibault et al., 2016). Thus, neurofeedback training holds promise as a possible treatment for neurological and psychiatric conditions (Sokhadze et al., 2008), and it contains protocols that can be used in addressing disorders such as chronic pain, depression, and anxiety (Thibault et al., 2016). However, there is limited evidence for the therapeutic efficacy of this treatment. Neurofeedback also involves training individuals to improve their flexibility in terms of physiologic responding. This feedback training can have a positive impact on individuals' learning, health, and performance (Koralek et al., 2013).

1.3 Principles of learning

Implementing neurofeedback involves a Brain-Computer Interface (BCI), which enables a special form of training using biofeedback (Birbaumer et al., 2013). Neurofeedback training involves modulation of brain activation in real-time. The signal intensities in the training are transformed to relate them to activities that reflect the main objective of the training, such as an intended percentage signal change compared to a resting period. Once this value is obtained, it is transformed into a feedback cue. A good example is a thermometer with filling bars, which reflect the level of the activity, and result in feedback given to the participant. The techniques used in neurofeedback training train the participants to gain control over the underlying signals that influence their feedback (Birbaumer et al., 2013).

Normally, classical operant learning needs an unconditioned signal (US) that can be considered to be a reinforced signal, and a stimulus signal, which is conditioned (CS) (Mendelsohn et al., 2014). In the neurofeedback training context, the conditioned signal represents the response of a brain that is being

trained, while the unconditioned signal constitutes the feedback signal to the participant, which acts as a reward (Mehler, 2018). During the training, the participants perform specific tasks such as mental imagery, which constitutes the operant behaviour, and which the training rewards. Research shows that learned upregulation of the motor areas being targeted through motor imagery training can be modulated by the presentation of cues that have been awarded in totally different contexts (Mendelsohn et al., 2014).

In the presentation of any reward-related cues, it is possible to enhance the activation of motor imagery areas and areas associated with motivation such as the ventral striatum. This shows that it is possible to modulate the relationship between US and CS by Pavlovian-instrumental transfer (PIT) learning. The findings also show that in neurofeedback training, mental imagery-based reinforcement can be used as an option for modifying behaviour and cognition (Cartoni et al., 2016).

The use of fMRI neurofeedback (fMRI-NF) is a more recent development (Weiskopf et al., 2003). When a participant is undergoing training in fMRI-NF, their blood oxygenation level-dependent (BOLD) signal represents the biological signal which they are trained to control BOLD signals are used to indirectly measure the neural activity of individuals, based on the fact that they are the biological basis of the deoxyhaemoglobin levels (a more detailed description is provided in Chapter two).

In real-time fMRI-NF training, the neural activity modulates the biological signals being given as feedback to the individual. In addition, the BOLD signal levels can be modulated by other non-neural factors, such as changes in heart rate, breathing, and carbon dioxide (Murphy et al., 2013). They largely depend on the ability of brain vessels to adopt local arterial blood supply by means of constriction and dilatation, in response to changing metabolic demands that result from variations in neural activity during the given task.

Birbaumer and colleagues (2013) hypothesised that for NF training to be considered successful, it must involve learning a skill, with the basal ganglia playing a central role in the skill learning, which forms a major structure in the

reinforcement of operant learning and reward processing. A recent meta-analysis (Emmert et al., 2016) supported this hypothesis and showed that fMRI-NF paradigms activate some parts of the basal ganglia and anterior insula cortex (AIC). However, it is important to note that this analysis did not account for attempts to self-regulate in the absence of feedback. Suggestions in earlier work claim that these areas and other structures, like supplementary motor areas, form a major part of an individual's frontoparietal network, which largely contributes to the cognitive control of the individual (Ninaus et al., 2013). This suggests that during fMRI-NF tasks, the identified specificity of neural correlates allows dissociation of self-regulation in true learning. Researchers have also proposed additional models to describe the learning mechanisms in neurofeedback (Sitaram et al., 2017).

Alongside the behavioural and neural effects that co-occur during neurofeedback training, the effects of training that take place after the training periods are also considered an area of interest. It is important to note that it is possible to achieve lasting training effects at different organisational levels, which represent different degrees of generalisability. For example, an individual can learn how to self-regulate in networks or areas from which they are not receiving any feedback. Depending on the calibration of feedback, there may be differences between individuals in regards to successful strategies in terms of modality and content. The ability of a participant to self-regulate an activity is predominantly tested by performance on activities that can be referred to as transfer runs, which are activities where a participant may apply the mental strategies that he or she has learned without expecting to receive any feedback (Robineau et al., 2017).

In addition, training aims to enhance the ability of an individual to mentalise specific content such as positive autobiographical mental imagery or motor imagery (Mehler, 2018). In this case, the fMRI-NF training presents the participants with a training approach that allows them to develop strategies which help them to mentalise successfully. It is important to note that a participant can test these training effects using mental imagery-based tasks or mental imagery questionnaires, and that reaction times and accuracy provide additional mental imagery performance measures (Sitaram et al., 2017). In

addition, one can associate additional training effects with successful training strategies, which can allow psychometric measures to detect and generalise a behavioural effect. Research shows that the generalisation of a behavioural effect beyond the training task largely constitutes the ultimate objective of the training interventions of fMRI-NF, based on the fact that they can modify the behaviour of an individual in ways that help the individual achieve the desired clinical outcomes (Mehler, 2018). For instance, these behaviours can be regulated by increasing compensatory or physiological behavioural strategies, and by reducing pathological strategies (Arns et al., 2017).

Scholars from different backgrounds have proposed different theories to explain the mechanisms of neurofeedback learning. These theories include two-process theory (Gaume et al., 2016), motor skill learning theory (Birbaumer et al., 2013) neural conditioning theory (Shibata et al., 2019), and system control theory (Ros et al., 2014). Most theories can be assigned to two major approaches. In the first approach, the theories depict neurofeedback learning as a way of active learning. In this case, an individual is given information and a choice to perform voluntary mental actions towards achieving an objective, such as regulating her or his brain activity through the use of cognitive tasks. Several cognitive aspects play an essential role in this view, such as motivation, awareness, and attention. The second approach does not consider how high-level cognitive purposes influence the brain activities of an individual, but instead focuses on characterising the learning activity of a person as an outcome which occurs after the individual is subjected to several pairings of stimulus-response activities. Normally, these pairings result in the weakening or strengthening of reinforcement-driven associations between the feedback signals and the brain signals (Birbaumer et al., 2013; Shibata et al., 2019).

The second approach is underpinned by the widespread idea that the learning activity of a person through neurofeedback can take place without a person being aware, which means that learning can only occur implicitly (Koizumi et al., 2016; Birbaumer et al., 2013; Shibata et al., 2019). The debate surrounding how awareness influences neurofeedback learning has increasingly become popular and has gained major relevance due to the development of neurofeedback paradigms in recent years (Megan et al., 2016; Ramot et al.,

2016; Watanabe et al., 2017). The debate has also gained awareness due to the criticism that several factors such as demand effects, experimenter bias, and placebo effects can contaminate learning in typical neurofeedback paradigms (Thibault et al., 2018, 2016, 2015).

1.4 Explicit versus implicit control over brain activation

It could be said that an individual's control over their brain activation can be learned through normal development, based on the fact that it is implicit. Implicit control can be said to be the most typical form of control underpinning the cognition and behaviour of individuals; in a normal setting, a person usually exhibits implicit and unwitting control over the activation of their brain. We know this because every voluntary perception or action results in some specific brain mechanisms being activated (DeCharms et al., 2008). A good example is that when an individual learns to play an instrument such as a piano, he or she develops implicit control over his or her motor cortex, and the ensuing learning produces motor performance. However, during the learning period, the person is not aware of the events that are taking place inside his or her brain, which means that he or she cannot make decisions based on these activities, and thus cannot shape the activities (DeCharms et al., 2008).
The explicit control over the activation of a brain can be said to be deliberately learned, which means that an individual knows about it and thus allows it to make volitional changes over their brain through the choices he or she makes (Sitaram et al., 2017). For instance, an individual can learn how they can control the way in which the brain region is activated by exerting exactly the type of action, intention, emotion, cognition, mental imagery, or perception that will minimise or maximise its activation.

An interesting question relates to the extent to which an individual can learn to have explicit control over the activation of their brain through specific training, and what would happen when the training was completed. If functional MRI is activated in real-time, it can bring the non-conscious processes of the brain into conscious awareness, with this process allowing the implicit control one has over the brain to be transformed into explicit control.

1.5 Awareness in human associative and motor learning

Throughout history, psychology has consistently tried to describe learning in terms of stimulus-response associations. In the early twentieth century, the traditional learning theories described by psychologists like Hull and Thorndike termed instrumental learning as the learning that happens between the actions of an individual and the outcomes. These psychologists described instrumental learning with regards to stimulus-response bonds, which are likely to be weakened or strengthened depending on the reinforcement (Hull, 1943; Yin and Knowlton, 2006). The approach used by these psychologists aimed at understanding learning by focusing on measurable inputs and outputs, which were expected to be free-form concepts such as representations and goals.

It is worth noting that associative learning in animal research is assumed to be detached from the processes of higher-order cognition (Lovibond and Shanks, 2002). However, learning can occur even from simple contiguity, which is considered to be a likely source of a primitive form of associative learning that is said to be present in many mammals and vertebrates (Bekinschtein et al., 2011; Heyes, 2012; Macphail, 1982). However, associative learning is not considered either necessary or sufficient for conditioning. Researchers claim that instead, associative learning can be perceived as a more complex process, which is driven by how an individual acquires and maintains their perception of the actions that lead to events in the world (Rescorla, 1988).

There is evidence showing that learning in human beings is accompanied by contingency awareness. Describing neurofeedback learning as implicit learning makes two assumptions. The first assumption is that neurofeedback learning can be termed as a type of motor skill learning (Birbaumer et al., 2013). The second assumption is that the motor learning process can be considered to be implicit. Scholars such as Dienes and Perner (2007) show that an individual can execute motor movement without awareness, and they also claim that an individual can act without their action being influenced by conscious intentions such as habits. However, scholars such as Krakauer and colleagues claimed that in order to understand motor learning, it is important to differentiate between motor learning and motor execution (Krakauer et al., 2019; Stanley and Krakauer, 2013).

Research conducted on motor learning in individuals shows that both explicit and implicit processes are involved in this type of learning. Thinking first of the explicit processes, it seems that they need more time to unfold, occur within faster time scales, and are sensitive to changes in reward contingencies and instructions. On the other hand, the implicit processes are said to be error-driven, need less time to unfold and act within slower timescales (Huberdeau et al., 2015). Learning can be affected by experimental manipulations, such as delaying feedback or using verbal instructions, which allows the individual to process implicit and explicit processes at different learning points (Schween et al., 2014; Taylor et al., 2014). Our main argument is that even though neurofeedback can be considered as a form of motor skill, it is not correct to dismiss the idea that explicit processes are used in the process of learning a skill.

1.6 Current views on the role of awareness in neurofeedback learning

The theory of neurofeedback provides potential reasons why a person can dismiss how awareness impacts learning. Verbal reports on the cognitive strategies used in neurofeedback performances shows a lack of consistency between individuals (Kübler et al., 2001; Neumann et al., 2003; Shibata et al., 2019); however, Kober et al. (2013) also shows a lack of consistent correlation between improvement in neurofeedback performance and verbal reports of strategies. When participants are given instructions for self-regulation purposes, the instructions are not always useful in the learning process, as participants sometime show progress even if they are not given instructions (Lacroix and Roberts, 1978; Sepulveda et al., 2016; Paret et al., 2019).

A participant is likely to learn even without being given neurofeedback, especially in a paradigm where they do not have explicit knowledge of the relationship between feedback and the neural activity (Amano et al., 2016; Shibata et al., 2011). Learning in individuals seems to take place where the neurofeedback setups are passive, especially when there are no objectives such as maximising a reward or passive settings. Birmaumer and colleagues (2013) argue that although participants are provided with abstract cognitive activities and imagery, they are motivated by instructions. This is based on the fact that

the brain learns, stores, and retains responses in ways that can be compared to motor skill as they follow implicit learning rules (Birbaumer et al., 2013).

These scholars argue that the neural activity of an individual manages to reach a certain pattern based on complex cognitive activities, which are then reinforced by implicit learning mechanisms. The study by Birbaumer et al. (2013) also shows that the cortical-basal ganglia loops are involved in the implicit learning process. Scholars such as Shibata et al. (2019) and Watanabe et al. (2017) support the idea that awareness is not needed for the learning process, with their argument being based on the supposition that tasks do not need initial instructions. Although the authors refer to these type of tasks as involving implicit neurofeedback, it is important to note that the signals were explicit, which means that the participating individuals had explicit knowledge about how their brain activity and the feedback they received related to each other. This idea also suggests that feedback instructs the brain activity to self-regulate (Shibata et al., 2019). However, the explanation given by Shibata et al. (2019) is that the participants were not aware of the experiment's purpose, and how the authors had focused on matching the induced fMRI to the purpose of the study.

In relation to the implicit tasks, exit questionnaires show that some of the participants failed to use particular strategies, which resulted in the authors suggesting that implicit learning mechanisms were involved. However, the participants were required to explicitly attempt self-regulation to modulate a signal, and therefore the role of explicit processes should not be discarded. Thus, it can be argued that the awareness of neurofeedback motivates one to carefully consider three dimensions: the measurement of awareness, communication of instructions to participants, and whether participants are exposed to passive or active learning situations. Understanding these three dimensions can help us to both understand the differences between the given tasks and identify the learning types involved. Thus, the following is a proposed taxonomy of neurofeedback paradigms (Muñoz-Moldes et al., 2020).

1.7 Real-time fMRI Neurofeedback

1.7.1 Definition of rt-fMRI neurofeedback

Real-time fMRI neurofeedback is a type of biofeedback in which real-time online fMRI signals are used to self-regulate brain function (Watanabe et al., 2017). It is a closed-loop system, making it possible to measure BOLD signals and process them in real-time. The fMRI neurofeedback can be provided by means of auditory or visual information that can be fed back to the subject, allowing them to control their brain activities (Birbaumer et al., 2013). Since the 1960s, studies have reported that many brain activities can be regulated using neurofeedback techniques like EEG and fMRI (Ruiz et al., 2014). According to these studies, the behaviour of an individual can be impacted by self-regulation neurofeedback training, which makes this technique a potential method for treating several neurological disorders (Marzbani et al. 2016). It is important to note that EEG neurofeedback has limitations, such as its inability to access the deep structures of the brain, and its low spatial resolution. FMRI, in contrast, has gained more popularity as a neurofeedback therapy tool, based on its ability to cover the whole brain, and its high spatial resolution (Sulzer et al., 2013, Thibault et al., 2018, Watanabe et al., 2017, Weiskopf et al., 2004). As such, fMRI is considered the first choice for developing neurofeedback systems. Real-time fMRI is a tool which is used to modulate the activities of the brain in real-time based on online feedback signals during the scanning, unlike traditional fMRI which uses offline data analysis. FMRI neurofeedback allows an individual to study the relationship between brain activity and behaviour as dependent variables and independent variables respectively.

1.7.2 Real-Time fMRI in healthy participants

Most studies about fMRI neurofeedback have trained healthy participants to modulate the activation of various regions of their brain, including the insula, anterior cingulate cortex (ACC) amygdala, sensorimotor cortex, and inferior frontal gyrus (IFG). These are the areas that relate to movement, perception, cognition, and emotion. Training an individual to self-regulate activity in their brain regions allows them to change the functional output of their brains, which leads to them experiencing behavioural and cognitive changes (Ruiz et al., 2014). Posse et al., (2003) conducted the first fMRI neurofeedback experiment,

which explored the ability of neurofeedback to regulate the activation of the amygdala during a paradigm which involved mood self-regulation.

The experiment involved the participants being presented with neutral and sad faces. Participants achieved self-induced sadness, and their amygdala activation levels were correlated with this low mood. Similarly, an experiment by Weiskopf et al., (2003) also successfully employed fMRI neurofeedback to upregulate the BOLD signal of the ACC. However, the study did not include any behavioural measurement. Caria et al., (2007) in an early work, used fMRI neurofeedback to regulate the activity of the anterior insular. In this case, the researcher successfully trained the participants to up-regulate the signals they had acquired from the right anterior insula by remembering autobiographical emotional events. The participants were able to achieve self-regulation without receiving feedback information after the neurofeedback training, which shows that the mental strategies learnt by individuals can persist after training.

Caria et al. (2010), in subsequent work, explored the relationship between self-regulation and emotional behaviour. This study presented the participants with neutral or emotionally negative pictures, and participants were required to rate the emotional valance of the given pictures. In a study by Hamilton et al. (2011), the authors studied the feasibility of downregulating the BOLD signal from the subgenual anterior cingulate cortex (sACC) using fMRI neurofeedback alongside positive affective strategies. In this study, the participants were able to modulate sACC activity, unlike the control group, who had been trained with sham feedback. In a study by Zotev et al. (2014), the researchers described the first implementation of simultaneous EEG neurofeedback and multimodal fMRI based on the integration of EEG and fMRI data streams. Participants used fMRI-EEG to modulate the left amygdala and frontal EEG power asymmetry simultaneously in high beta band during retrieval of happy autobiographical memories. As reported by Paret et al. (2016), it is possible to successfully down-regulate the amygdala activity in participants using neurofeedback by seeing aversive pictures was associated with a rise in functional connectivity of the right amygdala and ventromedial prefrontal cortex (vmPFC). Moreover, a study by Marxen et al. (2016) showed that participants were able to use neurofeedback to modulate the amygdala in certain directions after training

without feedback.

In addition to manipulating emotional regions of the brain, there have been attempts by researchers to induce changes in a person's behaviour by applying neurofeedback from other parts of the brain. For instance, researchers like Yoo et al. (2006) increased the auditory cortex's BOLD signal using fMRI neurofeedback during sound stimulation. According to the study's findings, individuals who receive feedback from the auditory cortex have a higher possibility of upregulating their activation in the auditory cortex, compared to individuals in control groups. In a study by Rota et al. (2009), the researchers trained individuals on how they could modulate the right IFG to have an impact on their language-related performance and speech processing. They used linguistic tests before and after the neurofeedback training to evaluate the impact they had on behaviour. In this study, people were able to regulate their IFG voluntarily, and they were also able to identify the accuracy of prosodic intonations of their emotions.

Researchers have also focused on sensorimotor areas, with these studies clinically impacting motor rehabilitation where an individual has a central nervous system injury. Studies on sensorimotor areas show that they can be used to create brain-computer interfaces. In a study by Yoo et al. (2008), the researchers noted that fMRI neurofeedback training had a long-term impact on the ability of a participant to regulate M1 activity during a motor imagery task (MI) while using the right hand. The participants of the study learned how they could regulate the BOLD signal of areas such as the M1 more effectively than participants in the control group, who had difficulties coming up with a mental strategy that could be used to maintain the regulation.

In a study by Chiew et al. (2012), the researchers trained the study participants on how they could maximise the laterality index (LI) of M1, which was considered the activity difference between ipsilateral and contralateral regions in a kinaesthetic MI task. An increase in the laterality of a motor-related activity is associated with better motor outcomes, which means that the use of neurofeedback to increase laterality can be used as a therapy for stroke patients (Ward, 2004; Neyedli et al., 2017). The findings of the study were mixed, with

only 50% of the participants managing to increase the value of LI. A study by Berman et al. (2012) reported that participants could learn how to modulate M1 activity during a finger tapping task. However, the participants failed to achieve self-regulation during the MI task. In a study by Johnson et al. (2012), the researchers tried addressing the delay experienced in the haemodynamic response, by comparing the intermittent and continuous presentation of feedback. The study results showed that if feedback information is presented intermittently, then it is more effective for the learning of self-regulation compared to the continuous feedback presentation.

In a study by Hui et al. (2014), the researchers studied how changes in the connectivity of the motor network in motor execution (ME) and motor imagery (MI) could be influenced by fMRI neurofeedback of the right part of premotor cortex (PMC). The findings of the study showed that there are connectivity changes in the ME network between the primary sensory cortex and right cerebellum of a person, and the MI network between posterior parietal cortex (PPC) and the PMC. In a study by Sepulveda et al. (2016), the focus was on examining the differential impact of monetary awards, explicit instructions, and feedback while participants were trained to up-regulate their SMA signal. The study involved dividing the participants into 4 groups and training them in a single protocol over two days. The groups received feedback as follows: feedback plus explicit instructions (MI task), feedback only, feedback plus monetary reward, and feedback plus instructions plus monetary rewards. As per the study's findings, the highest BOLD signal in SMA took place when the neurofeedback training was conducted using a monetary reward and feedback protocol. The findings also showed that the feedback protocol increased the BOLD signal between the first and second day significantly.

1.7.3 Clinical application of real-time fMRI

Researchers have recently become interested in studying real-time regulation training, based on the fact that it can be used in treating different clinical conditions. Although empirical evidence is needed to bolster some of these speculative therapeutic contributions, for some conditions it seems theoretically possible that an improvement would be seen. For instance, fMRI-NF training can be used to improve the ability of a stroke survivor to imagine movements with a

lesioned arm (Sharma et al., 2009; Sitaram et al., 2012).

In addition, fMRI-NF can be applied in supporting patients to achieve a certain mental state, by aiming at reducing certain symptoms. For instance, depressed patients might report that they cannot form positive thoughts, and thus fMRI-NF training based on regions that are associated with positive affect may aim to assess this process. These examples create supervised mental imagery training that involves the provision of a signal by feedback, which indicates activation in a specific region of the network that is of interest for the individual's condition. Researchers have conducted several neurofeedback experiments using methods of supervised mental imagery training (Sulzer et al., 2013).

The use of fMRI-NF, if compared to traditional EEG based BCI paradigms or EEG-NF paradigms, provides relatively high spatial resolution that makes it possible to target motor areas with higher specificity. Notably, the fact that the fMRI-NF is able to cover the whole brain makes it a promising technique for psychiatric and non-invasive neurological rehabilitation, which allows the provision of feedback from subcortical areas of the brain (Weiskopf, 2012). Most fMRI-NF protocols require participants to take part in mental imagery (Sulzer et al., 2013), although other areas such as those involved in motor execution can be the source for neurofeedback (Neyedli et al., 2017).

A number of researchers have piloted various fMRI-NF techniques to be used with patients who have psychiatric conditions (Arns et al., 2017; Sulzer et al., 2013) or neurological conditions (Wang et al., 2017). Proof-of-concept (PoC) studies have been used to study how fMRI-NF paradigms can be applied to psychiatric settings, with these paradigms being applied to patients experiencing different substance-related disorders such as cocaine and alcohol addiction (Hartwell et al., 2016; Karch et al., 2015; Kirschner et al., 2018; Li et al., 2012). Researchers have also explored how fMRI-NF training can be used for anxiety disorders, patients who experience post-traumatic stress disorder, pain, anxiety disorder, and patients showing phobia (Cordes et al., 2015; Gerin et al., 2016; Hampson et al., 2012; Keynan et al., 2016; Scheinost et al., 2013; Zilverstand et al., 2015). In studies such as Linden et al. (2012) and Young et al. (2014), the researchers have focused on understanding the feasibility of using fMRI-NF in individuals with

unipolar depressive disorder. Compared to the number of fMRI-NF studies with psychiatric applications, there is less published work focusing on people with neurological disorders.

In recent years, two PoC studies have attempted to understand the functions of cognition in rehabilitation, with one study aiming at understanding how memory can be improved in Alzheimer's disease (Hohenfeld et al., 2017). In addition, there have been studies focusing on understanding the training of higher visual areas, which attempt to reduce visuospatial neglect in patients with stroke (Robineau et al., 2017). There have been PoC studies focusing on motor rehabilitation, with studies such as Papoutsi et al. (2018) focusing on patients with Huntington's disease, Liew et al. (2016) and Sitaram et al. (2012) focusing on patients with stroke, and PoC studies such as Buyukturkoglu et al. (2013) and Subramanian et al. (2011) focusing on patients with Parkinson's Disease.

1.8 Motor simulation

Motor simulation refers to the way in which a motor programme is represented internally without any overt actions (Jeannerod, 2001). There are two common ways that motor simulation is thought to occur: action observation (AO), which means watching another person perform actions, and motor imagery (MI), which is explained as imagining how an action is executed, without a physical movement. People can perform AO implicitly or unconsciously, whereas for MI, participants perform the imagery explicitly.

1.8.1 Motor imagery (MI)

Research has seen a variety of terms being used in the field of motor imagery, with mental imagery being the most frequently used term. Mental imagery is defined by Richardson (1967) as the quasi-sensory or quasi-perceptual experiences of which we are self-consciously aware, and which exist for us in the absence of those stimulus conditions that are known to produce their genuine sensory or perceptual counterparts.
This definition mentions the three most important characteristics: the person performing imagery is consciously aware of the fact that she is imagining, imagery mimics perceptual or sensory experiences, and imagery can take place

without the presence of an immediate stimulus. Motor imagery involves a person imagining herself or himself making a movement without actually moving. We can add to Richardson's definition the fact that motor imagery primarily focuses on motor actions. The type of action performed depends on the environment and the actor's intentions.

For instance, one should be able to distinguish between an individual raising his or her hand above their head during stroke rehabilitation therapy (motor action) from the similar movement of the individual during a discussion (communicative action). With motor imagery being primarily focused on movement objectives, we can also add this characteristic to Richardson's definition by suggesting that imagery is not only a quasi-perceptual or quasi-sensory experience, but also a quasi-response experience (movement). It is also possible to distinguish three elements of motor imagery (Boschker et al., 2002). In the first element, an individual can imagine a situation from two different perspectives: an internal perspective and external perspective. From the internal perspective, the individual imagines things from his or her actual perspective, which can be from their body. From an external perspective, the individual observes him/herself from the perspective of a third person. In the second element, all the sensory modalities (taste, auditory, tactile, visual, olfactory, and kinaesthetic) are involved in internal motor imagery.

However, it is important to note that the external motor imagery only involves the visual modality. In the third element, one can frequently observe task-specific somatic responses during motor imagery (Boschker et al., 2002). Several other terminologies are used in literature, including terms such as guided imagery, mental movement, visual imagery, mental practice, motor imagery, and mental rehearsal. These terms include different imagery concepts that can result in confusion in determining what the correct terminology is. Different researchers consider mental practice as being a technique that can be used to rehearse imaginary tasks or scenes. Furthermore, mental practice can constitute imagined tasks or scenes, such as visual imagery of a person or object to improve memory or spatial navigation (travelling a route in mind).

Several researchers have provided evidence for an improvement in motor performance associated with motor imagery training (Gatti et al., 2013). In early research, participants were requested to conduct an action task with their fingers using either motor execution or motor imagery. Using transcranial magnetic stimulation (TMS) it was shown that the reorganisation of the motor cortex was similar in both tasks (Pascual-Leone et al., 1995). Gentili and colleagues (2010) found that motor imagery and motor execution training led to an improvement in performance. Mulder and colleagues (2004) reported that the degree of that effect depends on the degree to which an action falls within one's usual repertoire.

1.8.2 Motor imagery and movement execution

Different studies have shown that motor imagery shares certain characteristics with overt movement execution. Previous research has shown activation of specific cortical regions during motor imagery, including the supplementary motor area, superior and inferior parietal lobules, dorsal and ventral premotor cortices, pre-frontal areas, inferior frontal gyrus, superior temporal gyrus, primary motor cortex (M1), primary sensory cortex, secondary sensory area, insular cortex, anterior cingulate cortex, superior temporal gyrus, basal ganglia and cerebellum (Hanakawa et al., 2003; Lui et al., 2008).

1.8.3 Action observation

Action Observation (AO) can be described as the process of watching another individual act. Research conducted on how neuronal activity is mapped in primate motor areas in the 1990s led to the discovery of an unusual population of neurons. It was shown that the ventral premotor cortex has a set of neurons that discharge during motor actions, such as mouth and hand actions, as well as during observation of the same actions performed by others (Rizzolatti et a1., 1996). These neurons are known as ‘mirror neurons’, based on the fact that the observed actions seem to be reflected in the observer’s motor system. Studies such as Umilta et al. (2001) show that even when an action is not visualised but is implied, these neurons are active, which shows that they play an essential role in recognising an action and understanding its meaning. Researchers such as

Fogassi et al. (2005) have discovered that the inferior parietal lobule has a second population of similar neurons.
Furthermore, Buccino and colleagues (2001) have also discovered human mirror activation in the Brodmann's Area (BA), ventral premotor cortex (PMCv), secondary motor regions and inferior parietal regions.

1.8.4 Action observation motor imagery (AOMI)

Vogt et al. (2013) describe AOMI as when an individual imagines performing the action he or she observes. Traditionally, AO and MI were perceived as separate intervention techniques, where the researchers compared the two methods to define the most effective strategy to improve performance (e.g., Ram et al., 2007). Several studies have shown that similar regions are active during the motor imagery process and action observation, such as SMA and PMC (Jeannerod, (2006); Decety et al., (1994); Galdo-Alvarez and Carrillo-de-la-Pena, (2004); Grafton et al., (1996); Lacourse et al., 2005). Jeannerod (2006) highlighted that the inferior frontal gyrus in an individual is involved in mental imagery, execution of actions, and observation of actions, and plays an essential role in forming internalised action representations.

Furthermore, Jeannerod (2006) argues that the inferior frontal gyrus in an individual is involved in mental imagery, execution of actions, and observation of actions, and plays an essential role in forming internalised action representations (further information about regional activation during MI and AO will be provided in the next section). In recent times, researchers have started investigating how the combination of motor imagery and action observation impacts individuals by instructing participants to observe a given action and imagine the physiological, behavioural and sensation responses associated with these observed scenarios (Scott et al., 2018; Taube et al., 2014; Sun et al., 2016). These studies have proved that AOMI interventions result in motor regions of the brain showing increased activity compared to either motor imagery or action observation (Eaves et al., 2016). This means that the combination of these two approaches should be more effective in improving the learning and performance of motor skills compared to when either AO or MI is used independently (Romano-Smith et al., 2018).

1.8.5 Brain region activation during AO, MI and AOMI

In an analysis using activation likelihood estimation by Caspers et al. (2010), Hétu et al. (2013), and Hardwick et al. (2017), the researchers found that AO and MI activate motor-related regions that overlap with one another. The analysis of ME, AO, and MI has found that there are several areas of the frontoparietal motor network that are activated consistently.

1.8.5.1 Premotor Cortex (PMC)

There is consistent involvement of the dorsal premotor, bilateral ventral premotor, and supplementary motor area during AO, MI, and ME. The premotor cortex, according to Hoshi et al. (2007), is essential in the preparation, planning, and execution of an action. For both executed and imagined actions to be performed, equivalent amounts of time are needed, which suggests that motor imagery also involves preparation and planning phases before execution is inhibited (Guillot and Collet, 2005). A study by Davare et al. (2009) shows that the bilateral ventral premotor plays an essential role in the coordination of fine motor performance, with Dum and Strick (2005) showing that the dorsal premotor has minimal contribution in the execution of an action. Research has also shown that the supplementary motor area is the medial region of the premotor cortex which helps in linking actions and roles (Nachev et al., 2008).

1.8.5.2 Primary Motor Cortex (M1)

There is controversy regarding how M1 is involved in action simulation. In a study by Caspers et al., (2010), the authors found that motor imagery could only be recruited in AO, especially when an individual observes an action and intends to copy them. A study by Hétu et al., (2013) also found that M1 is not consistently recruited during motor imagery, with findings by Hardwick et al. (2017) showing that M1 is consistently involved during ME. In addition, a study by Jeannerod (2001) showed that when M1 is activated during AO and MI, this occurs to a lesser extent than during ME, which suggests that the activation of M1 only happens at lower levels.

1.8.5.3 Somatosensory cortex:

The somatosensory cortex is involved in motor imagery and reflects kinaesthetic aspects of MI, while in action observation, the recruitment of somatosensory cortex is proposed to extend the properties of the mirror system beyond the motor system (Keysers and Gazzola, 2009). Sensory inputs in ME give feedback on the accuracy of the movements, which allows one to compare the expected and actual sensory consequences (Muckli and Petro, 2017).

1.8.5.4 Parietal Cortex

A study by Block et al. (2013) showed that the parietal cortex is essential in processing visuomotor information when the movements of an individual are controlled online and guided by visual inputs. The Block et al. (2013) study showed that all modalities consistently activate the bilateral inferior parietal lobule (IPL) region. A study by Klann et al. (2015) shows that IPL is involved in different cognitive functions like processing tactile information, with studies by Cooke et al., (2003), and Rozzi et al. (2008) showing that the region is involved in storing different motor representations.

1.8.5.5 Other brain regions involved in MI, AO and AOMI

Schlerf et al. (2010) report that the cerebellum represents the body in multiple ways. They found data to associate the basal ganglia with the speed of executed and imagined actions and response selection.
Previous research has reported that neuronal activity increased as a result of AOMI in comparison to AO only in the inferior frontal gyrus, cerebellum, left insula, inferior parietal cortex, vPMC, supplementary motor area (SMA) and basal ganglia (Nedelko et al. (2012); Villiger et al., (2013) and Taube et al., 2015). Practical benefits have been seen with the use of AOMI. For example, Smith and Holmes (2004) used AOMI to improve individual performance in golf. In a clinical setting, AOMI has been used in rehabilitation programs, although it has mixed effects. For instance, some research showed that if AOMI is used on stroke patients with motor dysfunction in their upper limbs, it can improve the motor functions of these patients over an intervention period of four weeks (Ertelt et

al., 2007; Sun et al., 2016).

1.9 Previous rt-fMRI neurofeedback studies

Much research has been conducted using real-time fMRI. These studies have used many techniques and targeted many regions for different purposes. In this thesis, I will mainly focus on real-time fMRI research that has focused on motor regions. Table 1 summarises 38 previous studies that used rt-fMRI neurofeedback to regulate different brain regions. It provides information regarding the techniques and outcomes of every study listed in this research.

Table 1 Overview of the studies using rt-fMRI neurofeedback to regulate different brain regions

Study	ROI(s) and definition	Participants	Training sessions and feedback	Results
Al-Wasity et al. 2021)	Lt SMA; functional localiser	20 healthy participants (10 in experimental group and 10 in control group).	9 NFB runs 7 minutes each.	A gradual increase in SMA-related activity across the runs was detected in the experimental group only.
Kanel et al. (2019)	Rt anterior insula; anatomical localiser	20 healthy participants (10 participants in experimental group and 10 participants in control group).	16 NF runs and 4 transfer runs over two days.	Participants in the experimental group were able to up-regulate their right AI compared to the control group.
Neyedli et al.(2018)	Bilateral M1;	26 young healthy adults (13	4 runs of 6 min each, 1 day.	Young and older adults increased their lateralised

	functional localiser	controls); 18 elderly healthy adults (9 controls).	Continuous horizontal bar. Sham NF from a non-activated region.	activity between the motor cortices. Only young adults could maintain the lateralised activity during transfer.
Perronnet et al. (2017)	Left M1; functional localiser	10 young healthy adults (no controls).	3 runs of 6.7 min each, 1 day. Moving ball.	Unimodal fMRI-NF and bimodal EEG-fMRI-NF in a motor regulation task aided in learning self-regulation. Motor imagery-related haemodynamic and electrophysiological activity were both modulated during EEG-, fMRI- as well as EEG-fMRI-NF
Robineau et al.(2017)	Unilateral right V1/bilateral V1; functional localiser	9 elderly chronic stroke patients with left hemispatial neglect (2 experimental groups with 6 and 3 participants).	12 -15 runs of 3 min each, 3 days over 3 weeks. Auditory feedback between 0 (lowest) and 10 (highest) on ipsilesional V1 activity (unilateral group) or differential V1 feedback	Significant increase in activity levels over the training sessions. Recruitment of bilateral frontoparietal areas increased localisation to the contralesional hemisphere over the sessions. Significant decrease in errors in the line bisection task

			(bilateral group) every 6s No effects in the bilateral group, positive results in the unilateral group.	between the pre-training and session 3, and significant reduction of neglect severity according to conventional tests taken pre- and post-training.
Yamashita et al. (2017)	M1, lateral parietal cortex (PC); anatomical masks used to localise ROIs	30 healthy participants (13 in the increased functional connectivity group, and 12 in the decreased functional connectivity group) and 5 did not complete the behavioural study.	6 blocks, each of which was composed of 10 trials every day for 4 days.	Participants could increase or decrease the functional connectivity between 2 brain regions, and cognitive performance was significantly and differentially changed from pre-neurofeedback to post- neurofeedback training between the 2 groups.
Amano et al.(2016)	V1/V2; functional localiser for fMRI decoder	18 young healthy adults (6 controls).	3 runs on 3 days. Intermittent visual disc size. No NF training for the controls.	Induced associative learning between colour and grating orientation in the early visual cortex (V1/V2). Assessed with a forced-choice test after training, persisting for 3-5 months after training.

Habes et al. (2016)	PPA/FFA; functional localiser	9 young healthy adults (8 controls).	6 runs of 3 min each, 1 day. Continuous thermometer. No feedback for the controls, training in a mock scanner.	Successful upregulating of differential PPA/FFA activity. Binocular rivalry task performance showed no behavioural changes after training.
Liew et al.(2016)	Left M1 and thalamus; functional localiser	4 elderly chronic stroke patients with right hemiparesis (no controls).	18±3 runs of 4 min each, 2 days. Continuous thermometer.	Increased connectivity between the start and the end of the NF training in 3/4 participants. All participants showed an increased cortical -subcortical resting state connectivity. Individuals with greater motor impairment showed larger increases in learned self-modulation.
Sepulveda et al. (2016)	Left SMA; Functional localiser	20 healthy participants distributed equally into 4 groups.	4 runs and one transfer; 2 sessions.	The contingent feedback significantly increased their BOLD self-regulation. The contingent feedback with reward showed the highest BOLD

				signal amplitude in the SMA during the training.
Sherwood et al.(2016)	Left DLPFC activity; functional localiser	25 young healthy adults (7 controls).	5 runs of 8 min each, 5 days over 2 weeks. Continuous line graph. No feedback information for the controls.	Ability of ROI activity regulation significantly increased in the experimental group. Associated increase in working memory performance assessed with the 2-back task and dual-task scenario.
Subramania et al.(2016)	SMA; functional localiser	30 patients with Parkinson's disease; two groups (15 people each).	4 runs (3 sessions) for intervention group and no NF training for control group.	Patients in the NF group were able to upregulate activity in the supplementary motor area (SMA) by using motor imagery.
Ramot et al. (2016)	FFA and PPA; functional localiser	16 young healthy adults (no controls).	25 runs of 10 min each over 5-7days. Auditory feedback with positive/ negative sounds.	Induced modulation of FFA/PPA or PPA/FFA activity ratio in 10/16 participants without them being aware. Associated changes in functional connectivity in the auditory cortex.
Auer et al.(2015)	Left M1; anatomical and	14 young healthy	3 runs of 6 min each, 1 day.	Left M1 activity was lower during neurofeedback.

	functional localisers	adults (no controls).	Continuously vertically moving ball.	Isometric pinching task showed no change during pre- and post-training. Correlations between left M1 activation and performance.
Banca et al.(2015)	hMTþ/V5 complex; functional localiser	20 young healthy adults (no controls).	Self-paced training session, 1 day. Auditory feedback between (lowest) and 5 (highest).	Successful regulation of ROI activity through focused visual motor imagery in most of the participants. Recruitment of a novel circuit including putative V6 and medial cerebellum.
Blefari et al.(2015)	Left M1; anatomical and functional localisers	14 young healthy adults (no controls).	3 runs of 6 min each, 1 day. Continuously vertically moving ball.	Left M1 activity was lower during neurofeedback. Isometric pinching task showed no change during pre- and post-training. Correlations between left M1 activation and performance.
Megan et al. (2015)	Frontoparietal attention network,	80 young healthy adults (intervention	3 runs of max 2h each, 3-5 days.	Activity patterns for the faces versus scenes attentional states became more

	functional localiser.	group and 4 control groups, 16 participants in each).	Composite faces/scenes stimuli, proportion of task-relevant information related to how well the participant paid attention. Sham NF from the experimental group. No-NF: no feedback, outside the scanner. RT-feedback: response time feedback, outside the scanner. RT-sham control: random feedback from the RT-feedback group.	separable after training as assessed by MVPA. Sustained attention abilities improved in participants who received NF training.
Megumi et al. (2015)	Lateral parietal and M1 connectivity ; functional	33 participants (12 test group and two control:	5 runs of 4.5 min daily (4 sessions).	Participants successfully learned to increase the correlation of activity between

	and anatomical localisers	12 sham and 9 tapping-imagery).		the lateral parietal and primary motor areas.
Marins et al. (2015)	Left PMC; anatomical localiser	28 young healthy adults (14 controls).	3 runs of 6.5 min each, 1 day. Continuous vertical bar. Controls receive random signals without meaning, displayed for experimental purposes.	Increased activation in the ROI in the last NF run compared to the first run. Associated increases in activity of motor control regions, not present in the control group.
Scharnowski et al. (2015)	SMA and PHC; functional localiser	7 young healthy adults (no controls).	12-22 runs of 8 min each, 4-6 days; Continuous graph of differential SMA-PHC or PHC-SMA signal.	Significant increases in differential feedback signal associated with training, maintained in the absence of neurofeedback in transfer runs. Increased negative coupling between SMA and PHC. Improved reaction times during the motor task correlated with SMA activity, and performance in word memory correlated with PHC activity.

Xie et al. (2015)	Right dorsal PMC; functional localiser	24 young healthy adults (12 controls).	4 runs of 7.5 min each, 1 day. Continuous line graph. Sham NF from the experimental group	Associated decrease in connectivity be-tween bilateral PMC and right posterior parietal lobe.
Hui et al. (2014)	Right PMC; functional	28 young healthy adults (13 controls).	Localiser 4 runs of 7.5 min each, 1 day. Continuous line graph. Sham NF from the experimental group	Significant correlation between changes in ROI activity in the last run and network connectivity. Significantly increased performance in finger tapping task in both groups, but only correlated with functional connectivity in the NF group.
Robineau et al. (2014)	Visual areas in left and right occipital cortex; functional localiser	14 young healthy adults (no controls).	3 runs of 60 min each, 3 days. Continuous thermometer.	Consistent up-regulation of the target ROI activity in 8/14 participants. No significant improvement in bilateral target detection task and line bisection task.

Zhao et al. (2013)	Right dorsal PMC; functional localiser	24 young healthy adults (12 controls).	4 runs of 7.5 min. Continuous line graph. Sham NF from the experimental group.	Increase in connectivity from the dorsal PMC to other motor-related areas in the experimental group and progressive decrease in the control group. Significant improvements in the behavioural finger tapping task, higher in the experimental compared to the control group.
Zhang et al (2013)	Left DLPFC; functional localiser	30 young healthy adults (15 controls).	8 runs of 6.5 min each, 2 days. Continuous thermometer. Sham NF from the experimental group	ROI activity significantly increased between the first and last training session. Experimental group showed improved performance on the digit span and letter memory task.
Berman et al.(2012)	Left M1 and S1; functional localiser	40 young healthy adults (9 controls).	4 runs of 8 min each, 1 day. Intermittent feedback, monetary reward. Sham NF from the	Overall brain activity increase in the NF group and no significant change in the control group. Participants receiving NF showed significantly faster

			experimental group	reaction times with a coherent cue.
Chiew et al. (2012)	Bilateral M1; functional localiser	18 young healthy adults (5 controls).	4 runs of 8.5 min each, 1 day. Continuous arrow vector; length represents brain activity. Sham NF from the experimental group.	Increased laterality index between left and right M1 in 6/13 NF participants. Button press reaction time test showed no difference pre- and post-training in both NF and sham-feedback groups.
Johnson et al. (2012)	Left PMC; functional localiser	13 young healthy adults (no controls).	4 runs of 10.3 min each, 1 day. Continuous or intermittent thermometer.	Participants preferred intermediate over continuous feedback. PSC differences were more significant in the intermittent than the continuous condition.
Scharnowski et al. (2012)	Early visual cortex representing the left or right visual field; functional and anatomical localiser	16 young healthy adults (5 controls).	7 runs of 8.3 min each, 3 days. Continuous thermometer. Sham NF from an unrelated region.	Significant increases in visual cortex activity in 7/11 experimental participants. Associated increase in connectivity between the visual cortex and the superior parietal lobule (SPL).

				Significantly enhanced perceptual sensitivity in successful learners
Sitaram et al. (2012)	PMCv; functional localiser	2 elderly chronic stroke patients with right hemiparesis, 4 young healthy controls.	10 runs of 7.5 min each over 3 days. Continuous video feedback during runs 1-2, continuous thermometer feedback in the remaining runs.	Increased ROI activity and decreased intra-cortical inhibition over the course of the training. The visuomotor pinch-force task showed improved performance across trials in 1 patient and 3 healthy participants.
Hampson et al. (2011)	Bilateral SMA; functional and anatomical localiser	8 young healthy adults (no controls).	24 runs over 2 weeks. Continuous line graph.	Successful regulation of ROI activity in sessions 2-4, but no significant increase over the sessions. Decreased connectivity between the SMA and subcortical regions following training.
Shibata et al.(2011)	V1/V2; functional localiser for fMRI	Decoder 10 young healthy adults (no controls).	10 runs of 5 min each, 5-10 days.	Learned estimation of target-orientation likelihood, even

			Intermittent, solid green disk.	during the first neurofeedback day. Performance in orientation discrimination task significantly improved.
Rota et al. (2009)	Right IFG; anatomical and functional localisers	12 young healthy adults (5 controls).	4 runs of 9 min each, 1 day. Continuous thermometer. Sham NF from unrelated regions.	Progressive increase in ROI activation specific to the NF group. Improvements in the experimental group in interpreting emotional prosody but not syntax.
Yoo et al. (2008)	Left M1; functional and anatomical localiser	24 young healthy adults (12 controls).	7 runs of 1.2 min, 1 day; follow-up after 2 weeks. Continuous line graph. Sham NF from a non-activated region in an earlier session.	Successful regulation of ROI activity retained after 2 weeklong daily practice without NF. Recruitment of additional circuitries implicated in motor skill learning unique to the experimental group.
Bray et al. (2007)	Left M1 and S1; functional localiser	40 young healthy adults (9 controls).	4 runs of 8 min each, 1 day. Intermittent feedback,	Overall brain activity increase in the NF group and no significant change in the control group.

			monetary reward. Sham NF from the experimental group.	Participants receiving NF showed significantly faster reaction times with a coherent cue.
Yoo et al. (2006)	Left primary and secondary auditory areas; anatomical and functional localisers	22 young healthy adults (11 matched controls).	5 runs, 40 min total, 1 day. Intermittent auditory feedback of PSC. No neurofeedback information for the controls.	Required target level of regulation (40% increase from baseline) reached by 10/11 resp. 7/11 experimental and control participants. No significant difference between the pre- and post-training scans in either group. The experimental group showed a significant increase in activated volume and BOLD signal in the last NF run.
DeCharms et al. (2004)	Left M1 and S1; functional localiser	9 young healthy adults (3 controls).	3 runs of 20.5 min, 1 day. Continuous line graph, or virtual reality interface of a corresponding dynamic virtual object. Sham NF from a background	Successful regulation of ROI activity, specific to the experimental group.

			region at an earlier time-point in the same session.	
Yoo and Jolesz, (2002)	Left M1 and S1, parts of pre-motor areas; functional and anatomical localiser	5 young healthy adults (no controls).	1 run of 8 min, 1 day. Intermittent statistical map of pixel-by-pixel brain activity.	All achieved a 3-fold increase in the number of activated voxels in motor and somatosensory areas.

2 Chapter two: Magnetic resonance imaging (MRI) basics

2.1 History of MRI

In 1946, Purcell and Bloch first described the property of Nuclear Magnetic Resonance (NMR), for which they received a Nobel prize in 1952. NMR was first used to analyse chemical structure and composition. Lauterbur and Mansfield used NMR principles in 1973 to describe a technique for analysing and determining physical structure. This resulted in the development of Magnetic Resonance Imaging (MRI) which has since been used in chemical, biomedical and engineering applications.

2.2 Nuclear spin angular momentum

MRI can be understood through a thorough knowledge of the properties of atoms. The three main subatomic particles comprising atoms are the electron, the neutron and the proton. Neutrons are electrically neutral, protons positively charged and electrons negatively charged (e=1.6021773x10^{-19} coulombs). Neutrons and protons comprise the nucleus of an atom, with electrons orbiting their collective centre. The quantum mechanical description of atomic nuclei predicts the property of spin angular momentum. An atomic nucleus has an intrinsic angular momentum that can be referred to as spin. Spin has a magnitude known as I, which can be represented by the following formula.

$$|\mathbf{P}| = \hbar\sqrt{(\boldsymbol{I}(\boldsymbol{I}+\mathbf{1}))} \qquad 2.1$$

However, given the fact that P is a vector, it is vital to consider its orientation. The following formula can be used to find the value of the z-component of angular momentum in a magnetic field if it is applied along the z-axis.

P= $\hbar$m, where m = *I*, (*I* -1),(*I* -2)…..-I

where *I* is the value of magnetic quantum and $\hbar$ is Blank's constant\2π.

The spin quantum number, *I*, characterizes spin angular momentum such that I$\hbar$ is the total spin angular momentum. The *I* value can be said to be the intrinsic property of a nucleus. For a nucleus to show the property of magnetic resonance, it should have a non-zero value of *I*. The proton, (^{1}H), in medical applications is the nucleus of most interest, given that it has high natural

abundance. Usually, the spin quantum number of the hydrogen nucleus is *I* =1/2, where it gives high energy spin states of +1/2. Normally, the spin generates a magnetic field, which means that hydrogen protons possess magnetic moments. Other nuclei, such as ^{13}C, have low natural abundance relative to ^{12}C, which means that they can be used for tracer studies (see table 2).

Table 2 NMR active nuclei and their nuclear spin (I) and gyromagnetic ratio (γ).

Isotope	**Nuclear spin (*I*)**	**Gyromagnetic ratio (γ) (rads-1T-1)**
^{1}H	1/2	267.522
^{13}C	1/2	67.283
^{19}F	1/2	251.815
^{23}Na	1/2	70.808
^{31}P	1/2	108.394

2.3 Magnetic moment

A magnetic moment is a substance's ability to interact with a magnetic field. The magnetic moment can be said to be permanent in some substances such as a magnetic bar and compass needle. In most substances, magnetism is induced, which means that the magnetic moment appears only if there is an external magnetic field. This means that the interaction between the nucleus and magnetic field takes place only because of the magnetic moment. The angular momentum and magnetic momentum of a nucleus can be said to be vector quantities that relate to each other through a magnetogyric ratio, (γ), that measures the magnetic strength of the nucleus.

Based on this, the magnetic strength of a nucleus can be measured using the formula:

$$\mu = \boldsymbol{\gamma}\,\mathbf{P} \qquad 2.2$$

$$\mu = \mu_{0x^{-1}}\,\mathbf{V}\boldsymbol{\chi}\mathbf{B} \qquad 2.3$$

Where μ is the magnetic moment, μ_0 is the magnetic constant (= $4\pi\times10^{-7}$ $Hm^{-1)}$, B is the applied magnetic field, V is the object's volume and χ is the material's magnetic susceptibility. Magnetic susceptibility is a measure of how much a material will develop a magnetic moment when it is exposed to an external magnetic field.

If there is no static magnetic field, the ^1H protons are oriented randomly. However, if a static magnetic field is present, the ^1H nuclei magnetic moment relative to the magnetic field will become oriented. The spin quantum number usually determines the number of possible orientations. The spin number of ^1H is ½, where it can adopt two Zeeman energy levels with anti-parallel (spin-down) or parallel (spin-up) orientations to the external magnetic field. The orientations correspond to magnetic quantum numbers with low levels of energy (m = -1/2), where the vector of the nuclear spin can possess either low energy or high energy (m = +1/2), whereas the vector of the spin vector has high energy.

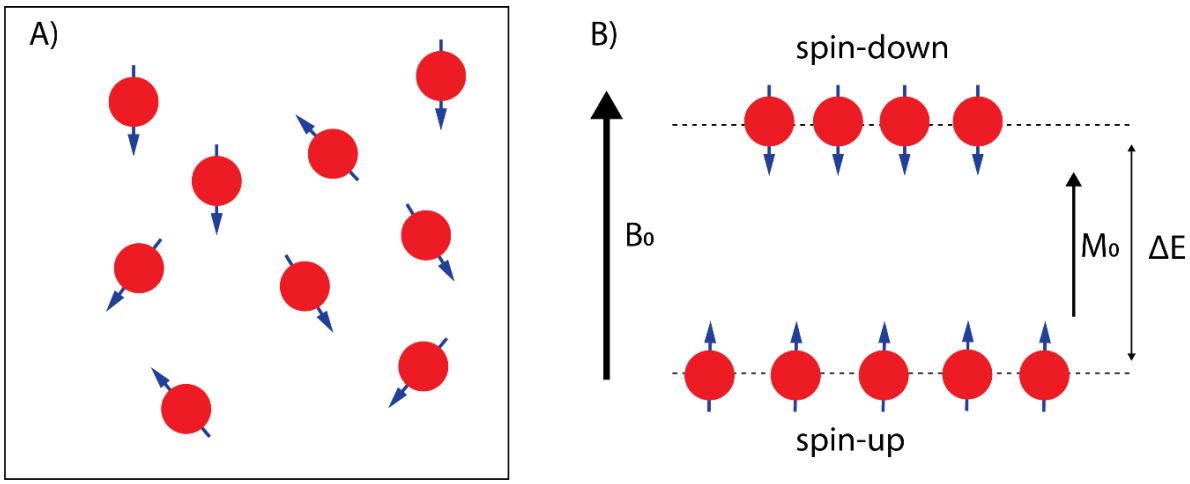

Figure 2-1 Alignment of NMR spins in the case of I = ½. A) Spins are randomly aligned due to the absence of an external magnetic field, however, each spin precesses about its axis. B) When an external magnetic field is present, more spins align parallel than anti-parallel to the field, creating a net magnetisation, M0.

The above behaviour is referred to as the Zeeman effect, where the following formula can be used to determine the interaction energy of each orientation:

$$E = -\gamma\hbar\, m_I B_0 \qquad 2.4$$

This means that the following formula can be used to represent the hydrogen nucleus (^1H) as the difference in energy between two spin states:

$$\Delta \mathbf{E} = \boldsymbol{E}_{\mathbf{m}_I=-\frac{1}{2}} - \boldsymbol{E}_{\mathbf{m}_I=\frac{1}{2}} = \left[-\left(-\frac{\mathbf{1}}{\mathbf{2}}\right)\boldsymbol{\gamma}.\hbar.\mathbf{B_0}\right] - \left[\left(-\frac{\mathbf{1}}{\mathbf{2}}\right)\boldsymbol{\gamma}.\hbar.\mathbf{B_0}\right] \quad 2.5$$
$$= \boldsymbol{\gamma}\hbar\mathbf{B_0}$$

A Boltzmann distribution can be used at thermal equilibrium to represent the populations of the two energy states:

$$\frac{\mathrm{N}_{\uparrow}}{N_{\downarrow}} = \mathrm{e}^{(-\Delta \mathrm{E}/\mathrm{K}_B \mathrm{T})} \quad 2.6$$

In this formula, $\mathrm{N}_{\uparrow}$ is the spin up state's population ($\mathrm{m}_{I=1/2}$) while $N_{\downarrow}$ is the spin down state's population ($\mathrm{m}_{I=-1/2}$). T is used to measure the temperature and K_B is the Boltzmann constant (1.3805 x $10^{-23}$$JK^{-1}$(joule per kelvin)). If the two states have different populations, there is a net magnetisation that represents the summation of vectors of the magnetic moments of the nuclei.

$$\mathrm{M_x} = \sum_{\mathrm{i}} \mu_x^i \quad 2.7$$

$$\mathrm{M_y} = \sum_{\mathrm{i}} \mu_y^i \quad 2.8$$

$$\mathrm{M_z} = \sum_{\mathrm{i}} \mu_z^i \quad 2.9$$

In the above, if the specific nucleus has μ_x, μ_y, μ_z as magnetic moment components, the directions are represented by x, y, and z. Net magnetisation, at equilibrium, is aligned in the(B_0) direction, which is the main magnetic field. This means that the formula below can be used to calculate the equilibrium net magnetisation (M_0):

$$\mathrm{M}_0 = \frac{\gamma^2 \hbar^2 \mathrm{B}_0 \mathrm{N}_\mathrm{s}}{4\mathrm{K}_\mathrm{B}\mathrm{T}} \quad 2.10$$

Where the number of spins is represented by N_s. It is important to note that the MRI signal is influenced by factors such as natural abundance, gyromagnetic ratio and scanner B_0 strength of the field strength of the particular nuclei.

2.4 Larmor Frequency

The net magnetisation produced in unit volume of material is a sum of the individual nuclear magnetic vectors.

M= Σ μ

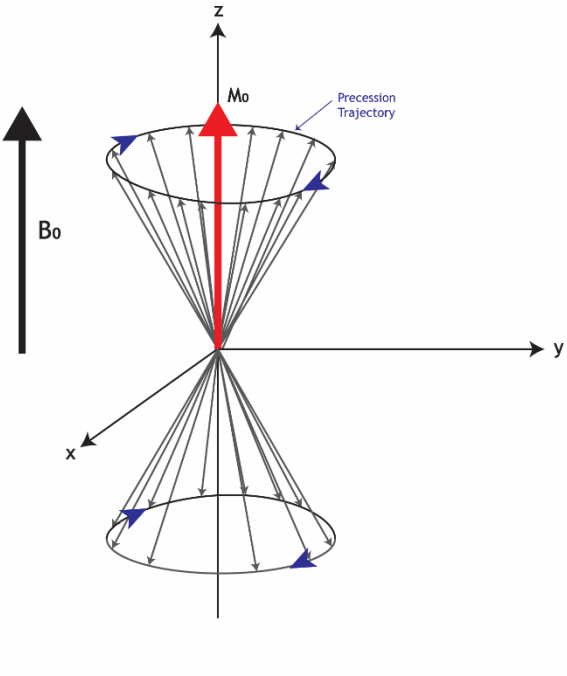

Figure 2-2 This figure represents the magnetic moment of a nucleus and its precession about a magnetic field, Bo.

Individual nuclear magnetic moments, μ, precess at a Larmor frequency, which depends on the field strength B_0 and $\boldsymbol{\gamma}$ as shown in the formula below:

$$\boldsymbol{\omega}_o = -\boldsymbol{\gamma} \boldsymbol{B}_o \qquad 2.11$$

With ω_o being the Larmor frequency, B_0 being the external magnetic field in T (Tesla), and γ being the gyromagnetic ratio (hydrogen =267.522 **rads-1T-1** and is equivalent to 42.58 MHz/T). The quantum theory of radiation asserts that the Larmor frequency is the frequency at which the nuclei absorb energy and is related to different amounts of energy between levels (ΔE). This means that the equation can be re-written as below:

$$\Delta E = \hbar \omega_0 \qquad 2.12$$

If the strength of the magnetic field is higher, the greater are ω_0 and ΔE and vice versa. The Larmor frequencies of different nuclei differ in that they have different gyromagnetic ratios.

2.5 Radiofrequency pulse

RF radiation can be described as electromagnetic radiation. It is also a combination of an oscillating magnetic field and an oscillating electric field (that does not interact with M_0) that are perpendicular to each other. Radiofrequency pulses (RF) occur by applying, perpendicular to B_0, a second magnetic field, B1, that rotates in phase with precessing nuclear magnetic moments at ω_1. B_1 can be determined using the formula below:

$$\omega_1 = -\gamma B_1 \qquad 2.13$$

In the formula above, the B_1 field can exert a constant direction torque only if (ω_1) is close to precession frequency (ω_0). The RF pulse's impact on M_0 can be visualized by considering a rotating frame of reference about the z-axis at radiofrequency ω1. The denotation of the new frame of reference is (x', y', z'), where it is considered in the context of the rotating frame, as shown below. The B_1 field in this rotating frame of reference seems to be stationary. The B_0 field's contribution is removed if $\omega_1 = \omega_0$ (On-resonance).

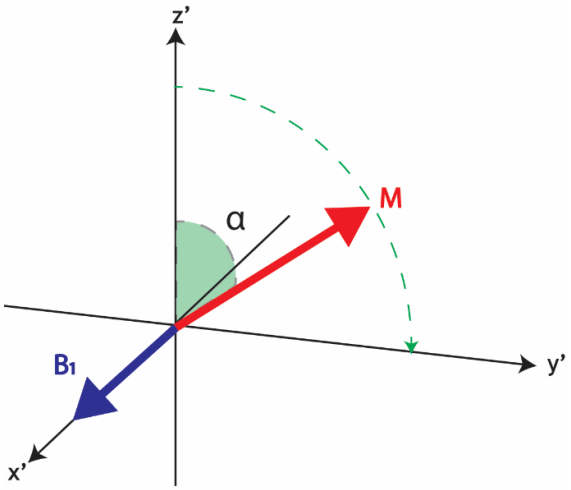

Figure 2-3 The tipping of the bulk magnetisation vector, M, under the application of an RF pulse, B1, in a rotating frame.

2.6 MRI Relaxation

2.6.1 Transverse relaxation

Transverse relaxation (T2) can be described as the spins' relaxation in a transverse plane. The relaxation takes place following the radiofrequency pulse when the variations in local magnetic field strength cause spins to lose phase coherence in the x-y plane because of the existence of different precession frequencies. An exponential relationship described by the formula below can be used to describe the loss of phase.

$$M_{xy} = M_o \, e^{\frac{-t}{T_2^*}} \qquad 2.14$$

The magnetisation is rotated into the x-y plane by applying a 90°rf pulse, which results in the spins losing phase coherence, where some spins precess slowly and some faster. The spins are inverted by applying a 180° rf pulse after a period τ, which causes spins to rotate in the opposite directions until they regain their previous lost phase coherence. When the spins are refocused completely after a period (τ) following a 180° rf application, an echo occurs. A spin cannot be refocused fully by a 180° pulse if it diffuses to a region whose magnetic field is slightly different. As a result, in the presence of local field inhomogeneities, free induction decay (FID) occurs.

The relaxation time of an FID is shorter than T2 in local field inhomogeneities ($D\boldsymbol{B}_0$). This relaxation time can be referred to as *T2**. The formula below describes the relationship between *T2** and *T2:*

$$\frac{\mathbf{1}}{\mathbf{T2}^*} = \frac{\mathbf{1}}{\boldsymbol{T2}} + \frac{\mathbf{1}}{\mathbf{T2}_{\mathbf{inhom}}} \qquad 2.15$$

In the above formula, $T_{2\ inhom}$ describes a signal's decay as a result of the inhomogeneity of the magnetic field.

$$\frac{\mathbf{1}}{\boldsymbol{T2}_{\mathbf{inhom}}} = \boldsymbol{\gamma} \mathbf{D} \mathbf{B}_{\mathbf{0}} \qquad 2.16$$

Where DB_0 is the extent of the variation of the applied strength of the magnetic field.

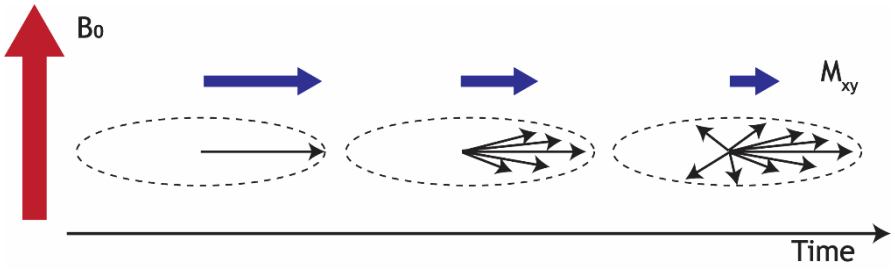

Figure 2-4 T_1 relaxation process. The diagram shows the transverse relaxation process after applying a 90^0 RF pulse. The black arrow (transverse magnetisation) initially has its maximum amplitude in the phase of spin rotation. The net transverse magnetisation amplitude decays in the process of the spins moving out of the phase (small black arrows).

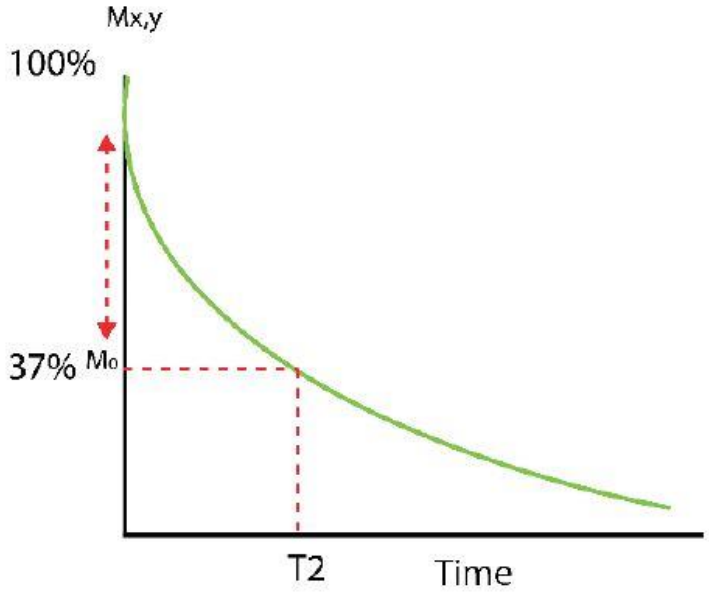

Figure 2-5 T2 decay curve, which represents the decay of magnetisation in the transverse plane.

2.6.2 Longitudinal relaxation

Longitudinal relaxation (*T1)* is when the magnetisation returns to *M*z, which is the equilibrium value. The rate of relaxation usually depends on local fluctuations in the local magnetic field that are generated as a result of the tumbling rate in the neighbouring molecules in which the spins reside.
The longitudinal relaxation (T1) in an exponential decay process is described in the following formula:

$$M_z = M_o(1 - e^{\frac{-t}{T_1}}) \qquad 2.17$$

Following the 90°pulse, M_z exponentially increases towards its equilibrium value, M_o parallel to B_0. The excited spins start to lose their energy to the surrounding lattice. This process is called spin-lattice relaxation.

T1 can be measured by using inversion recovery. The magnetisation is inverted by a pulse of 180°, which results in it residing along the negative z-axis. The magnetisation then starts to relax towards its thermal equilibrium position. After a period of time, τ (shorter than the relation time), a 90° pulse applied to flip the magnetisation onto the y⁻axis where an echo is acquired.

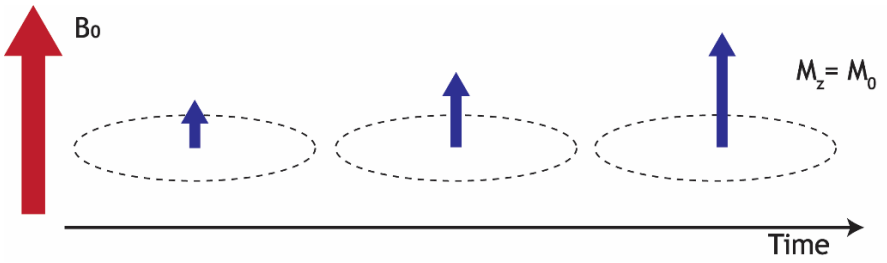

Figure 2-6 The T1 relaxation process. The diagram shows the T1 relaxation process after application of a 90^0 RF pulse. The z component of Mz is reduced to zero, although it gradually recovers to equilibrium value.

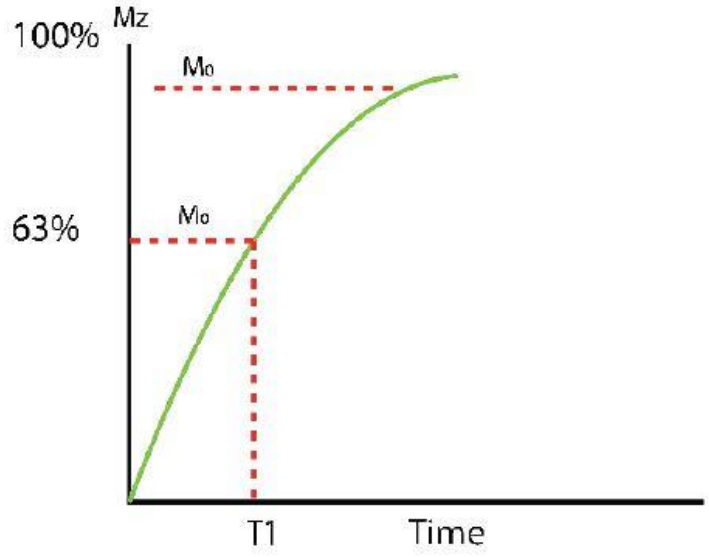

Figure 2-7 longitudinal recovery curve that represents the exponentially increasing longitudinal component of the net magnetisation.

2.6.3 Spin echo

The spin echo sequence can be described as the most basic method to measure relaxation time. The spin echo sequence has a 90^0 pulse, which is followed by a time known as TE/2 and a 180^0 pulse, where TE can be described as the echo time. Normally, the 180^0 pulse reverses the dephasing effects of magnetic field inhomogeneity where only the signal degradation is left due to spin-spin relaxation. The use of the 180^0 pulse is known as a refocusing pulse.

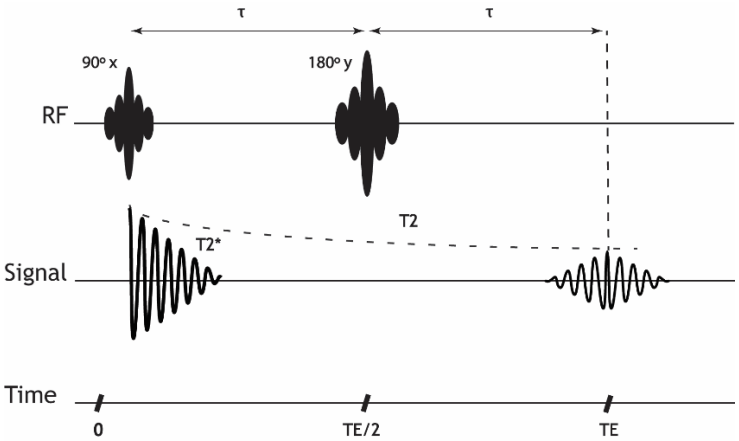

Figure 2-8 The figure above shows a 90^0 pulse, which is closely followed by a time of TE/2 and by a 180^0 pulse. A free induction signal (FIS) is generated by a 90^0 pulse in the signal strength of the initial amplitude. The FIS has a decay that is determined by T2 and the magnetic field's homogeneity. An echo signal is formed as a result of the 180^0 refocusing pulse (Eklund, 2010).

A 90^0 pulse is applied along the x-axis with B1 which results in the magnetisation vector, M, tipping from its equilibrium position onto the y' axis. Throughout the sample, the applied magnetic field has inevitable variations that result in the magnetisation vectors, which contribute to M, starting to dephase relative to one another. The magnetisation vectors arising from this region precess into an anticlockwise direction due to the fact that the frame rotates at ω_L, while the magnetisation vectors that arise from the regions where the local fields are higher than B_0 precess clockwise in the rotating frame.

Some spin groups may precess faster than others due to the slight difference in the local microscopic field. The total transverse component of M decays rapidly over time. A 180^0 pulse applied at TE/2 after a 90^0 pulse causes the complete dephasing of magnetisation vectors to rotate 180^0 on the x' axis. Magnetisation vectors can dephase completely to rotate 180^0 on the x' axis if the magnetisation vectors remain intact at the end of the 180^0 pulse, however, now they are centred on the y' axis. The faster magnetisation vectors still precess in a clockwise direction but now towards the y' axis. The magnetisation vectors in low field regions also precess in an anticlockwise direction in the rotating frame but they move towards the y' axis. At time TE after the 90^0 pulse, all the magnetisation vectors are aligned precisely along the y' axis. They have been refocused and rephased by the 180^0 pulse. Since M is formed by sum of all magnetisation vectors, the transverse components reach a maximum value at

this time which corresponds to the centre of the spin echo sequence. The magnetisation vectors then dephase again, leading to a fast drop in the NMR signal.

2.6.4 Multi spin echo sequence

The Multi spin-echo sequence technique is based on the Carr-Purcell-Meiboom-Gill (CPMG) sequence, in which transverse magnetisation, following a slice of selective 90º pulse, is refocused by a train of slice-selective 180º pulses, resulting in a series of echoes (Meiboom and Gill,1958).

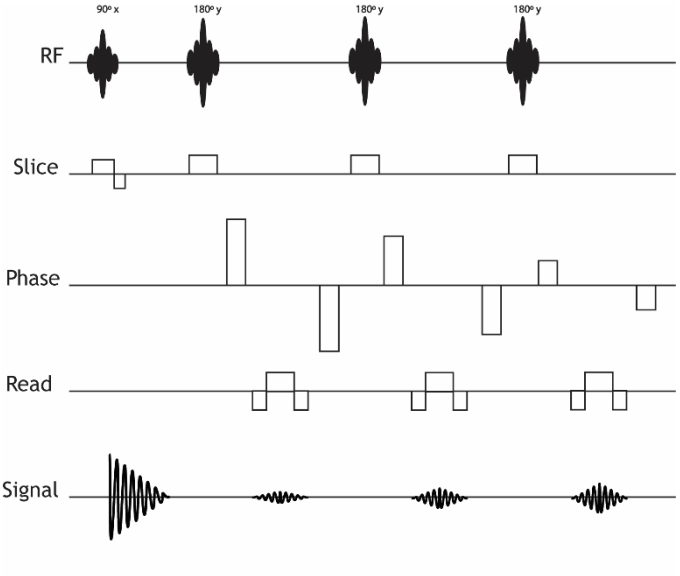

Figure 2-9 Simplified pulse diagram of multiple spin echo imaging sequence (Eklund, 2010).

2.6.5 Gradient echo

A gradient echo can be formed by applying a negative gradient after the excitation pulse, resulting in spins dephasing rapidly. This is followed by the application of a positive gradient that results in the spins rephasing. The spins then phase again after some time, resulting in the echo. However, gradient echoes are impacted by the inhomogeneity of magnetic fields, resulting in poor image quality compared with the spin echo sequence. This is represented as T2*. One remarkable thing about gradient echoes is the potential to vary the flip angle (*a)*, which can result in the repetition time (TR) being shortened. Figure 2.10 below shows the time courses for the gradient fields and the RF pulse when using a gradient echo to sample a line.

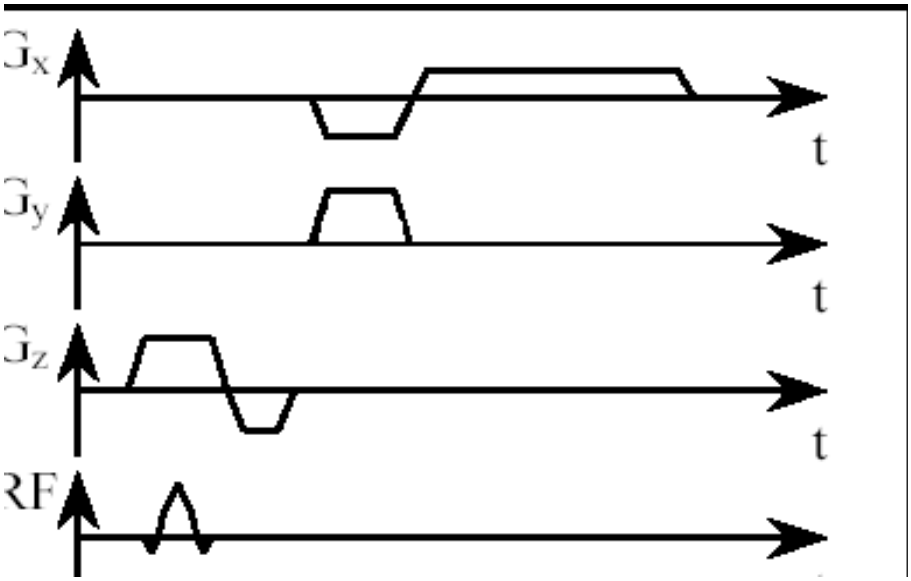

Figure 2-10 Gradient echo is used to sample a line using gradient fields. This is achieved by applying Gz, a slice selective gradient field, at the same time as the RF pulse create a specific slice. The current line can be selected using Gz in k-space. Given that the slice selection is performed in the z-direction, the Gz can be referred to as Gss (Eklund, 2010).

2.6.6 Echo Planar imaging (EPI)

Echo planar imaging (EPI) allows the acquisition of whole slices within a fraction of a second (Mansfield 1977), therefore, the whole brain can be covered within 2-3 seconds. This is achieved by reversing the readout gradient, thereby producing a train of echoes following a single RF excitation pulse. During EPI, k-space is acquired continuously, therefore, all lines of k-space are filled after each RF excitation.

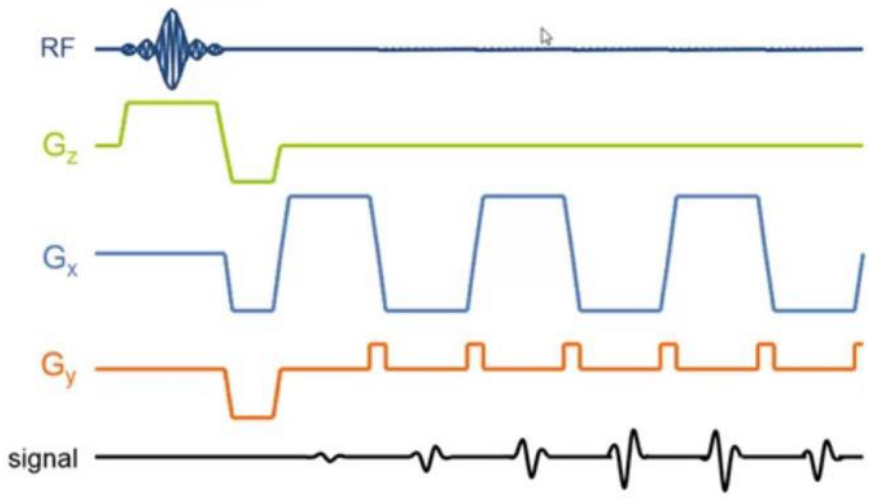

Figure 2-11 A schematic diagram of an EPI sequence. The slope of the frequency encoding gradient (x-gradient) is rapidly alternated, generating a train of gradient echoes. A phase

encoding gradient 'blip' is applied between each frequency encoding gradient to ensure each gradient echo fills a different line of k-space (Author's own, 2021).

2.7 Generating MR signals

If the magnetisation has a transverse component, the detection of its precession around B_0 can be examined. To detect the signal, the same RF coil that transmits B1 can be used. The precessing net magnetisation causes a change in magnetic flux, Φ, which results in induction of an electromotive force (emf). Faraday's law of induction can be used to calculate the emf in a coil induced by magnetic flux change as shown below.

$$\mathrm{emf} = \frac{-\mathrm{d}\phi}{\mathrm{dt}} \qquad 2.18$$

The following mathematical formula can be used to express the MRI signal resulting from precession of net transverse magnetisation:

$$\mathbf{s} \propto \mathbf{e}^{((\mathbf{i}\boldsymbol{\varphi}))} \qquad 2.19$$

Where φ is the phase of transverse magnetisation. The following formula show this as a function of time:

$$\boldsymbol{\varphi} = \boldsymbol{\omega}\mathbf{t} \qquad 2.20$$

$$\boldsymbol{s} \propto \mathbf{e}^{((\mathbf{i}\boldsymbol{\gamma}\mathbf{B\_0}\,\mathbf{t}))} \qquad 2.21$$

Normally, MR imaging is used to obtain spatial information of the given sample. This means that it is important to encode the resonance frequency of nuclei as a function of their spatial position. For this to be achieved, magnetic field gradient pulses can be used, where they form the basis of MRI. Magnetic field gradients can be applied in the direction where spatial encoding is needed for the nuclear spins to be spatially encoded, as shown by the formula below.

$$\mathrm{G_x} = \frac{\partial \mathrm{B_z}}{\partial \mathrm{x}}\,, \qquad \mathrm{G_y} = \frac{\partial \mathrm{B_z}}{\partial \mathrm{y}}\,, \qquad \mathrm{G_z} = \frac{\partial \mathrm{B_z}}{\partial \mathrm{z}} \qquad 2.22$$

The Larmor frequency of the spins at position X_1 is then a function of the applied gradient:

$$\omega_{(x_1)} = \gamma(\mathrm{B_0} + \mathrm{G_x}.\mathrm{x_1}) \qquad 2.23$$

The rotating frame of reference concept can be used conveniently if the rotation of the new reference frame is on the z-axis at ω_1, the same frequency as the B_1 field of the RF radiation. The net magnetisation at resonance ($\omega_1 = \omega_0$) will

appear to be static as a result of the disappearance of the effects of the B_0 field. The following formula shows how the signal intensity can be acquired as a function of time and the applied gradient.

$$s \propto e^{(i\gamma G_x . x_1 t)} \qquad 2.24$$

As shown by the figure below, the MRI data acquired with respect to time and to gradient strength and duration is referred as k-space.

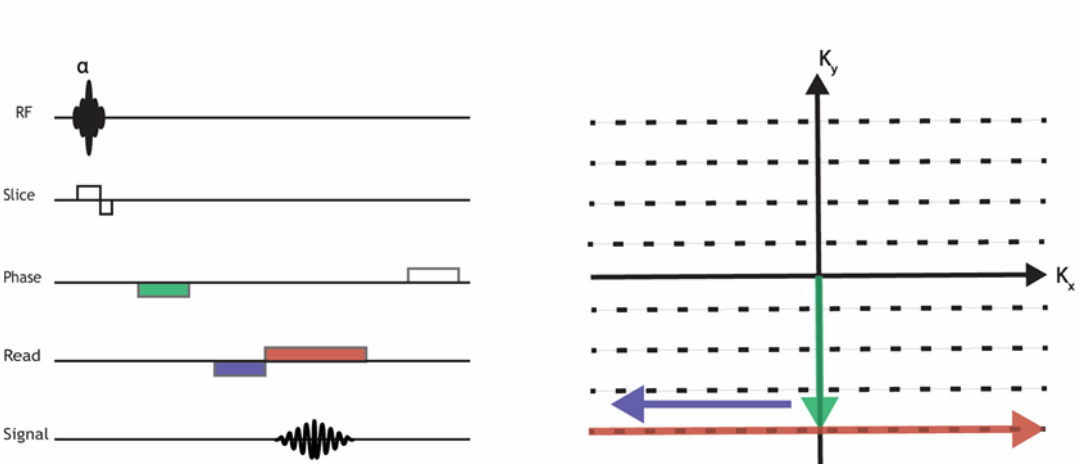

Figure 2-12 this figure shows how MR imaging data are acquired in k-space. Data are acquired in an echo if the read gradients fill the k-space on horizontal lines. The strength of the encoding gradient, which is applied in the pulse sequence, is used to determine vertical positions of k-space lines. The application of two Fourier transformations/transforms, which take place in the first and second direction of k-space data, is used in the reconstruction of an image (Author's own, 2021).

As shown in the formula below, the position and separation of points along each axis of K-space are defined by the gradient duration (t) multiplied by the gradient strength:

$$k_x = \frac{1}{2\pi} \gamma G_x . t_x \ , \qquad k_y = \frac{1}{2\pi} \gamma G_y . t_y \qquad 2.25$$

If the substitution $k_x = \frac{1}{2\pi} \gamma G_x . t_x$ is used and the signal is integrated over the sample, the following formula can be used to express the total signal.

$$S_{(k)} = \int_{-\infty}^{+\infty} \rho(x)\, e^{i2\pi(k_x . x)} dx \qquad 2.26$$

In the above formula, $\rho(x)$ is the spin density. It shows that the $S_{(k)}$ signal is the Fourier transform of the spin density ($\rho(x)$). A 2D MR image can be generated through the Fourier transformation of the data in k-space in both the phase direction of (ky) and the read direction (kx), as shown in the formula below:

$$S_{(k)} = \int_{-\infty}^{+\infty} \int_{-\infty}^{+\infty} \rho(x, y)\, e^{i2\pi(k_x.x + k_y.y)} dx\, dy \qquad 2.27$$

Transverse magnetisation, Mxy, is generated for MR imaging only from spins positioned in small and well-defined areas of the whole volume. To achieve this, a shaped RF pulse is applied during the magnetic field gradient's application with a frequency bandwidth Δω.

2.7.1 Slice selection

Applying a frequency selective RF pulse and magnetic field gradient simultaneously can help in achieving slice selection along vertical or horizontal planes. A magnetic field gradient causes nuclei to precess at different frequencies in the desired direction for the slice selection. The bandwidth of excited frequencies can be controlled if a shaped RF pulse is applied (Gaussian or sinc function). The magnetisation vectors spread undesirably from different regions due to the slice gradient, leading to a reduced signal. However, the spread in magnetisation can be cancelled by applying a refocusing gradient after slice selection, which can be done using a gradient of the same sign after the 180º pulse or a gradient of the opposite sign after a slice gradient. If the z-gradient is used in slice selection and the field gradient is applied perpendicular to the z-axis, the spins will experience a magnetic field at the given position, Z.

$$\mathbf{B} = \boldsymbol{B_0} + \mathbf{Gz}\,\mathbf{Z} \qquad 2.28$$

With the gradient applied, the Larmor frequency becomes dependent on the spin's position along the z-axis:

$$\boldsymbol{\omega} = \boldsymbol{\gamma}(\boldsymbol{B_0} + \mathbf{Gz}\,\mathbf{Z}) \qquad 2.29$$

This means that the frequency-selective RF pulse will excite a slice containing nuclei with the same bandwidth frequencies. It is possible to change the slice thickness by adjusting the field gradient, Gz's, magnitude and the RF pulse's bandwidth Δω.

$$\boldsymbol{DZ} = \frac{\boldsymbol{Dw}}{\boldsymbol{\gamma Gz}} \qquad 2.30$$

2.7.2 Frequency Encoding (readout)

A spatial encoding gradient is applied along the encoding frequency after the RF pulse is switched off. This magnetic field causes the magnetisation at different positions to precess at different frequencies based on their position, resulting in labelling their spatial position in the frequency encoding direction.

2.7.3 Phase encoding

The direction of phase encoding is usually visualized, in addition to the readout direction, in a two-dimensional (2D) image. The application of a phase-encoding gradient results in some spins precessing faster than others, which converts phase differences into magnetisation depending on the position of the spins within the gradient. This is a result of the linear variation in the magnetic field gradients in the phase encoding direction. In k-space, the acquired data in each excitation acquisition form single lines of the raw matrix during the performance of the phase encoding step.

2.8 Magnetic resonance instrumentation

2.8.1 Main magnet

In the whole scanner, the magnet is the most expensive part. In most modern scanners, superconducting magnets are used, which is unlike the earliest systems where water-cooled resistive magnets were used. Modern scanners, however, can still use permanent magnets. The permanent and resistive magnets of the whole body are limited to a field strength of approximately 0.3T before their weight becomes excessively large. Most clinical MRI systems use superconducting systems. A good example of an MRI's superconductor is a Niobium-Titanium (NbTi) alloy. This alloy is placed in a copper matrix with 50 to 400 km of the wire being required for a modern MR magnet. The NbTi coils are kept mostly at approximately 4.2 kelvin, liquid helium's boiling point. Current in the coils flows indefinitely providing that the temperature levels are kept below the critical temperature to ensure liquid helium can be used as a cooler. The magnetic fields from such magnets are very stable with time, which is essential for an MRI system.

2.8.2 Shimming

Shim coils can be said to be the first unit from the inner bore of the magnet. For a magnet to reach acceptable homogeneity levels, it is necessary to be able to shim the magnet to correct field distortions. Generally, there may be combinations of both active and passive shims. Active shims can be said to be a matrix of electromagnets (coils) inside the cryostat, where the coils carry different currents. On the other hand, passive shims can be explained as arrays of thin metals found in bore trays. They focus mainly on removing Bz inhomogeneities. The shim coils produce small magnetic fields which vary as a function of position (such as dBz/dx, d^2Bz/dx^2). The small fields superimpose on the B_0 field to improve B_0 homogeneity.

2.8.3 Gradients

Gradient coils are required to produce a linear variation in one direction of the field as well as to have high efficiency, low resistance, and low inductance to minimise the current requirements and heat deposition. The gradient coil set

normally has three active shielded gradients, described as x, y, and z. These gradients make the magnetic fields vary with position, providing spatial encoding of the Larmor precessional frequency and allow the system to determine the origin of the MR signal in 3D space. The quality of a gradient system relies on the maximum gradient strength (G_{max}) and the ratio G_{max} over the shortest time needed to switch on the gradient.

2.8.4 RF coils

The RF coil is the piece of equipment closest to the patient. The RF coil is the third component of the MRI scanner. Coils have different designs, although they fall into two main categories, namely, volume coils and surface coils. A surface coil, just as the name implies, rests on the surface of the imaged object. A surface coil, in its simplest form, can be said to be a coil of wire that has a parallel capacitor. The inductance of the coil and resonant circuit are tuned to have the same frequency as the spins to be imaged.
A transmitter RF coil delivers pulsed, radiofrequency radiation at the Larmor precessional frequency and then generates a magnetic field, B1, that is orthogonal to the B_0 field (i.e. in the x-y plane). Transmission coils can be used to receive the MR signal. The MR signal can be received using transmitter coils.

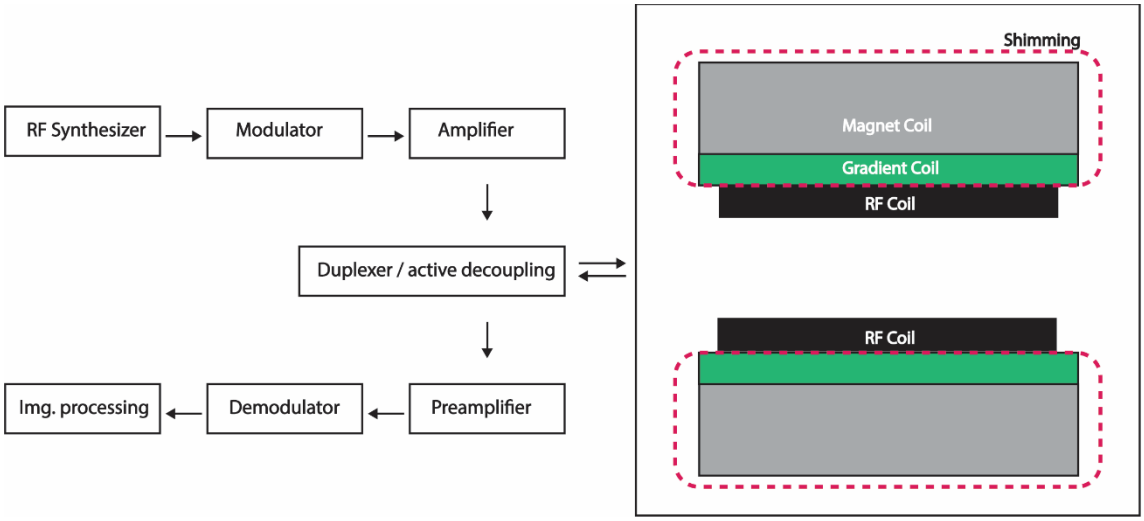

Figure 2-13 MRI Scanner represented by its basic components (Author's own, 2021).

2.8.5 RF transmission / MR signal reception and digitization

2.8.5.1 RF synthesizer

The RF frequency, $\omega_{1,}$ is controlled by the central computer controls. The RF synthesizer generates an oscillating electrical signal with a well-defined frequency, resulting in an RF wave oscillating at a frequency of the spectrometer reference, namely, $\omega_{ref.}$ The following formula is used to calculate the RF synthesizer output:

$$\boldsymbol{S}\,(\boldsymbol{synth}) = \cos\,(\mathrm{wref.\,t} + \mathrm{f(t)}) \qquad 2.31$$

With ϕ(t) being the RF phase and τ being the time coordinate.

2.8.5.2 RF modulator

The RF modulator function is to modulate the RF reference wave into RF pulses with modified amplitude and time according to the sequence design.

2.8.5.3 RF amplifier

The RF amplifier function is to scale up the RF transmission to a high power (from 300-1000 kW) to produce large-amplitude RF pulses for transmission to the RF transmitter coil.

2.8.5.4 Decoupling box

The function of the decoupling box is to switch the receiver coil off resonance during pulse transmission and to move the transmit coil off resonance during signal acquiring.

2.8.5.5 RF preamplifier

The RF receiver coil detects the MR signal, which is usually extremely weak. Signals are amplified immediately to higher power signals through pre-amplifiers to prevent environmental noise from contaminating the signal.

2.8.5.6 RF demodulator

The MRI signals are transformed into audio frequency ranges after passing into receiver units. For this to take place, the signals are mixed with reference frequency through demodulation. It allows the discrimination between frequencies either side of the carrier or central frequency.

2.8.5.7 Image digitization

Analogue signals are changed into digital signals through an analogue-to-digital converter (ADC). The dynamic range of the signal receiver is determined by the number of bits available in the analogue-to-digital converter and the sampling rate determines the bandwidth of the acquisition.

2.9 Functional magnetic resonance imaging (fMRI)

Functional magnetic resonance imaging (fMRI) is a non-invasive imaging technique used to measure and localise specific functions of the brain without the application of radiation and contrast agents. In an fMRI experiment, the brain of the participant or patient is scanned repeatedly using the fast-imaging technique of echo planar imaging (EPI). Participants are required to perform some tasks during the scanning. These tasks consist of activity periods and rest periods. During the activity, the MR signal increases in the brain region that is involved in the task, as the flow of the oxygenated blood increases in that region. The signal processing is then used to reveal these regions.

2.9.1 BOLD Contrast

FMRI, which is usually based on the contrast of BOLD (blood oxygenation level-dependent), has been used as a tool to visualise the human brain's neural activities. The human brain's main source of energy is glucose, with oxygen facilitating the efficient conversion of the glucose into energy. The change in the rate of glucose metabolism in brain regions is associated with an increase in the amount of blood flowing in that brain region. This can be determined using the formula, $C6H12O6 + 6O2 = 6CO2 + 6H2O$. For every glucose molecule needing to be oxidized, six oxygen molecules should be consumed. For an oxygen-to-glucose index (OGI) to be considered ideal, it should have a ratio of 6:1 if the

glucose entering the brain is metabolized oxidatively.

In haemodynamics, the human body is required to respond to physical activities by homeostatically adjusting its blood flow to deliver different nutrients, such as glucose and oxygen, to stressed tissues, thereby allowing them to function. Haemodynamic response (HDR) allows the fast delivery of blood to active neuronal tissues.
Oxyhaemoglobin is a diamagnetic molecule whereas deoxyhaemoglobin is paramagnetic. If a blood vessel has deoxyhaemoglobin, it results in the vessel and the tissue surrounding it having susceptibility differences. This can result in the MR signal being dephased, resulting in a reduction in the T2* value. In a T2* weighted image, if the blood vessels have deoxyhaemoglobin, the image of the voxels darkens. It is possible to observe changes in blood oxygenation as the T2* weighted images record signal changes. However, oxyhaemoglobin cannot produce the same dephasing since it is diamagnetic.

The shape of HDR varies with the stimulus properties and the underlying neuronal activity. Increasing the neuronal activity would, therefore, lead to an increase in the HDR amplitude. Furthermore, increasing the extent of neuronal activity would increase the HDR width. The following figure summarises the physiology of the BOLD response in three stages shown in (Huettel et al., 2004):

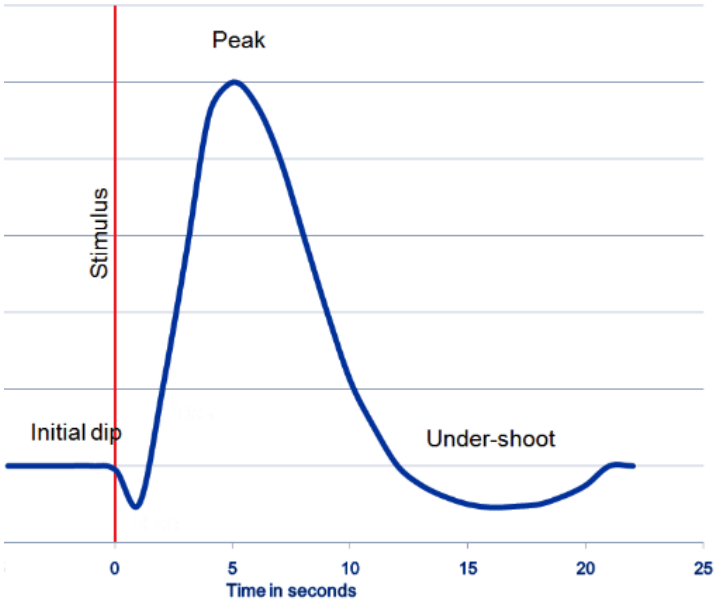

Figure 2-14 Schematic representation of BOLD haemodynamic response (Huettel et al., 2008).

Initial dip: this lasts for 1 to 2 seconds and has been attributed to the temporary increase in the amount deoxygenated haemoglobin and temporary decrease in blood volume resulting from rapid capillary dilatation in the voxel.
Peak: increased neuronal activity occurs due to an increase in metabolic demand, increasing the inflow of oxygenated blood. This means that the amount of oxygen being supplied to an area is more than the amount extracted, resulting in a drop in the concentration of deoxygenated haemoglobin. This results in an increase in the BOLD signal over the baseline approximately two seconds after the onset of the neuronal activity, then rising to a maximum value at approximately five seconds.

Undershoot: the amplitude of the BOLD signal decreases after discontinuation of neuronal activity to below baseline levels, remaining at that level for an extended interval (Huettel et al., 2004).
In summary, the BOLD signal depends on the deoxygenated haemoglobin that is found in the brain region and is largely dependent on the balance between the supplied oxygen and oxygen consumption. An increase in neuronal activity increases the amount of oxygen consumed, leading to more deoxygenated haemoglobin which results in a darker MR image. However, the increased neuronal activities leads to an increase in the T2* signals.

2.9.2 Functional Mapping using the BOLD Effect

After the BOLD effect was discovered, it resulted in attempts by many groups to map the activation of the human brain using the technique. An introduced contrast agent was used in the first MR brain activation study of a human being, with a contrast agent being introduced to map the visual cortex. The BOLD effect was introduced later and was used to map the motor and visual functions of the brain. Articles reviewed on the subject have shown many references to fMRI experiments in the initial stages. For one to successfully use fMRI to study the functioning of the brain, the brain should be imaged repeatedly. Such studies require a suitable stimulus.

Three aspects define the experiment's success, namely, the data analysis method, the stimulus paradigm design and the scanning sequence used. The

magnitude of the static magnetic field is critical to the percentage signal change obtained on activation. The reason being that susceptibility differences have greater signal dephasing at higher magnetic fields. Initially, the fMRI studies were conducted at a strength of on 1.5 Tesla, but now most MRI facilities are conducting fMRI procedures using 3 - 7 Tesla scanners. The BOLD's effect increases as the field strength increases, therefore, higher magnetic fields appear to be desirable when conducting fMRI studies. Most fMRI studies apply T2* weighted imaging because it is sensitive to the BOLD signal [Ogawa et al., 1990]. T2***** relaxation refers to the decay of the transverse magnetisation that is seen with gradient-echo (GRE) sequences, as it is one of the main determinants of image contrast with GRE sequences (Chavhan et al., 2009).

The amount of T2* weighted in the image depends on the TE echo time. This means that the T2* curves will display little difference between the resting state and activated state if the TE is short. However, there will be no signal in either state if the TE is too long.
The echo planar imaging (EPI) technique has been widely adapted in fMRI imaging to shorten encoding duration and increase temporal resolution (Lu et al., 2015). EPI makes it possible to detect the activation response to short stimuli since it allows acquisition of images in 20–100 msec. It also eliminates motion-related artifacts, therefore, imaging of rapidly changing physiologic processes becomes possible (Poustchi-Amin et al., 2001).

The contrast-to-noise ratio of BOLD signals depends on voxel size and slice thickness. The BOLD signal is low when the voxels are small due to the limited signal-to-noise ratio (SNR), but it is also reduced with large voxels due to partial volume effects and physiological noise. Therefore, the optimum voxel size can be chosen that depends on the size of the activated region (Glover and Krueger, 2002).

3 Chapter Three: General Methodology

3.1 Experimental Design

Functional Magnetic Resonance Imaging (fMRI) experiments are conducted with the aim of testing scientific hypotheses. In order to test a certain hypothesis, Huettel *et al.*, (2004) suggests that an experiment must be well designed to use a dependent variable (BOLD signal) using independent variables (stimuli). fMRI experiments should be conducted in a controlled environment, considering the temporal characteristics of the BOLD signals and any possible confounding effects. Experiments require that a stimulus paradigm be designed, to instruct the participant on what to do, and to help them understand when to start and end the activity.

fMRI experiment designs can be split into two distinct groups: block designs and event related designs. Block designs are commonly used to average neural responses across many trials grouped together in one block. This is done in order to increase the Signal-to-Noise Ratio (SNR). In contrast, event related design experiments allow us to study the transient changes in brain activity in reaction to a particular stimulus (Petersen and Dubis, 2012).

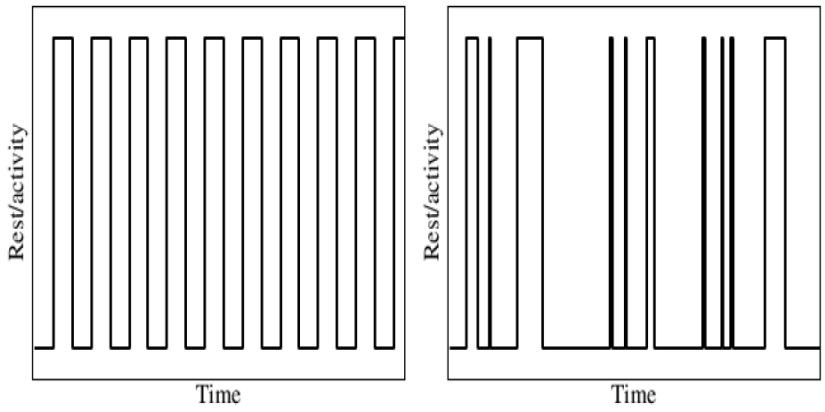

Figure 3-1 Left: The graph on the left illustrates a block stimulus paradigm where the activity and rest periods are usually even, for example 20 seconds long. Right: The graph on the right shows an example of an event related paradigm where the active period consists of blocks or spikes of variable lengths (Eklund, 2010).

The experimental design is convolved with the haemodynamic response function to predict the BOLD response. The BOLD signal illustrated in figure 1.2 below is an impulse response (IR), which contains a peak appearing at between 4-6 seconds, followed by an undershoot from 10-30 seconds. The shape of this response varies between participants, and between different brain regions

within the same participant. In other words, Henson (2007) suggests that IR acts as a low pass filter that passes the low frequencies and reduces the high frequencies.

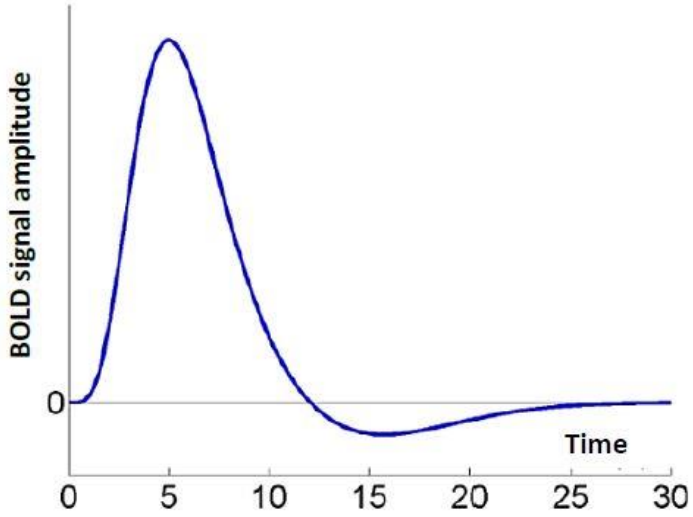

Figure 3-2 An impulse response represented by the BOLD Signal (Henson, 2007).

In a block design, the stimuli of one condition are presented continuously for a period of time before being followed by either a null block or a different block of conditions. For a block of 5 stimuli presented every 4s, alternating with 20s of null block, the expected fMRI response is demonstrated in figure 3.3 below.

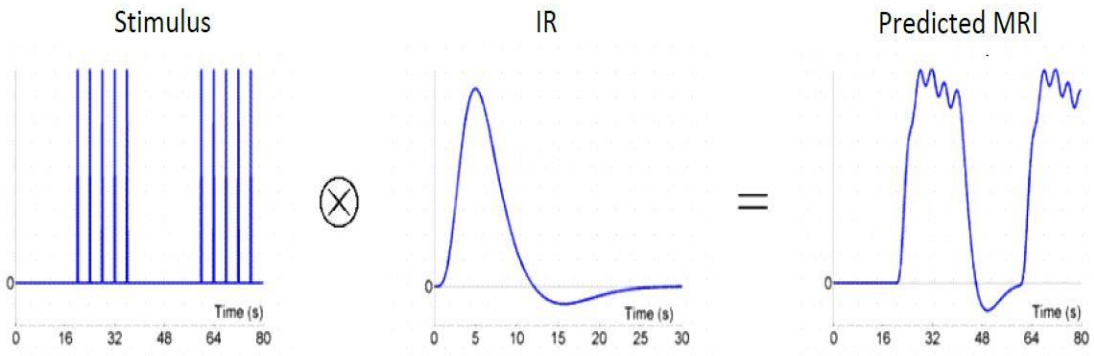

Figure 3-3 Convoluting the IR with a block of 5 stimuli presented every 4 seconds, alternating with 20 seconds of null block (Henson, 2007).

Event related designs show a single stimulus at a time and then compare the fMRI response with a baseline or with other responses. For example, if there are stimuli that are presented every 4s and 16s, the convolution results with the IR are shown in figure 1.3 below. Event related designs are not efficient in this

case because most of the stimuli energy has been eliminated during high pass filtering.

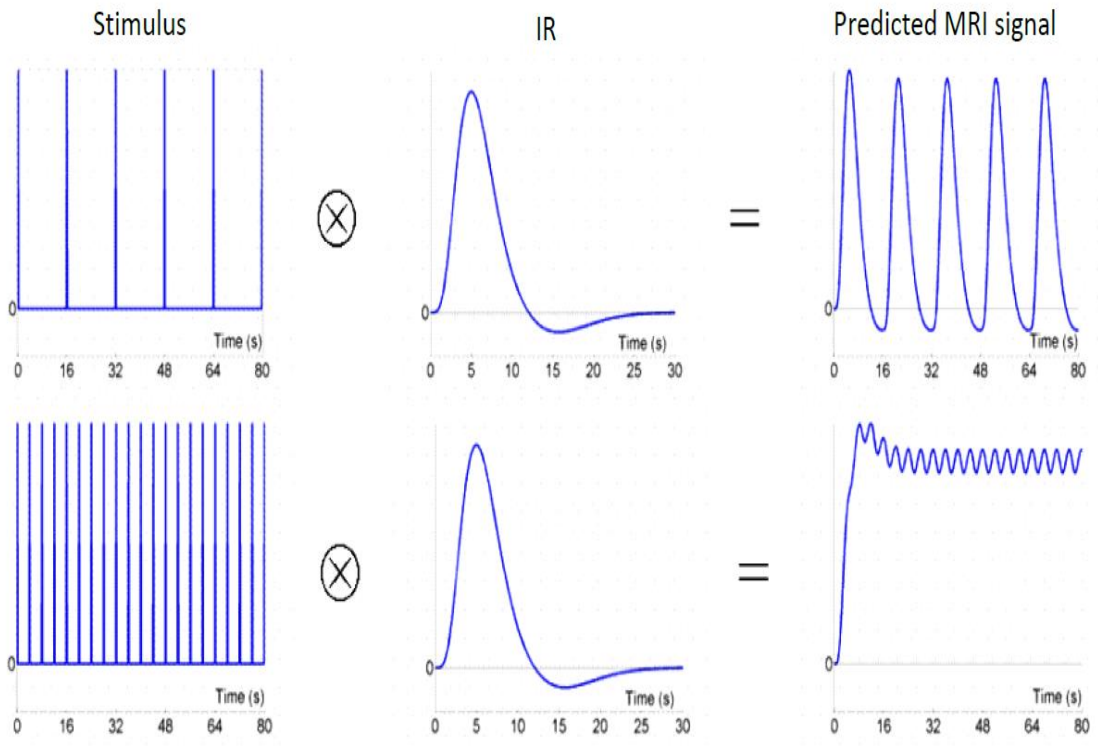

Figure 3-4 Convolving IR with a stimulus presented every 4s (bottom row) or 16s (top row) (Henson, 2007).

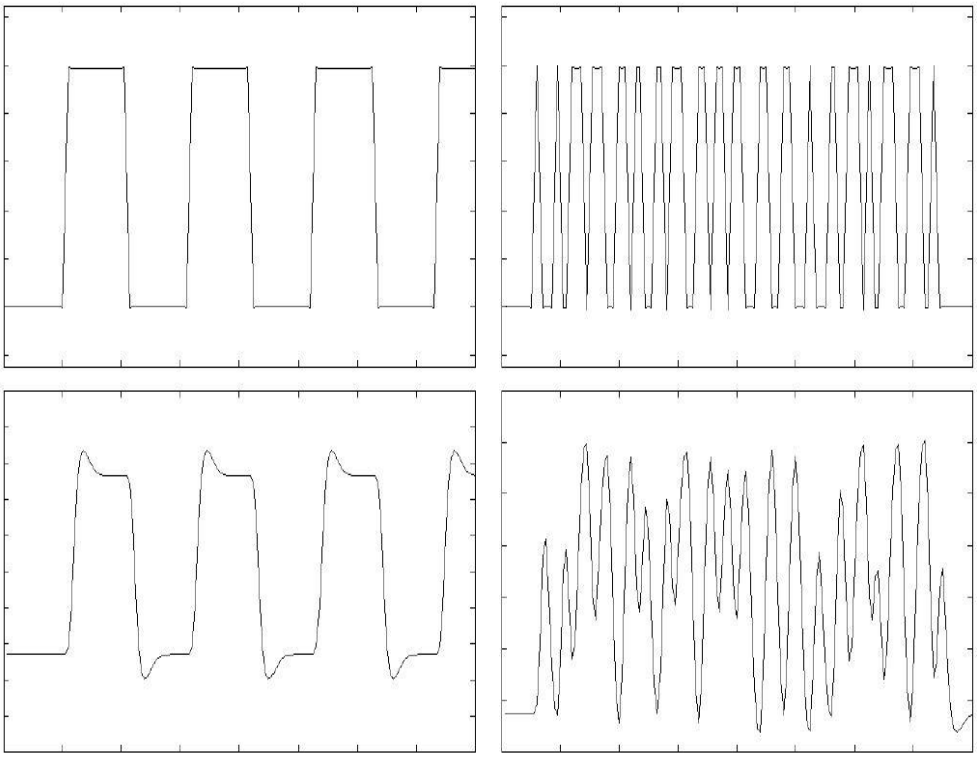

Figure 3-5 Top left: The graph shows a block-based design rest and activity periods, with rests usually being evenly long, for example 20 seconds. Top right: The graph shows an event related design where the activity and rest periods are shorter and frequently randomised. Bottom Left: This illustrates the block-based design convoluted with the haemodynamic response operation. Bottom right: This graph shows the event related design convoluted with the haemodynamic response function (Eklund, 2010).

3.2 Preprocessing of fMRI data

Identifying brain areas that are activated by tasks is the most common objective of fMRI studies. However, the signal that comes directly out of the scanner is poorly matched to this objective. The preprocessing of fMRI data encompasses all the changes needed to prepare the data for task-related analysis. Preprocessing refers to all the steps taken to refine the signal and eliminate sources of noise.

The variability in raw fMRI data is so great that it can simply eliminate the small variations in the BOLD response induced by most cognitive tasks. Some of this variability is inevitable, in the sense that it is a result of uncontrollable or unmeasurable factors, for example system and thermal noise. However, other sources of variability are systematic. For instance, when a participant moves his

or her head, the BOLD response sampled from each spatial position within the scanner suddenly changes in a predictable manner as a result of head motion. Preprocessing aims to remove these systematic non-task-related sources of variability.

3.3 Functional Data Preprocessing

Normally, fMRI data encompasses a three-dimensional matrix (volume) of volumetric pixels (voxels) that is repeatedly measured over time. Every voxel contains a BOLD signal, which varies over time and represents an indirect measurement of neural activity. An fMRI experiment might have a total volume of 70x70x32 voxels which are sampled every 1-3 seconds for 5-10 minutes, depending on the experimental design. Prior to statistical analysis, preprocessing is carried out on the raw data to reduce artefact and noise-related factors of the BOLD signal and prepare it for further analysis.

3.3.1 Slice time correction

FMRI data are gathered in the form of slices selected by radiofrequency excitation pulses, followed by simultaneous data collection throughout the slice. The slices of each volume are selected to have equal spacing in time across one repetition time (TR). This can be done by collecting the data either in descending or ascending slice order (Ashby, 2011). Recently, most fMRI scans have used interleaved slice acquisition, where all the odd-numbered slices are collected first, then the even-numbered slices are collected. This is done to prevent cross-slice excitation between adjacent slices. The downside of this method is that the BOLD signals of contiguous parts of the brain are obtained at non-adjacent time points. Hence, slice acquisition time correction solves this difference by temporally interpolating the voxels' time courses, so that it is assumed they are being collected simultaneously. The most common forms of interpolation are linear, cubic spline and Sinc interpolation (Huettel et al., 2004). The BOLD signal in contiguous slices is separated in time, with implications for the voxels in neighbouring slices. In this situation, slice timing correction enables each voxel's time course to be considered simultaneously (Friston et al. 1995).

3.3.2 Motion Correction

Head motion during scanning can considerably affect imaging data. This head movement arises because it is difficult to entirely constrain a participant's head during a scan that might run for several minutes (Buxton, 2009). Head motion is considered to be one of the main sources of MRI timeseries variations (Lindquist, 2008)
Minor head movement during scanning can negatively affect the imaging data (Huettel et al., 2004). In fact, if the movements are too numerous or too large, a participant may need to be eliminated from the experiment, hence, it is important to apply motion correction to the measured volumes.

Motion correction amends existing minor variations in motion across different functional images by aligning them to a reference image (Buxton, 2009). This is to ensure that each voxel will have similar co-ordinates throughout a time series, and all images will have matching orientations. The first image is selected as the reference image, having discarded the initial images to ensure equilibration in the field. Every subsequent image will be registered and re-sampled to ensure it is in the same orientation as the first image. Six parameters are normally used for a rigid-body transformation of the data into the initial functional image. The three rotation parameters are along the x, y and z axis, and the three translation parameters are: forwards-backward, known as '*yaw*', up-down, known as '*pitch*', and left-right, known as '*roll*'. These values are iteratively calculated using an optimisation algorithm to reduce the summation of the square of the variations between the reference image and each subsequent image (Friston et al., 1995). According to Huettel *et al.,* (2004), the tri-linear sinc interpolation approach is used in order to detect head motion using linear interpolation, and to correct it.

3.3.3 High pass filter and low frequency drift

As a result of physiological noise and scanner imperfections, there are trends and drifts in the fMRI data which should be eliminated before statistical analysis. Voxel time courses can indicate low frequency fluctuations or drifts caused by physiological noise, as well as scanner related fluctuations such as temperature changes. These fluctuations reveal themselves as low frequency 'falling' and

'rising' over the sequence of a task block. Signal drifts considerably reduce the power of statistical analysis, and can be eliminated using 'frequency filters', with the caution that condition-related signal variation may also be mistakenly eradicated. A high pass filter is used separately on each individual voxel, as neighbouring voxels may have different rates of drift.

Correcting drifts is one of the most significant preprocessing steps, and can be eliminated by using a high-pass filter. One way to achieve this is by using linear filters or by using general linear model (GLM) with Fourier basis. The GLM is used to estimate the presence of low frequency in a voxel's time sequence. According to Huettel et al., (2004), the projected time course from a GLM based on the predictors (sines and cosines for low rates) will then be subtracted from the original data, creating a filtered time course.

3.3.4 Spatial Smoothing

This is conducted before data analysis to enhance inter-participant registration, and to minimise noise in the BOLD signal by blurring residual anatomical differences. Spatial smoothing means that data points are averaged with their neighbours. This has the effect of a low pass filter, meaning that high frequencies of the signal are removed from the data, while low frequencies are enhanced. The result is that sharp "edges" of the images are blurred, and spatial correlation within the data is more pronounced (Formisano et al., 2006). In regions that are spatially larger than the imaged spatial resolution, smoothing may lower random variance in individual voxels. This also helps to increase the ratio of signal-to-noise ratio within the region, by providing a weighted average of the local signal (Huettel et al., 2004).

3.3.5 Anatomical Data Preprocessing

Intensity inhomogeneities in anatomical images (T1) can considerably lower the accuracy of segmentation and functional co-registration, as shown in figure 3.6A. A commonly used method for Intensity Inhomogeneities Correction (IIC) is based on a surface fitting approach, where low-order polynomials are used to model low frequency intensity changes called field bias (see figure 3.6B) in a division of selected voxels belonging to the white matter. Field bias is then

eliminated from the data, providing a homogeneous intensity image, as shown in figure 3.6C (Vovk *et al.*, 2007).

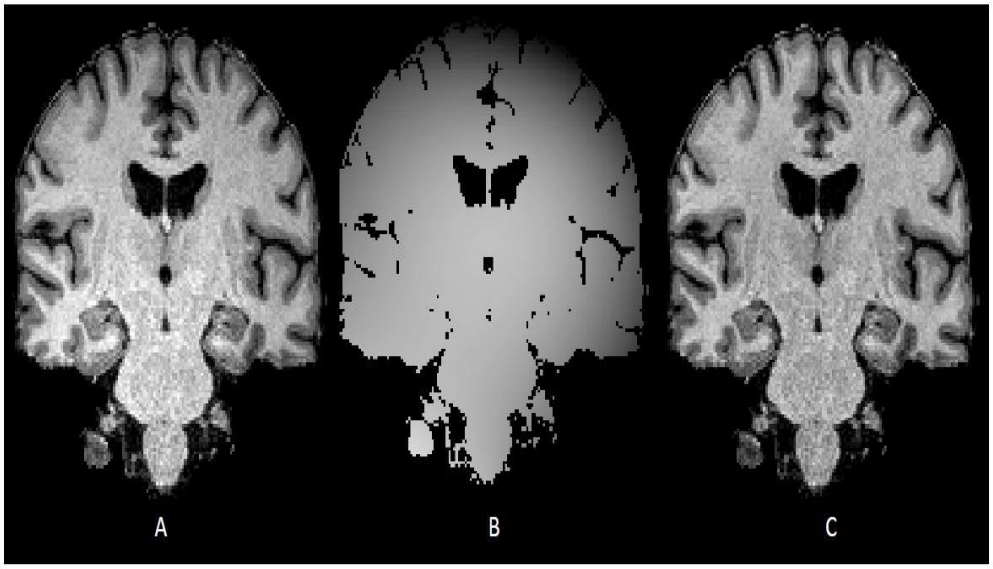

Figure 3-6 Intensity inhomogeneity difference before and after the IIC (Vovk et al., 2007).

3.3.6 Co-registration

Differences between the anatomical and functional images are clear. Normally, the functional images have low resolution, with blurry and unidentified structures, as shown in figure 3.6A. In contrast, the anatomical images appear remarkably detailed, with clear borders of the gyri and sulci and clear outlines between the white and grey matter, as observed in figure 3.6B (Huettal *et al.*, 2008). Co-registration is therefore required to enhance the spatial localisation of the functional images. Images with low resolution are aligned to the high-resolution structural images using a rigid body transformation (3 translations and 3 rotations).

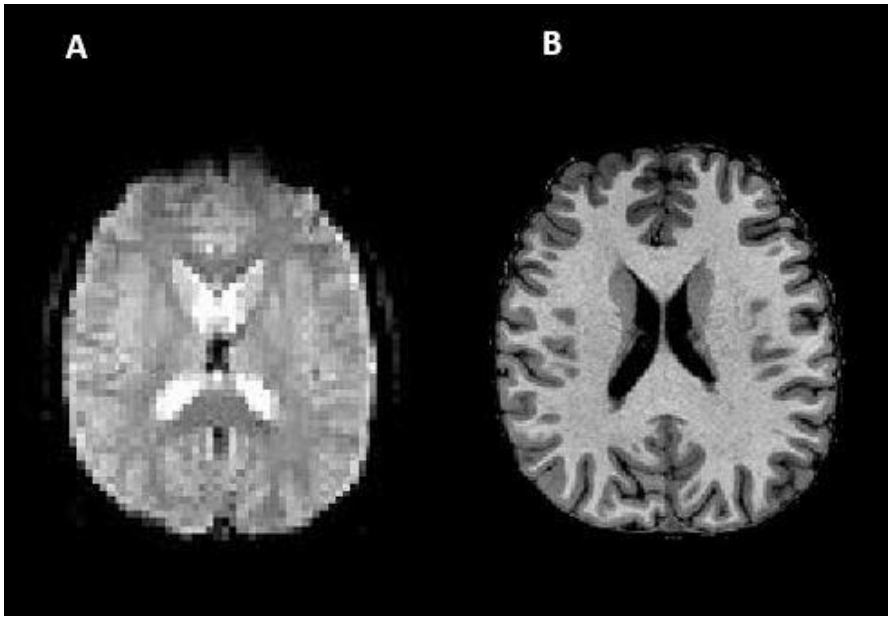

Figure 3-7 Comparison of functional image (A) and anatomical image (B). Structural landmarks that are clear in one structural image might not be distinguishable in functional images of the similar slice. (Author's own, 2021)

3.3.7 Spatial Normalisation

Human brains vary in shape and size. These differences extend to every distinguishable brain region, implying that even basic landmarks such as the calcarine sulcus can have different orientations and positions. Therefore, normalisation is used to warp participants' anatomical images into a standardised anatomical space, utilising templates such as Montreal Neurological Institute prototype (MNI) (Evans et al., 1993) or Talairach space (Talairach and Tournoux, 1988). Normalisation allows for group level statistical analyses to be conducted and compared across studies and subjects at particular anatomical coordinates.

3.4 General Linear Model (GLM)

GLM is one of the most common statistical methods in fMRI univariate analysis. The General Linear Model models the BOLD signal of a certain voxel as a weighted summation of one or more independent variables, along with unresolved noise or variance (Huettel et al., 2004).

GLM is the most widely used multiple regression model in univariate analysis of fMRI data. Its basic foundation is that a prediction informs the design of the model which best explains the experimentally modulated neural activity as it

takes into account the timing and duration of events; the predictions are weighted in order to reduce the impact of error on the subsequent measurements. The data in this case is encompassed in volumetric space, contiguously mapped by tens of thousands of isotropic voxels. Significantly, the model testing is conducted on an individual voxel basis, which forms the basis of the univariate approach. The spatial structure of fMRI data is in fact not used in the model. The voxels are instead treated independently and are arranged along a single dimension per time point for simplicity of calculation. The following expression describes this:

$$Y = X\beta + e \qquad 3.1$$

The *data matrix* is expressed by **Y,** comprised of **V** voxels by **n** points. The *design matrix,* **X,** identifies the linear model to be assessed and is made up of *regressors* **M,** each **n** times points in length. Each of the regressor's weight is integrated into a parameter matrix β**.** Lastly, an error matrix, **e**, is included.
It is important to consider the statistical level of uncertainty in this analysis. The solutions to the general linear model equation (3.1) are the estimated model parameters (also referred to as beta-weights). Under the null hypothesis, dividing these parameters (explained variance) by the residual error (unexplained variance) should follow a statistical distribution commonly known as the F-distribution. Their significance can be assessed as a function of the available degrees of freedom, which depend on the various regressors and time points (Huettel et al., (2004); Jezzard et al (2001)).

Analysis of fMRI data typically includes different participants, sessions and often more than one group. In order to perform generalisation to the population from which those subjects were obtained, two methods are implemented for intersubject analysis; these are known as fixed effect and random analyses. The fixed effect analysis (FFX) assumes that the experimental impact on the BOLD signal is fixed across all participants. The data from all participants are treated as deriving from a single participant, through concatenating all runs of all participants. Therefore, the statistical inference of FFX analysis is restricted to the sample of participants used in the study. A random effect (RFX) is used to measure variability of the effects across subjects, in order to make an inference about the population from which the participants were sampled. In this analysis,

participants are considered to be a representative sample of a population (Huettel et al., 2004).

3.5 Real-time fMRI neurofeedback system

Real-time fMRI neurofeedback is a tool that enables processing of BOLD signals in real time to provide participants with feedback about their brain activation while they are inside the MRI scanner (Mizuguchi et al., 2013). This technique allows participants to have voluntary control over the activity in a selected region of their brain. In this thesis, I used this tool to modulate motor connectivity neurofeedback in healthy participants. This section provides a brief discussion of the technical requirements of a real-time fMRI neurofeedback system.

Generally, most fMRI neurofeedback systems consist of the subject, signal acquisition, signal preprocessing, signal assessment and feedback.

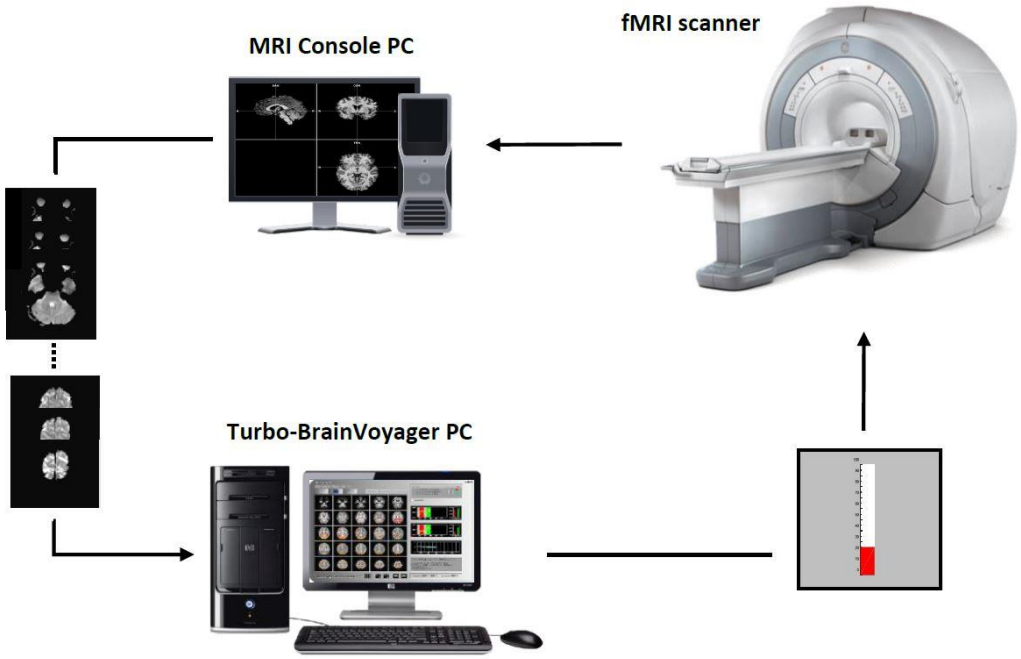

Figure 3-8 A schematic diagram of a real-time fMRI neurofeedback system.
The three major components comprise signal acquisition, pre-processing and assessment, which are performed by two different computers attached through a fast TCP/IP correlation.

3.5.1 Signal acquisition

MRI neurofeedback analyses were performed using a 3 Tesla Siemens Tim Trio MRI scanner at CCNi with a 32-channel head coil. Whole brain images were obtained using an Echo-Planar Imaging (EPI) sequence. Images were sent in real

time, volume by volume to the analysis computer, which hosted Turbo-BrainVoyager (TBV) (Brain Innovation, Maastricht) through a TCP/IP protocol.

3.5.2 Signal pre-processing

TBV was used to pre-process the attained volumes in real time. This comprised 3D motion correction, Co-registration, slice timing correction, de-trending and spatial smoothing using a Gaussian kennel with full width at a half maximum (FWHM) of 8mm, then added to a cumulative GLM.

3.5.3 Signal Analysis

The average time courses of chosen regions of interest (ROIs) were distributed to a custom script running on MATLAB (Natick, MA, Mathworks Inc., USA) to compute the feedback signal.

3.5.4 Single-ROI fMRI neurofeedback paradigm

The feedback signal was computed based on the following equation,

$$\text{bar height(t)} = \left(\frac{ROI_{target\,(t)} - ROIt_{base}}{ROIt_{base}}\right) - \left(\frac{ROI_{reference\,(t)} - ROIr_{base}}{ROIr_{base}}\right) \qquad 3.2$$

where, *ROI target(t)* and ROI reference*(t)* are the average BOLD signals of target and reference ROIs during the neurofeedback block at time *t*. *ROIr_base* and *ROIt_base* are the average BOLD signals of the previous three volumes in the fixation target block and reference ROIs respectively. The reference ROI, used to correct for comprehensive scanning effects, incorporated a rectangular region covering all the voxels in the axial slice away from the target region.

3.5.5 Connectivity neurofeedback paradigm

The significance of the feedback signal was assessed using Pearson correlation, illustrated below,

$$\boldsymbol{bar\ height} = 50 * (Corr + 1) \qquad 3.3$$

$$\mathbf{Corr}(\mathbf{x},\mathbf{y}) = \frac{\sum_{i=1}^{n}(x_i - \overline{x})\,(y_i - \overline{y})}{\sqrt{\sum_{i=1}^{n}(x_i - \overline{x})^2}\sqrt{\sum_{i=1}^{n}(y_i - \overline{y})^2}} \quad 3.4$$

where x, y are time courses of ROI_1 and ROI_2 respectively calculated from a descending window. $\overline{x}$ and $\overline{y}$ are the average BOLD signal within the sliding window of ROI_1 and ROI_2 respectively, and *n* is the time of window (in volumes) as per Liew et al., (2016). **50** is a scale factor.

3.5.6 Feedback Signal

This was represented as a variable thermometer bar proportionate to the percentage variation of the BOLD signal computed using equation 3.4. An LCD projector was used to project the thermometer onto a rear projection screen that could be seen through a mirror fitted on the head coil. The delay associated with the feedback was a result of the image processing and acquisition time. As a result of new innovations in computer technology, the time used in processing one volume did not typically exceed 100ms.
However, the BOLD signal, which is an indirect measure of brain activity, has an intrinsic delay of about 4-6 seconds following the stimulus onset (Hirano et al., 2011; Yeşilyurt et al., 2008). The feedback was updated continuously (continuous feedback) every TR, also intermittent feedback could be presented, as highlighted by Johnson and his colleagues (2012), by presenting the feedback signal at the end of every task block. This method enables averaging of the feedback signal, meaning that participants do not have to consider the BOLD delay. In my research, an intermittent feedback approach was used.

The Matlab code used in this neurofeedback research is derived from previous purpose-built code of the lab and its functions are to estimate the feedback signal and display it to the participants in real-time as a thermometer bar. This code has been used in previous research such as Kanel et al. (2019) and Al-Wasity et al. (2021) to upregulate single brain regions such as Anterior Insula and SMA. However, in my research, the code was modified to calculate the connectivity feedback from two regions of interest (2 ROIs) instead of calculating the feedback from a single ROI. The following flowchart explains the

logic behind the Matlab code used for the real-time fMRI connectivity experiment.

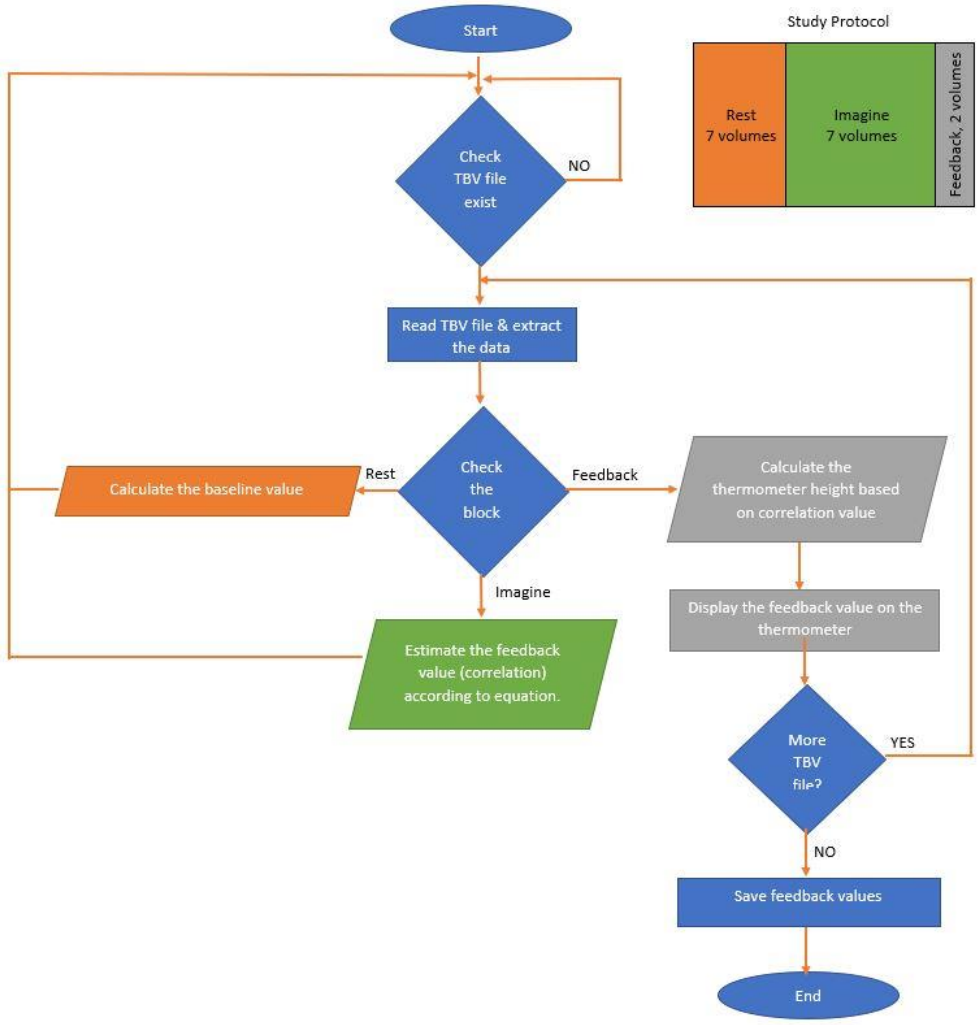

Figure 3-9 Flowchart for MATLAB used in real-time fMRI experiments

In brief, using an intermittent feedback design, the Matlab code reads in signals from two ROIs over a given time duration, calculates their Pearson correlation coefficient (see equation 3.4) and scales this correlation (see equation 3.3) for presentation as a thermometer bar.

3.5.7 FMRI neurofeedback design considerations

The design of the neurofeedback experiment relies on its goals, which often aim to show that self-regulation impacts behavioural functions in healthy participants (Shibata et al., 2011; Sitaram et al., 2012; Scharnowski et al., 2015). Furthermore, it may be used for clinical improvements in patients (DeCharms et al., 2005; Ruiz et al., 2013). Most fMRI neurofeedback research uses the same experimental method, which includes the following:

3.5.8 Definition of the target region

The regions of interest depend on the behavioural changes that are being studied. For instance, experiments that aim to modulate motor reaction time may focus on activity in the motor cortex such as the primary motor cortex (M1) (Chiew et al., 2012), or supplementary motor cortex (Scharnowski et al., 2015) respectively. A few experiments have been conducted for clinical purposes such as modulating pain perception by voluntarily controlling the rostral cingulate cortex (rACC) (DeCharms et al., 2005), and sensorimotor-targeted regions can be used in motor rehabilitation related to stroke and neurological disorders (DeCharms et al., 2005; Subramanian et al., 2011b; Sitaram et al., 2012; Linden and Turner, 2016). The feedback signal might be the average BOLD signal of a particular ROI (Blefari et al., 2015), the activity difference between two ROIs (Neyedi et al., 2017), connectivity between two brain networks (Megumi et al., 2015) or the output of a Multivariate Pattern Analysis (MVPA) classifier (Shibata et al., 2011). ROIs can either be delineated functionally using a functional localiser, as highlighted by Berman et al. (2012) and Aurer et al. (2015b), or anatomically defined using a brain atlas or macroscopic anatomical landmarks (Marins et al., 2015).

3.5.9 Instructions

One unresolved issue of the neurofeedback learning method is the role of instructions. There are two different strategies that may be used for self-regulation: explicit and implicit mental strategies. Explicit strategies involve the participant being asked to use a particular approach for moderating the brain activity, whereas with implicit strategies, the participants are given no information, and they are allowed to look for an applicable and effective mental approach. Explicit guidelines help subjects to learn the task faster, hence reducing the costly scanning time. However, the explicit strategies might contribute to cognitive confounds (Lubianiker et al., 2019). Nevertheless, recent studies have investigated the implementation of implicit approaches in learning self-regulation in a single RT-fMRI session (Shibata et al., 2011; Sepulveda et al., 2016). Other research has illustrated the implementation of an implicit approach together with monetary reward being the optimal strategy for self-regulation,

compared to implicit, explicit or explicit with monetary reward (Sepulveda et al., 2016).

3.5.10 Task Design

Most fMRI neurofeedback experiments use block design for the modulation task. This type of experimental design is effective in increasing SNR and defeating the delay that is inherent to BOLD responses. The block design consists of a task block of 15-50 seconds where subjects are directed to regulate the BOLD signal, followed by a rest block of similar period, during which participants are instructed to relax and/or count numbers (Hanakawa, 2011). Typically, a single run comprises fewer than 10 blocks to avoid fatigue and loss of focus, and is repeated 2-10 times within one experimental session. The number of neurofeedback sessions varies, from a single session (Caria et al., 2007; Blefari et al., 2015) to 12 sessions Auer et al (2015). Scharnowski et al (2012) employed a different number of sessions per subject based on the individuals' ability to attain success in regulation.

3.5.11 Transfer after neurofeedback training

One objective of neurofeedback research is to see the behavioural changes that occur during the neurofeedback learning maintained after the learning has ended i.e., when participants are not seeing the feedback thermometer, or are outside the MRI. In clinical applications, maintaining learned skills after neurofeedback training and applying them in real-life situations is the ultimate objective.

Previous real-time fMRI neurofeedback research has shown that once learned, self-regulation can also be achieved in transfer runs without feedback information, however this only holds true for transfer runs immediately following the neurofeedback training (deCharms et al., 2004, 2005; Hamilton et al., 2011; Lee et al., 2012; Scharnowski et al., 2012; Sitaram et al., 2012; Ruiz et al., 2013). Other research has shown that the lasting neurofeedback training effects can differ between studies.

For example, neurofeedback training using real-time fMRI induced plastic brain changes that lasted for at least 1 day after the training (Shibata et al., 2011; Harmelech et al., 2013). However, Megumi and colleagues (2015) highlight that their neurofeedback training induced changes in resting state fMRI and these changes lasted at least 2 months. However, the resting state effects demonstrated plastic changes, but they were not associated with applying learned self-regulation by the participants. In clinical applications, Scheinost and colleagues (2013) showed that patients with obsessive-compulsive disorder who successfully learnt to increase activity in the orbitofrontal cortex using real-time fMRI had persistent changes in resting state connectivity and a significant reduction in contamination anxiety for several days following the neurofeedback training.

3.5.12 Experimental control conditions

Control groups have been used to prove that feedback knowledge is necessary for the self-regulation of brain activity, compared with the impact of repetitive training using simple instructions. These findings suggest that neurofeedback effects result from modulating specific targeted areas (Lubianiker et al., 2019). There are several different kinds of control conditions that can be used for real-time fMRI research. These conditions include providing feedback from an alternative region (alternative neurofeedback), modulation of the experimental neural target in the opposite direction (inverse neurofeedback), presenting participants with sham feedback recorded from a matched subject from the experimental group (yoked sham) and applying mental strategies with no feedback presentation (mental rehearsal) (Zhao et al., 2013; Hui et al., 2014; DeCharms et al., 2005; Scharnowski et al., 2012; Lubianiker et al., 2019).

In addition, active neurofeedback control conditions may introduce two main classes of confounds: modulations of additional processes that are not engaged in the experimental intervention, and modulations of the general processes of neurofeedback which substantially vary from the experimental group. To remove these confounds, neurofeedback control conditions must involve the same general process modulations as those of the experimental group, without any additional process engagements (Lubianiker et al., 2019). Lubianiker and

colleagues (2019) highlight that the ideal control condition requires a valid neurofeedback intervention that manipulates the same general processes, but without any specific modulations over and above the general neurofeedback processes.

3.5.13 Behavioural changes due to neurofeedback training

The key objective of neurofeedback training is to obtain behavioural changes that result from participants learning to regulate their brain activity. These impacts rely on the function of the targeted ROIs. In this thesis two behavioural tasks were used: a Go/No go task, and a switching task.

The Go/No-go task measures Reaction Time (RT), and reflects the relationships between the inhibitory and activational components of motor control. Measurement of reaction times is an essential concept in cognitive psychology. Reaction time is calculated as the time between the onset of a stimulus or response cue and a participant's response (Fillmore et. al. 2006).

The switching task involves quantifying the changing time associated with switching between sequence operations. Switching deficit has been implied from differences in the probability of performing or maintaining a switch. In this thesis, the switching task was used to measure the time required to execute a switch between sequential operations. This method not only examines the probability of successfully implementing a switch, but also evaluates the ability of the participant to execute the switch itself (Hayes et al., 1998).

3.5.14 Intermittent vs continuous feedback

Several approaches have been used by researchers to present RT-fMRI feedback, such as scrolling a graph display, display of verbal feedback, display of whole-brain activity, visual scale approaches and a combination of feedback displays (Hellrung et al., 2018). The first report of RT-fMRI used intermittent feedback, and showed that a functional map was updated after each rest-task block. Several other RT-fMRI studies have used continuous feedback, in which the visual displays are updated after an acquired volume is attained (Johnson et al., 2012).

There are several advantages to using continuous feedback. An individual has more opportunities to modify their brain activity and thoughts the more they get feedback, which in the process allows them to manipulate the functioning of their brain. When one gets continuous feedback, a person may have greater engagement or interest in participating in the feedback paradigm (Hellrung et al., 2018). The provision of continuous feedback may also have disadvantages. The fMRI measure of BOLD signals is variable, and results from slow haemodynamic responses, which can make it hard for one to link the feedback given with the thoughts that took place earlier (Hellrung et al., 2018). However, this challenge can be addressed by training and instructions about the delay.

Additionally, the fMRI signal's noise is typically dealt with by using traditional approaches of signal averaging and filtering. This means that is important for constant feedback to use these non-traditional approaches to prevent noise from impacting the continuous feedback. It is important to note that the cognitive load and visual attention of evaluating the feedback given can be confounding, which can result in it distracting an individual from undertaking the given tasks (Johnson et al., 2012). This means that when feedback is given frequently, it can have a negative impact, since it can distract one from the given task. Alternatively, the technique of presenting intermittent feedback at the end of a regulating block has been used in few RT-fMRI studies (Posse et al., 2003, Shibata et al., 2011, Yoo and Jolesza, 2002).
The advantages of intermittent feedback are improving learning of self-regulation in comparison to continuous feedback, and also reducing distraction factors (Johnson et al., 2012).

These considerations show that in RT-fMRI neurofeedback procedures, it is better to have intermittent feedback than continuous feedback. If feedback is given at the end of a task, it is not necessary for the participant to know about any haemodynamic delay for averaging and filtering a signal (Johnson et al., 2012; Hellrung et al., 2018).

3.5.15 Challenges of real-time fMRI neurofeedback

Regardless of the great development of real-time fMRI neurofeedback over the last decade, there are still different challenges that remain. These include the

need to optimise the setup, prove its effectiveness in clinical therapy and determine the target populations that will benefit most from neurofeedback.

3.5.16 Online computation and presentation of feedback

Feedback signals typically represent the motion-corrected signal from one area, or the differential feedback from one area in contrast to a control region (Rota et al., 2009). Differential feedback has the benefit of nullifying physiological noises such as pulse artefacts or breathing noises, which have been demonstrated to impact the BOLD signal (Nikolaou et al., 2016). However, non-physiological noise would be amplified by this procedure, hence reducing the SNR. Regarding the presentation of feedback, a typical paradigm is a thermometer-like demonstration. At times the activation may be depicted as colour variation (for instance from yellow=high to blue=low) (Bruhl et al., 2014), or the position and colour may be integrated as feedback information. Another simple visual representation includes a burning fire or a facial expression (Mathiak et al., 2010). The implementation of feedback in a computer game or in a virtual reality setting have also been trialled (Goebel et al., 2004). Some experiments have used a closed-loop approach, where the feedback in turn controls the salience of the stimulus, for instance by opacity or picture size (Sokunbi et al., 2014). Besides visual feedback, one could also receive feedback from tactile, auditory or even olfactory cues. To date, of these only auditory feedback has been studied in a pilot study (Posse et al., 2003).

4 Chapter Four: Functional localisers for motor areas of brain using fMRI

Abstract

With the advance of neuroimaging technology, researchers are able to investigate changes in the response of brain regions under various conditions. One example of such technology is functional MRI (fMRI), a non-invasive brain imaging method. Looking specifically at motor areas, there are many localisers that can identify these brain regions, based and functional properties of these areas. Localising the brain region/s is an integral part of the neurofeedback procedures.

The aim of this research is to develop and test localisers for different motor areas such as M1, SMA, motor cerebellum and motor thalamus using fMRI which are then used target regions of interests (ROIs) for subsequent neurofeedback procedures.

Eighteen right-handed participants were recruited in this research to test the feasibility of five localisers for primary motor cortex (M1), supplementary motor area (SMA), premotor cortex (PMC), motor cerebellum and motor thalamus. The study was conducted between February 2018 - February 2019 using a 3T Siemens Tim Trio MRI scanner at the Centre for Cognitive Neuroimaging (CCNi) at the University of Glasgow.

A motor execution task, namely hand clenching, was tested to functionally activate M1, SMA and motor cerebellum. A combined action observation and motor imagery (AOMI) task was tested to functionally activate PMC. Finally, the use of a mask based on Talairach coordinates was examined in order to identify motor thalamus.

Our results show that all localisers are feasible and successfully activated the desired regions of interest. Motor execution successfully activated M1, SMA and motor cerebellum. The novel localiser based on AOMI successfully activated PMC and finally, the motor thalamus mask that was created offline, based on thalamus atlas, was successfully implemented on each participant.

Motor execution actions, such as hand clenching, can be used to functionally activate many motor areas including M1, SMA, cerebellum. AOMI successfully activated PMC. All five localisers tested in this research were feasible and can be used for applications such as real-time fMRI (rt-fMRI) neurofeedback research to define the regions of interest.

4.1 Introduction

Functional magnetic resonance imaging (fMRI), a non-invasive functional imaging technique, is well known to provide high spatial resolution in imaging brain functions (Ogawa et al.,1992; Kwong et al.,1992). It has been widely used for functional localisation and identification of brain areas in humans (Brett et al., 2002). The use of fMRI scans to first identify brain areas of functional significance and then to examine brain activity more closely in the area is popular in neuroimaging and is known as 'functional localisation'. This approach requires conducting an independent experiment to a localised targeted region for each individual participant. After being defined, it can then be used to analyse a task of interest in a constrained way (Inuggi et al., 2010). The term 'functional localiser' refers to functional experiments such as fMRI and it distinguishes this localisation from anatomic information that are obtained from computed tomography (CT) or structural MRI.

If the localiser is identified accurately, it provides a remarkable increase in sensitivity as it diminishes issues that occur due to covering large volumes of the brain. The anatomical constraints afforded by functional localisers usually take the form of regions of interest (ROI). These are defined operationally by reliable effects in the localiser (Friston et al., 2006).
During an experiment using a functional localiser, after the ROI is determined, analysis is restricted to the responses (activation) within the ROI (i.e., responses averaged over voxels within the ROI). As a result, there is one statistical inference and therefore no need to adjust the p-value for multiple comparisons and responses elsewhere in the brain are ignored (Duncan et al., 2009).

The implementation of ROI designs in brain imaging began in the late 1980s as researchers reported their results using ROIs defined using structural anatomy, perfusion, or receptor binding. These ROIs were based on defining characteristics of the underlying tissue and did not reflect any functional role of these areas. These ROI were considered useful as they showed the distribution of the induced activation. However, the problem was that ROIs did not provide information about where region-specific responses are expressed (Friston et al., 2006).

Usually, functional localiser scanning is conducting separately from the main experiment. Thus, localisers introduce some inevitable confounds of both time and order. The localiser will be inappropriate if the activation pattern later changes due to time effects, for example effects such as learning could reduce activation in some areas and increase it in other areas. Furthermore, the localiser and main experiments usually have different aspects such as scanning parameters (e.g. number of scans), design (e.g., blocked vs. event-related), task, or stimuli used. This implies that the precision with which localising and experimental effects are estimated can differ profoundly (Friston et al., 2006; Duncan et al., 2009).

The localisation of motor areas has been the object of several previous research studies (Inuggi et al., 2010). Many tools, such as EEG and fMRI have been used to localise motor regions such as M1 on the precentral gyrus (PcG). There are several fMRI-based techniques with different accuracy that have been conducted to localise motor areas in the literature, such as voluntary movement stimulation to activate regions of interest (ROI) (He and Liu, 2008; Wagner et al., 2000) and operative electrical stimulation (Yousry et al., 1995). In this research, the aim was to develop and test localisers for different motor areas such as M1, SMA, motor cerebellum and motor thalamus using fMRI.

4.2 Methods

Eighteen participants were recruited for this research. They were separately recruited into three groups to test the localiser for different motor regions in the brain. All participants were right-handed, and their ages and genders are listed in Table 3 below.

Table 3: Demographic characteristics for participants in groups 1,2 and 3

	Group 1	Group 2	Group 3
Number of participants	12	3	3
Age (mean in years)	28.75	27.33	28.33
Gender	7 M , 5 F	2 M , 1 F	3 M

This research was conducted between February 2018 - February 2019 using a 3T Siemens Tim Trio MRI scanner at the Centre for Cognitive Neuroimaging (CCNi) at the University of Glasgow.
The research has been approved by the ethics committees of the College of Science and Engineering at the University of Glasgow. Consent was obtained from each participant for the experiment.

Imaging parameters and fMRI neurofeedback platform

This experiment was performed in the Centre for Cognitive Neuroimaging (CCNi) at the University of Glasgow. The MRI unit is a 3T Siemens Tim Trio MRI scanner. A32-channel head coil was used and T1 weighted image structural images were acquired using the following parameters: TR=2000ms, TE=2.52ms, 192 sagittal slices, 1 mm^3 isotropic voxels and image resolution 256×256.
fMRI data was collected using a T2*-weighted gradient echo (EPI) pulse sequence (TR=2000ms, TE=30ms, whole brain coverage with 32 axial slices, 0.3 mm gap and 3 mm^3 isotropic voxels).

4.2.1 First group: localisation of motor regions

Twelve right-handed healthy participants were recruited to test the localiser for motor regions. This localiser aims to identify M1, SMA and motor cerebellum. Each region was localised based on anatomical landmark and functional localisation (Hou et al., 2016). The anatomical landmark for M1 is a sigmoidal hook or omega sign, which is a term used to denote the appearance of the hand motor area (hand knob). The anatomical landmark for SMA is defined as the area of the medial frontal cortex in the superior frontal gyrus lying dorsal to the cingulate sulcus, rostral to the primary motor cortex, and caudal to the vertical commissure anterior line (Kim et al., 2010). The cerebellum is located within the posterior cranial fossa of the skull, caudal to the cerebrum and tentorium cerebelli, and dorsal to the brainstem. In the anterior region transverse fissures extend uninterruptedly to the lateral margin of the cerebellum. This anterior region can be subdivided into the anterior lobe and the lobules simplex by the deep primary fissure (Voogd and Glickstein, 1998). A high-resolution anatomical

scan (T1 weighted image) and a functional localiser run was conducted on each participant

The localiser run was composed of 7 fixation blocks (16s) interleaved by 6 blocks of bimanual hand clenching (30s).

During the functional scanning of the localiser, participants were instructed to either to count letters or numbers if “REST” appeared on the screen. This was done to control the baseline activity (Hanakawa, 2011; Berman et al., 2012). Participants were instructed to clench their fists if “MOVE” appeared on the screen.

The functional data was pre-processed and analysed online with an accumulative General Linear Model (GLM) embedded in the Turbo-BrainVoyager and offline using BrainVoyager. The ROIs were defined in each participant in the native space.

4.2.2 Second group: localisation of premotor cortex (PMC)

Three right-handed healthy participants were recruited in order to test the localiser for PMC.

A high-resolution anatomical scan (T1 weighted image) and a functional localiser run was conducted on each participant

The localiser run took approximately five minutes and was composed of seven fixation blocks (16s) interleaved by six blocks of action observation and motor imagery (AOMI) (30s).

During the functional scanning of the localiser, participants were instructed to either count letters or numbers if “REST” appeared on the screen and to watch videos of hand actions and imagine these actions at the same time if “IMAGINE” appeared on the screen. The ‘Rest’ block lasted for sixteen seconds then an ‘Imagine’ block appeared for thirty seconds.

The functional data was pre-processed and analysed online with an accumulative General Linear Model (GLM) embedded in the Turbo-BrainVoyager and offline using BrainVoyager. The ROIs were defined in each participant in the native space.

4.2.3 Group third: localisation of motor thalamus

Three right-handed healthy participants were recruited in this experiment in order to test the localiser for motor thalamus. A high-resolution anatomical scan (T1 weighted image) and a functional localiser run was conducted on each participant.
Since a reliable functional localiser for motor thalamus could not be defined, the thalamus was defined by using a thalamus mask obtained from a thalamus atlas. The thalamus mask was created offline using the Talairach atlas (Talairach et al., 1988; Lancaster et al., 2000). This mask covered motor parts of the thalamus, including ventral lateral nucleus and ventral anterior nucleus (Fang et al., 2006). This mask was used in the experimental group when M1-thalmus connectivity was targeted. The mask was implemented individually to each participant from the anatomical scan. After implementing the mask, it was visually checked to see if it accurately applied to localise the thalamus.

4.3 Results

4.3.1 Localisation of primary motor cortex (M1):

All subjects showed activations in several areas, which are part of the "classical" sensorimotor network, including the primary motor cortex (M1).
M1 is anatomically identified visually by a sigmoidal hook or omega sign, which is a term used to denote the appearance of the hand motor area (hand knob) (Yousry et al., 1997). Figure 4.1 shows the activation in M1 to hand clenching movement in all participants.

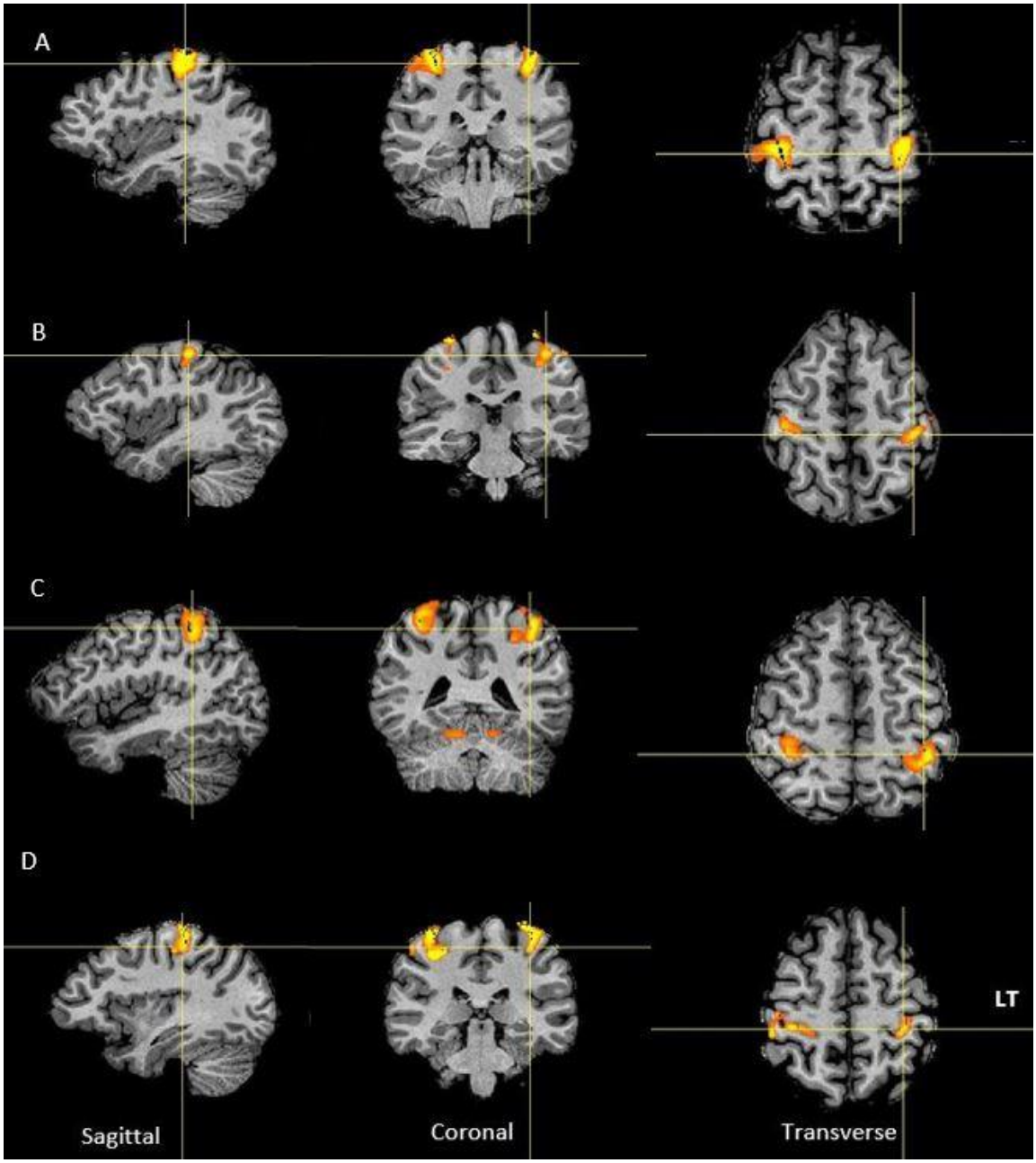

Figure 4-1 Activation in bilateral M1 as a result of hand clenching. A, B, C and D show sagittal, coronal and transverse images of four participants.

4.3.2 Localisation of supplementary motor area (SMA):

Hand clenching also introduced activations in bilateral SMA in all participants as seen in Figure 4.2.

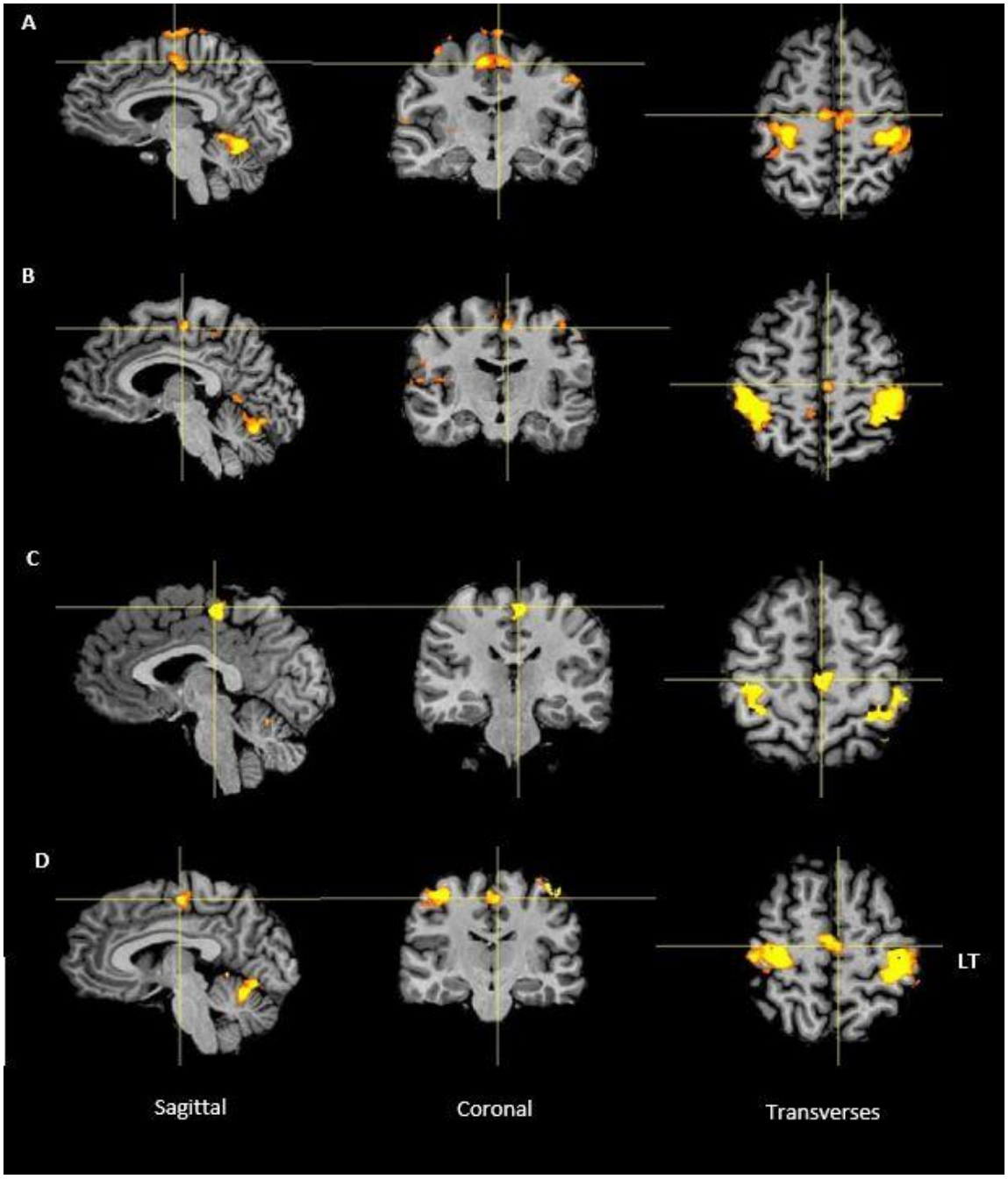

Figure 4-2 Activation in bilateral SMA as a result of hand clenching. Panels A, B, C and D show SMA activations in sagittal, coronal and transverse images of four participants.

4.3.3 Localisation of motor cerebellum

All participants showed activations in the cerebellum as a result of hand clenching as seen below in Figure 4.3. These activations include dentate nucleus, lobules IV and V.

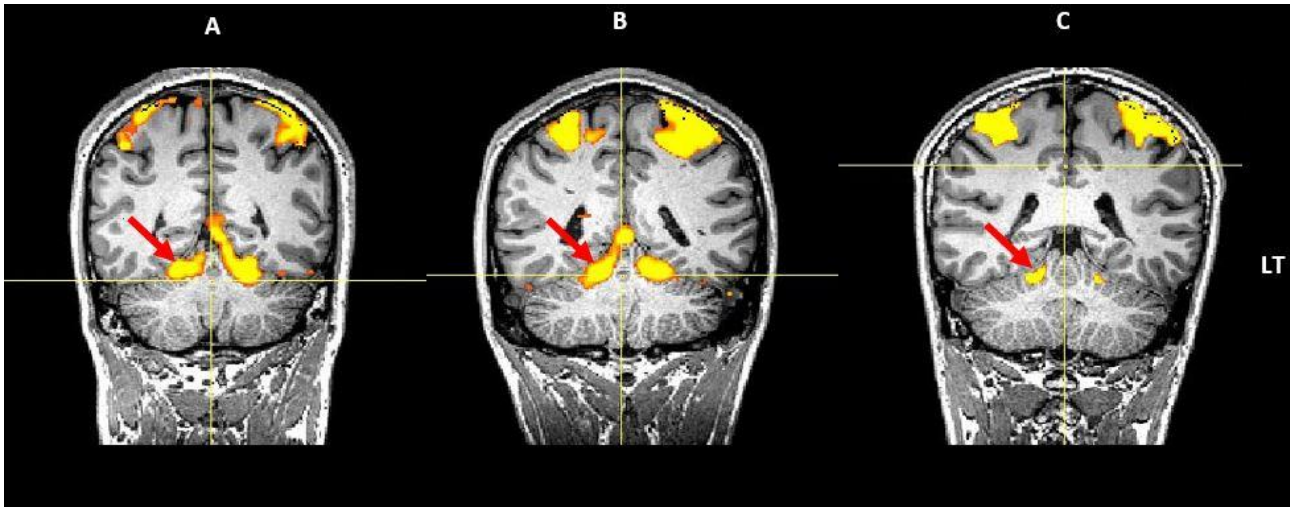

Figure 4-3 . Activation in bilateral cerebellum as a result of hand clenching. Panels A, B, C and D show cerebellar activation in coronal images of three participants. Red arrows indicate activation in right anterior motor cerebellum.

4.3.4 Localisation of premotor cortex (PMC)

All participants showed activations in left PMC as result of AOMI as seen in Figure 4.4. An additional activation can be seen at motor regions such as bilateral M1. Additional activation can be seen at areas thought to be involved in motor imagery and action observation, such as SMA and visual cortex.

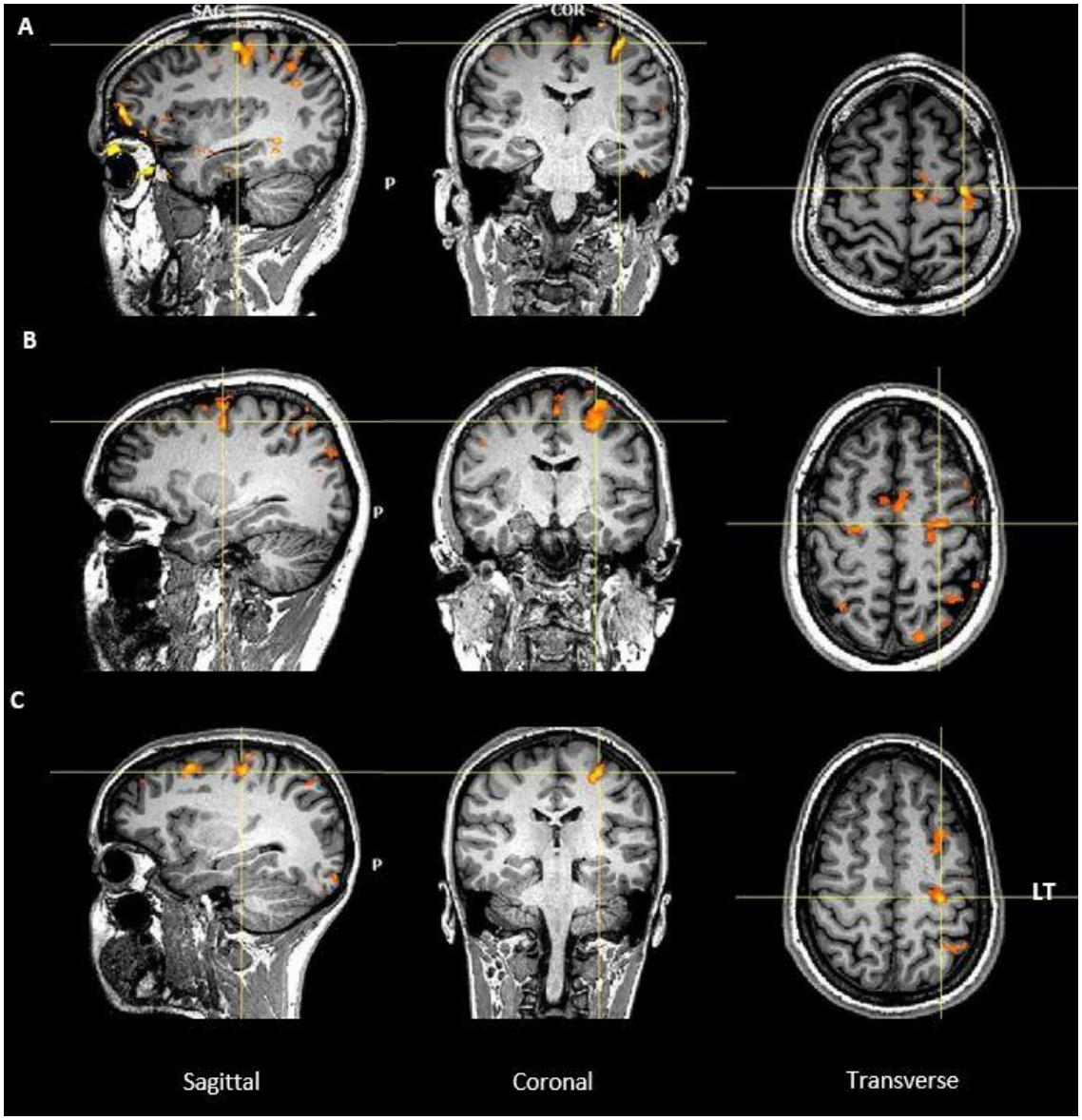

Figure 4-4 Activation in bilateral left as a result of motor imagery and action observation. Panels A, B and C show sagittal, coronal and transverse images of first, second and third participants respectively.

4.3.5 Localisation of motor thalamus

Figure 4.5 shows thalamus mask applied on anatomical images of the participants. The anatomical image (T1 weighted image) was converted to Talairach space using BrainVoyager before implementing the thalamus mask because this mask was created based on the Talairach atlas.

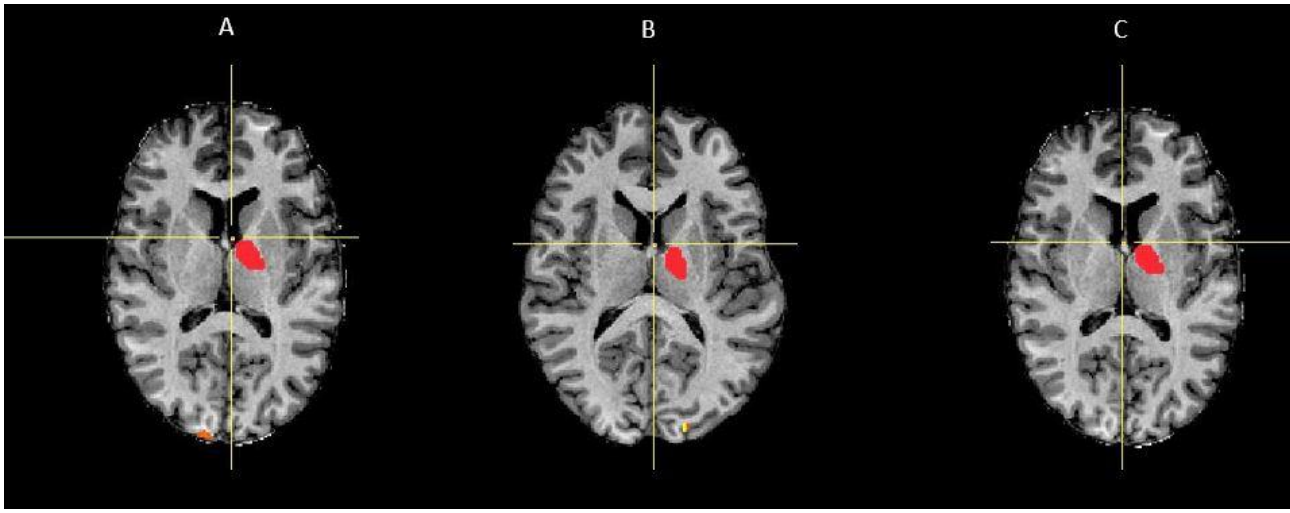

Figure 4-5 Shows thalamus mask (red cluster) which successfully implemented on the anatomical image.

4.4 Discussion

The present study investigated aspects of localising motor areas. First, motor execution of bimanual hand actions, namely hand clenching, was used to activate and localise M1, SMA and cerebellum. This technique has been widely used in the field of real-time fMRI. For M1 localisation, these results are with line with many rt fMRI studies that targeted M1 for modulation using hand actions, such as clenching (Chiew et al., 2012) fingers tapping (Berman et al., 2012; Mehler et al., 2018) and active isometric pinching (Blfari et al., 2015). These studies successfully localised M1 using localiser runs based on motor execution of actions. M1 was anatomically located by identifying the precentral gyrus and hand knob region for each participant (Yousry et al., 1997) then M1 was functionally localised for each participant by analysing BOLD signals in real time during motor execution tasks, such as clenching and a square ROI was centred on the voxel with the maximal signal change during clenching relative to the resting blocks. Then each ROI was overlaid onto the individual's anatomical image (T1) for all participants (Berman et al., 2012).

The SMA localiser in this study successfully activated the SMA as a result of motor execution stimuli (hand clenching). Our results are in line with Sepulveda et al., 2016 who used motor execution to localise SMA and also in line with Scharnowski et al. (2015), Mehler et al. (2018) and Al-Wasity et al. (2021) who

used finger tapping as a motor action to activate and localise SMA.

In addition, a motor execution task, namely hand clenching, was used to activate the motor cerebellum. Motor cerebellum has typically been localised in previous fMRI studies by using a cerebellum mask based on an atlas (Stoodley et al., 2012). However, previous fMRI research has also found that motor execution activates motor cerebellum (Mostofsky et al., 2009) especially lobules IV and V (Stoodly et al., 2009) and dentate nucleus (Dimitrova et al., 2006). Therefore, we hypothesise that a motor execution task can be used to activate motor cerebellum to provide a functional localiser. Our results supported this hypothesis as an activation was found at the cerebellum as result of hand clenching in all participants. Therefore, this localiser is suitable for motor cerebellum and can be used for rt fMRI neurofeedback research targeting cerebellum modulation.

In the second group, the aim was to functionally localise PMC using a novel technique which used action observation and motor imagery together (AOMI) stimuli. According to our knowledge, this type of localiser has not been used before to localise PMC. Previous rt-fMRI research targeted PMC used techniques to localise PMC, such as a PMC mask based on an atlas (Pereira et al., 2019), motor execution (Marins et al., 2015), anatomy reference or action observation (Sitaram et al., 2012). The bilateral ventral premotor cortex and dorsal premotor cortex have all been consistently implicated in motor imagery and action observation (Hardwick et al., 2017). Therefore, the idea that it can be identified using AOMI stimuli (Friesen et al.,2017) was supported by our results. In conclusion, AOMI can be added to techniques or tasks that activate PMC and therefore it can be used as a localiser for fMRI studies.

In the third group, a thalamus mask was used to localise the thalamus. Since the thalamus is a deep subcortical structure, it is difficult to localise it functionally. As a result, a mask based on a thalamus atlas to identify the thalamus has been previously used in fMRI studies (Kang et al., 2018). However, Liew and colleagues (2016) used a functional localiser to identify the thalamus in their research, but they did not provide any information about the technique or task used. Here, the thalamus mask was created offline using the Talairach atlas

(Talairach et al., 1988; Lancaster et al., 2000). This mask covered motor parts of the thalamus including ventral lateral nucleus and ventral anterior nucleus (Fang et al., 2006). This mask was successfully fitted individually onto each participant. Therefore, it can be used to define motor thalamus during rt-fMRI NF research.

4.5 Conclusion

Motor execution, namely hand clenching, can be used to functionally activate many motor areas. These results showed that this technique successfully activated M1, SMA and motor cerebellum functionally. Furthermore, the novel technique of an AOMI task was successfully used to functionally activate PMC. Finally, a mask of motor thalamus was created and tested on participants. The results showed that this motor thalamus mask was accurately fitted onto each participant's anatomical image. It was concluded that all localisers used in our research appeared feasible and can be used to define the regions of interest for rt-fMRI research.

5 Chapter Five: Modulation of functional connectivity between M1 and thalamus during motor imagery using real-time fMRI connectivity neurofeedback

Abstract

Real-time fMRI-based neurofeedback (rt-fMRI-NF) is a technique in which participants are able to voluntarily modulate the brain activity of different regions of the brain by undertaking a mental task, namely, motor imagery. This includes providing feedback about the connectivity between brain regions. Enhancing connectivity between cortical and subcortical regions holds promise for improving motor functions. In the present study, we aimed to investigate the effect of functional connectivity during motor imagery using rt-fMRI neurofeedback. The primary motor area (M1)-thalamus connectivity was targeted as these regions play a role in performing motor actions.

Twenty healthy participants were recruited for this research. Each participant carried out the Vividness of Movement Imagery Questionnaire-2 (VMIQ-2), switching task and Go/No Go task. They were then assigned randomly into one of two groups (10 participants each). Participants in the first group (experimental group) received feedback from M1-thalamus connectivity while the participants in the second group (control group) received feedback from M1-Supplementary motor region (SMA) connectivity.

The results showed a significant increase in connectivity neurofeedback in the experimental group (M1-thalamus) while there was no such enhancement in the connectivity found in the control group (M1-SMA). The behavioural tasks showed a significant reduction in the switching time in the experimental group only, while the Go/No Go task showed a significant reduction in the reaction time in the control group only.

In conclusion, rt-fMRI-NF is a useful tool to modulate functional connectivity between M1 and the thalamus using motor imagery and it facilitates the learning of new mental strategies by participants to upregulate M1-thalamus connectivity. The switching task is a recommended behavioural task for the M1-thalamus and the Go/No Go task is a recommended behavioural task for the M1-SMA. Upregulating the connectivity neurofeedback using rt-fMRI could be used to enhance the motor performance of patients with motor impairments such as those resulting from stroke.

5.1 Introduction

Functional magnetic resonance imaging (fMRI) is a popular tool for mapping human brain functions. It measures the changes in blood oxygen level dependent (BOLD) which allows the active areas in the brain to be defined. Investigation of brain connectivity has attracted the attention of researchers who want to understand how brain areas communicate, coordinate and interact with each other to perform cognitive and psychological functions (Heuvel et al., 2010). Many studies using fMRI have explored brain connectivity in the past three decades. These studies provided information about the complex integrative networks that link brain areas functionally and structurally (Heuvel et al., 2010). Recent advances in MRI technology allow one to analyse the data in real time and, thus, provide feedback while the participant is still inside the scanner. This technique is called real-time fMRI-based neurofeedback.

Real-time fMRI neurofeedback systems have also been developed to enable participants to voluntarily regulate brain activation over multiple areas. Such systems measure the neural activity of participants and represent this activity to them as visual or auditory signals in real time to enable self-regulation of neural activity (Mizuguchi *et al.*, 2013).

Currently, there are three types of neurofeedback training based on the differences in feedback information. The first, univariate neurofeedback, uses the average BOLD signal within a specific brain region of interest to increase or decrease the average activity in that region (deCharms et al., 2005). Secondly, decoded neurofeedback is the process of inducing knowledge in a subject by increasing patterns of neural activation in predetermined regions in the brain, such as the motor and visual cortex. This is attained by measuring neural activity in these areas using fMRI, comparing this to the ideal pattern of neural activation in these areas (for the intended purpose) and providing feedback to subjects on how close their current pattern of neural activity is to the ideal pattern (Shibata et al., 2011, 2016; deBettencourt et al., 2015; Amano et al., 2016). Thirdly, connectivity neurofeedback uses the functional connectivity between two brain areas to modulate connectivity (Koush et al., 2013; Megumi et al., 2015; Liew et al., 2016).

The influence of connectivity neurofeedback on brain regions provides a physiological measure for rt-fMRI-NF training (Weiskopf et al., 2007; Caria et al., 2012) and many studies have found that rt-fMRI-NF is a useful technique to modulate the connectivity among brain areas (Marins et al., 2015; Xie et al., 2015).

In the literature, there are many studies which have focused on modulating motor cortex activity using rt-fMRI-NF. These studies aimed either to upregulate or downregulate many motor areas such as M1 (Yoo et al., 2008; Berman et al., 2012; Chiew et al., 2012; Blefari et al., 2015; Neyedli et al., 2017), SMA (Hampson et al., 2011; Scharnowski et al., 2015; Sepulveda et al., 2016; Al-Wasity et al., 2021) and PMC (Sitaram et al., 2012; Zhao et al., 2013; Hui et al., 2014; Marins et al., 2015). Although most rt-fMRI-NF studies focussed on training participants to modulate single areas, a few recent studies have established the ability to modulate functional integration between interconnected brain areas (Desseilles et al., 2011; Seghier et al., 2010). Although such integration between different brain areas has proven more difficult to assess, recent developments in data analysis techniques make it possible to study connectivity using resting-state fMRI or rt-fMRI-NF to modulate the connectivity neurofeedback between different brain areas in real time (Friston et al., 2003; Koush et al., 2013; Megumi et al., 2015; Liew et al., 2016; Yamashita et al., 2017).

Several studies have reported that cognitive functions are associated with specific brain networks and that any abnormality in these networks leads to mental disorders. (Broyd et al., 2009; Stam, 2014; Fornito et al., 2015; He et al., 2007; Barch et al., 2013; Thompson et al., 2013; Liu et al., 2015). This indicates that the use of connectivity neurofeedback is a promising approach to therapeutic intervention for psychiatric and neural disorders and to improve cognitive functions. For example, stroke commonly causes damage to the motor system including areas such as M1, SMA and PMC which play an important role in the planning and execution of movement. Although stroke commonly occurs in elderly patients, it may occur at any age. Approximately 25% of strokes occur before the age of 65. Because motor deficits following stroke are common and have a significant impact on life quality, motor rehabilitation strategies are

needed to promote brain recovery and motor functions. Neurofeedback (NF) is a technique that has shown therapeutic success in many applications such as stroke rehabilitation (Nan et al., 2019). Research has shown NF to be effective and potentially useful in many disorders such as epilepsy and attention deficit disorder, as well as the recovery of motor function following stroke (Wang et al., 2018). This implies that connectivity neurofeedback is a helpful approach for stroke recovery because it enhances the activation in the affected motor areas, resulting in the improvement of motor functions (Liew et al., 2016).

The mechanisms of stroke recovery using fMRI neurofeedback are still under investigation (Soekadar et al., 2014). Buch and colleagues (2012) showed that simultaneous activation of inputs and outputs to the motor cortical areas trigger Hebbian plasticity, which strengthens cortical-subcortical connectivity. Hebbian plasticity is a form of synaptic plasticity which is induced by, and further amplifies, correlations in neuronal activity (Zenke and Gerstner, 2017).
Motor imagery (MI) is a cognitive process in which people simulate actions or movements internally without any apparent movement (Blefari et al., 2015). MI aims to enhance motor skills in healthy and clinical populations (Alkadhi et al., 2004) and it is usually undertaken in motor learning skills (Mizuguchi et al., 2013). MI could be beneficial in athletics, skill acquisition and rehabilitation (Ietswaart et al., 2011).

Improvements in cortical-subcortical connectivity are associated with better motor recovery after stroke (Jang et al., 2012). Previously, electro- or magnetoencephalography (EEG/MEG) was used to regulate cortical areas, however, they are very limited because they cannot be used to regulate deeper brain areas or sub-cortical brain regions. Rt-fMRI-NF overcomes this limitation by providing full brain coverage, allowing feedback from both cortical and subcortical regions (Weiskopf et al., 2003).

Using rt-fMRI-NF connectivity is a promising technique to enhance the connectivity between motor areas in patients with stroke. Carter and colleagues (2012) demonstrated that the reduction in functional connectivity in stroke patients between bilateral M1 areas may be related to motor dysfunction of the upper limb.

The present study aimed to determine whether healthy participants can enhance the connectivity neurofeedback between M1 and thalamus using rt-fMRI-NF. It also aimed to investigate whether successful fMRI-NF of M1-thalamus connectivity will translate to changes in behavioural measures. The connectivity between M1 and the thalamus was targeted due to its importance in motor functions as cortical to subcortical areas are important in stroke recovery (Megumi et al., 2015; Liew et al., 2016, Yamashita et al., 2017). The motor thalamus encompasses thalamic nuclei that are strategically located between motor areas of the cerebral cortex and two subcortical networks, namely, the basal ganglia (BG) and the cerebellum. The motor thalamus plays a role in the complex cognitive and proprioceptive control of movement, respectively (Middleton and Strick, 2000). It also plays a role in maintaining posture, general movements and motor learning (Bosch-Bouju et al., 2013). The ventral lateral nucleus of the thalamus (VL) serves as a central integrative centre for motor control, receiving inputs from the cerebellum, striatum and cortex and projects to the primary motor cortex (Bosch-Bouju et al., 2013).

M1 and its association with other motor regions such as PMC and SMA and subcortical regions such as the thalamus play an important role in the planning and execution of movements. Previous studies have shown that M1 plays a supportive role in motor function recovery after stroke. Other studies have demonstrated that enhanced activity in the contralesional M1 may impair the recovery of motor function (Stinear et al., 2015). The connectivity between these areas has been investigated by Liew and colleagues (2016) and the results showed that three patients had positive results, as they successfully manged to enhance the connectivity between M1 and thalamus. However, their study was limited by sample size and the condition of the participants.

If connectivity neurofeedback between M1-thalamus is modulated by motor imagery based rt-fMRI-NF, then, significant changes in behavioural measures would be recorded either in the Go/No Go task or the switching task or in both tasks as a result of connectivity neurofeedback training. Participants in the current study underwent training with intermittent feedback of the temporal correlation (functional connectivity), based on Pearson's correlation, between

BOLD signals in M1 and the thalamus after each trial (Megumi et al., 2015; Liew et al., 2016, Yamashita et al., 2017).

5.2 Methods

5.2.1 Participants

Twenty participants with normal or corrected-to-normal vision were recruited for this study. Participants verified that their visual acuity was sufficient to resolve images and text presented on the screen without any correction or they were provided with sufficient correction. All participants were right-handed, as determined by the Edinburgh Handedness Inventory (Oldfield, 1971). Participants were all proficient in written and spoken English. The mean age in the M1-thalamus group (experimental group) was 25.9 years (four male participants, six female) and the mean age in the SMA-M1 group (control group) was 25.4 years (five male participants, five female participants). Participants were not informed which group they were assigned to and they did not have any prior experience with neurofeedback.

Each participant undertook a test called the Vividness of Movement Imagery Questionnaires-2 (VMIQ-2) (Callow and Roberts, 2010) to measure their ability to perform the motor imagery tasks.
The VMIQ-2 is a revision of the Vividness of Movement Imagery Questionnaire (VMIQ) (Isaac et al., 1986) which comprises 12 items that assess the ability to image a variety of movements. Participants are required to image each item in two ways: using internal visual imagery (first-person perspective) and external visual imagery (third-person perspective) and rate the vividness on a five-point Likert scale from 1 (perfectly clear and vivid) to 5 (cannot imagine at all). The VMIQ-2 has shown acceptable factorial validity, construct validity and concurrent validity. Characteristics of the participants are shown in Table 4.
The experiment was explained to each participant before scanning. All participants completed an MRI safety checklist prior to MRI scanning. The research was approved by the ethics committee of the College of Science and Engineering, University of Glasgow. Each participant provided informed consent for their participation in the experiment.

Table 4: Demographic characteristics for participants in the NF and control groups

	M1-Thalamus (NF group) (Mean±SD)	M1-SMA (control group) (Mean±SD)	P-value (two tailed t-test)
Age (years)	25.9±5.28	25.4±4.58	0.832
Handedness	90±13.33	88±10.32	0.712
MI vividness (third person perspective)	23.8±7.36	18.8±10.03	0.22
MI vividness (first person perspective)	18.1±7.26	18±4.44	0.971

5.2.2 Behavioural tasks

5.2.2.1 Switching task

Each participant carried out a switching task before and after the NF training. The task paradigm was designed using Presentation software (Neurobehavioral Systems, Inc) which provides a set of tools for neurobehavioral experiments. The paradigm was adapted from Hayes et al. (1998). The switching task provides a measure of the time associated with switching between sequential operations. During the experiment, the 1,2 and 3 keys on a computer keyboard were tapped using the index finger. Participants learned to associate visual presentation of the letter A with keypress sequence 123 and letter B with key press sequence 132. A double-letter stimulus was displayed on the screen: AA, BB, AB and BA and the participants' task was to respond as rapidly as possible by tapping the three keys associated with the first letter followed by the three keys associated with the second letter.

We predicted that the switching point between two sequences would occur between taps 3 and 4. At this point, the intertap interval would increase as result of the occurrence of the second subsequence, hence, the switching. The first intertap interval reflects the reaction time following the onset of the double-letter stimulus. The second and third intertap intervals decrease below

the initial rection time. The intertap interval after the 3rd tap increases due to the switching as the sequence is either repeated or altered at this point (Hayes et al., 1998). The switching time would be greater when changing from one action sequence to a different one. The switching time is predicted to be larger in the experimental group compared to the control group.

A 3 ×3 mixed effect ANOVA (group × pre/post × switch/no switch) was used to analyse between and within group effects. Next, a paired-sample *t* test was performed as a *post hoc* test to compare the pre-post experiment inter-response time of each group.

5.2.2.2 Go/No Go task

Each participant carried out a Go/No Go behavioural task before and after each NF session (Fillmore et al., 2006). The Go/No Go task was used previously by Al-Wasity et al. (2021) and shown to be sensitive to motor training using neurofeedback. The Go/No Go task design involves two stimuli which are the Go stimulus (Green shape) and No-go stimulus (Blue shape). Participants were instructed to respond rapidly to the Go stimulus with a button-press and to withhold responding to the No-go stimulus. This task lasted approximately ten minutes.

Every participant completed 250 trials of this task before and after the NF training session. Participants were instructed to use their right index finger to press the space bar of a conventional keyboard as quickly and accurately as possible when a Go-trial appeared on the screen (green target) and to hinder their response (that is, to keep the index finger positioned above the space bar without pressing) when a No-go trial was presented (blue target). The task was based on Inquisit 5 software. Each trial consisted of a fixation point (+) presented for 800 ms, followed by a blank white screen for 500 ms, followed by a rectangular cue (horizontal 2.5 × 7.5 cm, or vertical 7.5 × 2.5 cm, where stimulus orientation was not informative) that was displayed for one of five intervals (100, 200, 300, 400 and 500 ms) to decrease the temporal warning effect. Finally, Go and No-go targets were coloured green and blue, respectively, and were presented for 1000 ms or until participants responded (Fillmore et al., 2006). A paired-sample *t* test was performed as a *post hoc* test to compare the pre-post experiment inter-response time of each group.

Imaging parameters and rt-fMRI neurofeedback platform

The study was performed on a 3T Siemens Tim Trio MRI scanner at the University of Glasgow Centre for Cognitive Neuroimaging (CCNi) with a 32-channel head coil. A T1-weighted high resolution anatomical scan was acquired at the beginning of the experiment (TR=2000ms, TE=2.52ms, 192 sagittal slices, 1 mm^3 isotropic voxels and image resolution 256×256). T2*-weighted functional scans were collected with an Echo Planar Imaging (EPI) sequence (TR=2000ms, TE=30ms, whole brain coverage with 32 axial slices, 0.3 mm gap and 3 mm^3 isotropic voxels).

For the NF runs, the data were sent volume by volume from the scanner to Turbo-BrainVoyager (TBV) via a network connection. The functional data were then pre-processed in real time. Custom-made MATLAB code was used to estimate the connectivity between the two regions and this connectivity measure was displayed as a thermometer bar on the screen.

Data were collected over two sessions. During each MRI session, a T1-weighted anatomical scan, a functional localiser and ten neurofeedback runs were obtained for each participant. During the NF blocks, participants were instructed to increase the height of the thermometer bar by imagining complex hand actions. The height of the thermometer bar indicated connectivity between M1 and the thalamus as calculated using Pearson's correlation. We used an intermittent feedback paradigm that updated and displayed the thermometer bar level after each NF block.

Every participant carried out 10 NF training runs for each session, with each single NF training run comprising eleven 32s blocks (14s motor imagery, 14s rest and 4s thermometer display).

5.2.3 Localiser

5.2.3.1 Functional Localiser

The experiment began with a functional localiser run to identify the left primary motor region (M1) and SMA which would provide one of the regions from which the feedback connectivity signal could be obtained. The localiser run took approximately 5 minutes and comprised 7 fixation blocks (16s) interleaved with 6 blocks of bimanual hand clenching (30s).

During the procedure, participants were instructed to count letters or numbers if "REST" appeared on the screen and to clench their fists if "MOVE" appeared on the screen. The functional data were pre-processed and analysed online with an accumulative General Linear Model (GLM) embedded in Turbo-BrainVoyager. The ROIs were defined in each participant's native space and subsequently used for the NF training runs to derive the NF signal. The M1-ROI was delineated from the active voxels (threshold of t > 5.0) within a rectangle where the precentral gyrus bulges posteriorly, also known as the sigmoidal hook or omega sign, which is a term used to denote the appearance of the hand motor area (hand knob) (Figure 5.1). In the control group, the SMA-ROI was delineated from the active voxels (threshold of t > 5.0) within a rectangle, anterior to the precentral sulcus and superior to the cingulate sulcus, as shown in figure 5.2.

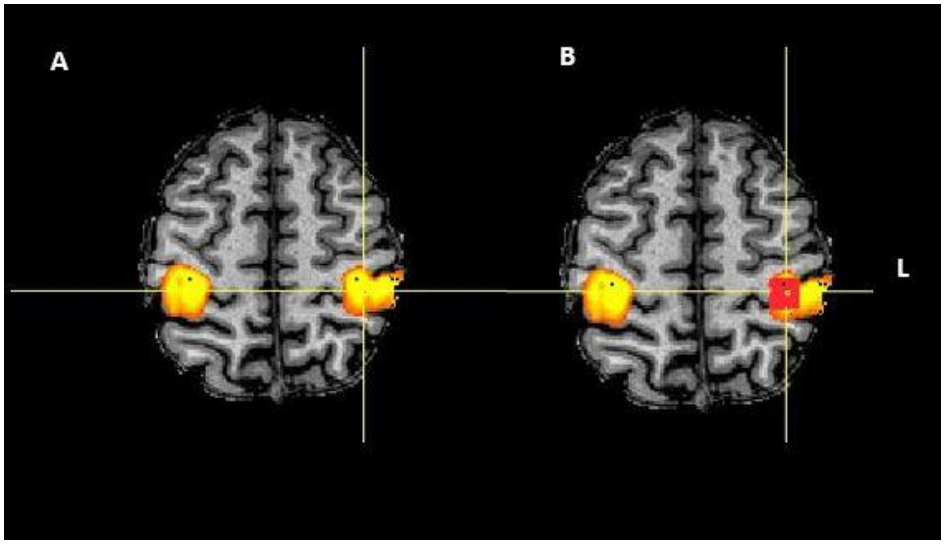

Figure 5.1 This figure illustrates the location of left primary motor cortex (M1) which was defined functionally during the localiser by a contrast of hand clenching to rest (crosshairs). A) shows the activation of M1 (yellow). B) indicates the selection of M1 voxels as a targeted area for NF (red cluster).

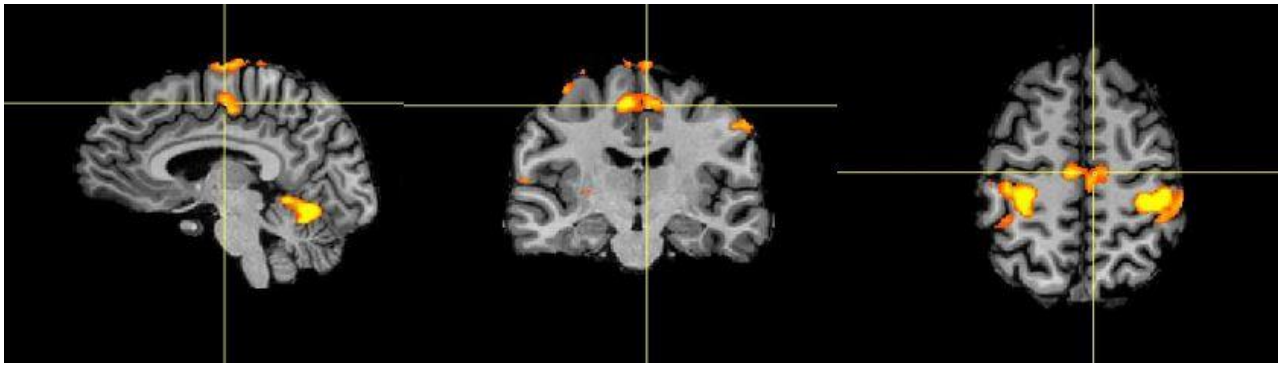

Figure 5.2 This figure illustrates the location of the supplementary motor cortex (SMA) which was defined functionally during the localiser (crosshairs).

5.2.3.2 Motor thalamus mask

Because we could not identify a reliable functional localiser for the thalamus, it was defined by using a thalamus mask obtained from a thalamus atlas. Here, the thalamus mask was created offline using the Talairach atlas (Talairach et al., 1988; Lancaster et al., 2000). This mask covered the motor parts of the thalamus including the ventral lateral nucleus and the ventral anterior nucleus (Fang et al., 2006). This mask was used in the experimental group when M1-thalmus connectivity was targeted. This mask was applied individually to each participant from the anatomical scan obtained at the beginning of the experiment. After applied the mask, it was visually checked to see if it accurately applied to localise the thalamus (Figure 3.3).

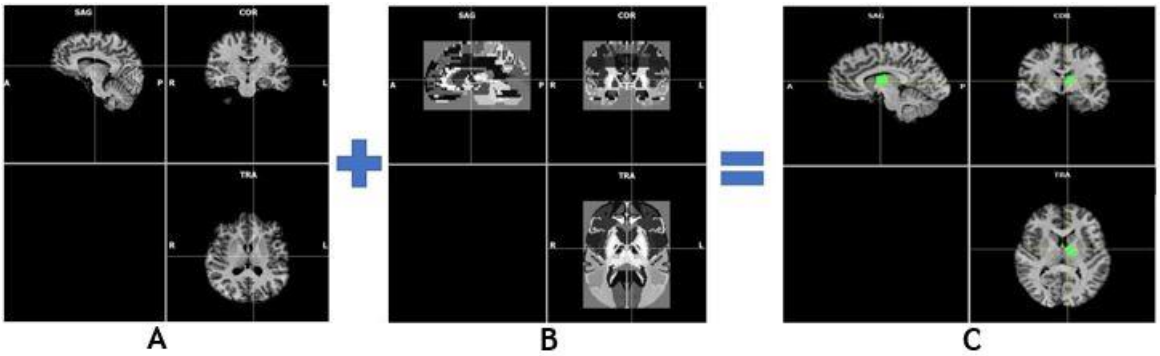

Figure 5.3 This figure shows the thalamus mask that was used in this experiment. Panel A represents the anatomical image of brain that was obtained from structural T1 scanning. This image was then converted into Talairach space. Panel B shows the thalamus mask that was created offline based on Talairach atlas. Panel C shows the final image of the thalamus mask after loading it on the participant's anatomical image.

5.2.4 Rt-fMRI neurofeedback

Every participant carried out ten NF training runs of 400s duration. Each NF training run consisted of 32s blocks. Each block comprised 14 seconds of rest, 14 seconds when participants were asked to regulate their brain activity and 4 seconds when a thermometer bar was presented with the feedback signal (Figure 5.4).

Participants in the experimental group saw feedback which presented connectivity between M1-thalamus, while participants in the control group saw feedback which was provided from the M1-Supplementary motor area (SMA) connectivity.

During the NF blocks, participants in the experimental group were instructed to increase the activation of M1-thalamus connectivity by imagining complex action for 14 seconds.

Next, the thermometer bar was displayed for 4 seconds after each NF block to represent the level of M1-thalamus connectivity during the task. However, in the control group, the thermometer bar showed the connectivity of M1-SMA. During the rest block, participants were instructed to count numbers or letters for 14 seconds to keep the baseline low (Hanakawa, 2011; Berman et al., 2012).

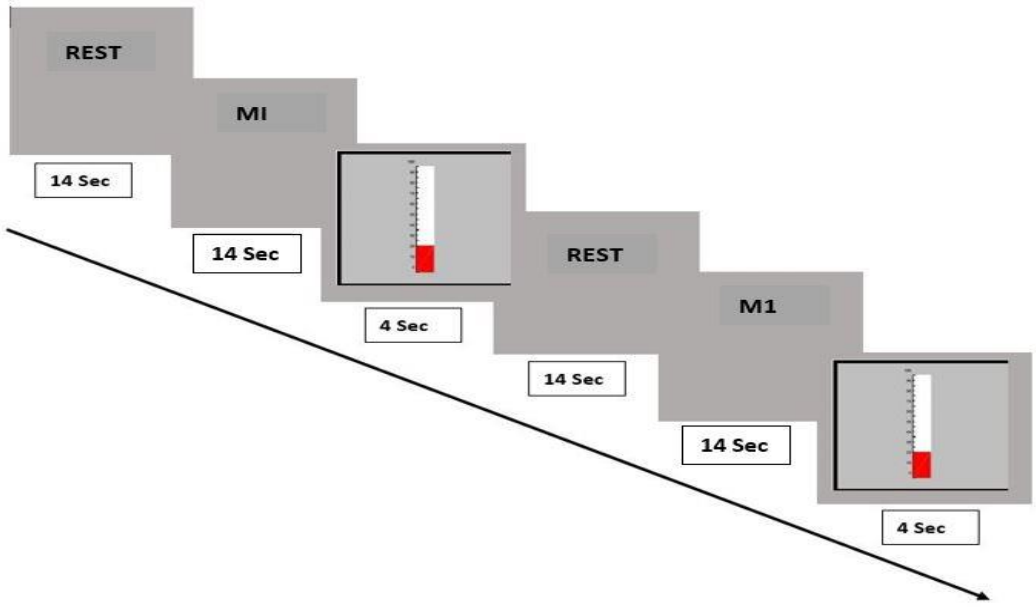

Figure 5.4 fMRI NF training paradigm design. A run lasted 400s and comprised eleven 14s NF blocks alternating with eleven 14s fixation (rest) blocks and eleven segments when the thermometer bar was shown for 4 seconds.

5.2.5 Online data analysis

Turbo-BrainVoyager software and MATLAB were used to perform rt-fMRI data analysis and NF presentation. The data were sent volume by volume from the scanner to Turbo-BrainVoyager via a network connection. Next, the functional data were pre-processed in real time.

The intermittent feedback signal consisted of a thermometer bar of varying height which was updated and displayed after each NF block based on the following equation:

$$\boldsymbol{bar\ height} = 50 * (Corr + 1) \qquad 0.1$$

Where scale is an arbitrary scale value to optimise visibility of the thermometer bar.

$$\mathbf{Corr}(\mathbf{x}, \mathbf{y}) = \frac{\sum_{i=1}^{n}(\boldsymbol{x_i} - \bar{\boldsymbol{x}})\,(\boldsymbol{y_i} - \bar{\boldsymbol{y}})}{\sqrt{\sum_{i=1}^{n}(\boldsymbol{x_i} - \bar{\boldsymbol{x}})^2}\sqrt{\sum_{i=1}^{n}(\boldsymbol{y_i} - \bar{\boldsymbol{y}})^2}} \qquad 0.2$$

Where **x** is a 14-s time series of M1, $\bar{\mathbf{x}}$ is the mean activation of M1 during a MI block, **y** is a 14-s time series of the Thalamus and $\bar{\mathbf{y}}$ is the mean activation of the Thalamus during a MI block for the experimental group and $\bar{\mathbf{y}}$ is the mean activation of SMA during a MI block.

5.2.6 Whole brain analysis

The data were analysed offline using Brain Voyager QX 2.8.4 (Brain Innovation, Maastricht, the Netherlands) and custom-written MATLAB scripts (Version 8.2, The MathWorks Inc., Natick, MA, 2000). Anatomical T1 images were corrected for inhomogeneity and normalized to Talairach space. EPI data were slice-time corrected. Spatial alignment of all volumes to the first volume of the localiser was performed to correct for head motion. The fMRI data were co-registered to T1 images based on anatomical landmark points and co-registration was manually corrected if necessary. The data were then normalised to Talairach space using rigid body transformation and scaling. Linear drifts were removed and a temporal high-pass filter (2 cycles) was used to eliminate non-linear drifts

in the time series. Data were spatially smoothed using a Gaussian kernel with 6 mm full width at half maximum. Data were convolved with a hemodynamic response function and covariates derived from six head motion parameters (Johnston et al., 2010; Dijk et al., 2012). All the pre-processed functional data of each subject were analysed using a General Linear Model (GLM) with two predictors (fist clenching and rest for analysis of the localiser, feedback and rest for analysis of NF). Group data were evaluated based on a second level random effect analysis general linear model (RFX-GLM) (Goebel *et al.*, 2006).
False Discovery Rate (FDR) at a threshold of $q < 0.05$ was applied to report activations to address the issue of multiple statistical comparisons across all voxels (Benjamini et al., 1995). Using FDR, we control for the number of false positive voxels among the subset of voxels labelled as significant. Finally, a cluster threshold of 108 mm^3 was applied to eliminate small clusters (Herbec et al.,2015).
Finally, a *t* test was run between the NF and control cluster maps to create contrast maps, highlighting any significant differences between the two groups.

5.2.7 Statistical analysis

For each group, a paired *t* test was used post-hoc to compare the mean connectivity value of the first run with the mean connectivity value at the last run. Furthermore, a linear regression of the average connectivity values over neurofeedback runs was used to examine the upregulation over runs.

5.3 Results

5.3.1 Connectivity Analysis

Each participant completed twenty runs over two sessions (ten runs in each session). Figure 5.5 shows the activation levels of the experimental group (M1-thalamus) and the control group (M1-SMA) over two sessions. The first session was from run 1 to run 10 and the second session started at run 11 and ended at run 20. The results for M1-thalamus showed a gradual, but noisy increase from runs 1 to 20. This was confirmed by a linear regression that showed an increase in the mean M1-thalamus activity across runs in the NF group, indicating a learning effect (Intercept coefficient = 0.193, with $R^2 = 0.272$, X variable coefficient = 0.0047, $p = 0.0185$). On the other hand, the results for M1-SMA

showed no apparent consistent change from runs 1 to 20, which was consistent with the linear regression analysis which showed no increase in the mean M1-SMA activity across runs in the control group (Intercept coefficient = 0.2449, with R^2 = 0.0226, X variable coefficient = 0.0013, p = 0.518).

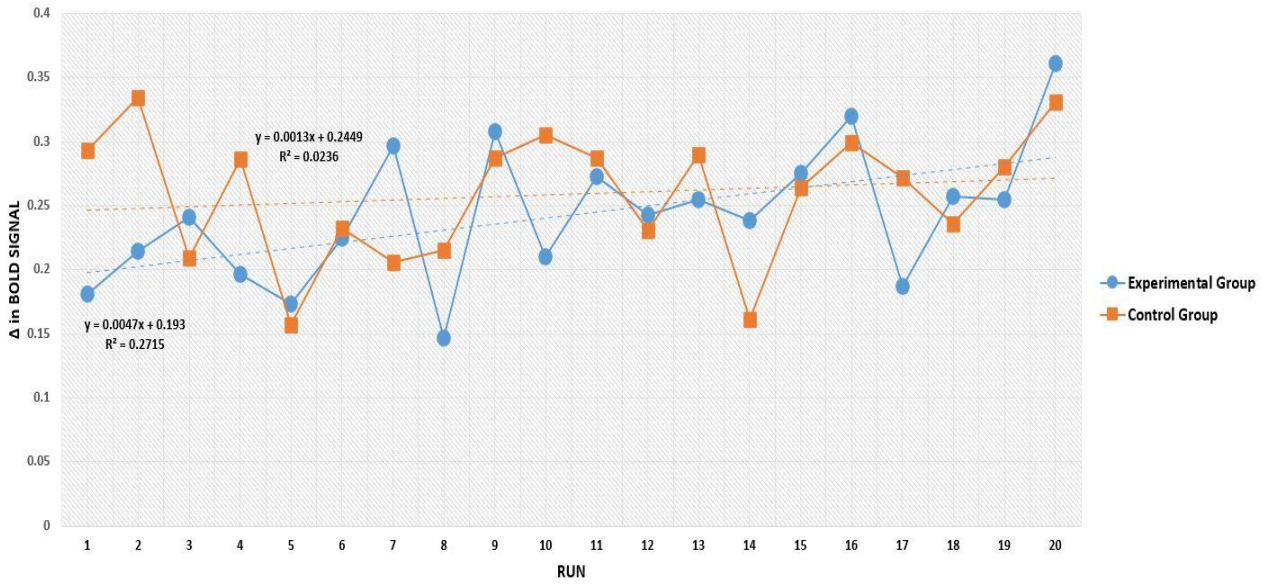

Figure 5.5 this figure shows the M1-thalamus connectivity average across runs for the experimental (blue) and control (orange) groups. Dashed lines represent the trend for each group.

The success of training is clear when comparing the first run of the first MRI session with the last run of the second MRI session. The correlations show an increase for both the experimental and control groups, as seen in Figure 5.5. The paired t test revealed a significant increase in M1-Thalamus connectivity from the first to the last run ($t(9) = -2.53$, $p<0.01$), however, the paired t test did not

show a significant increase in the activation level between run 1 and run 20 in the control group ($t(9) = -0.53$, $p<0.3$) (see Figures 5.6).

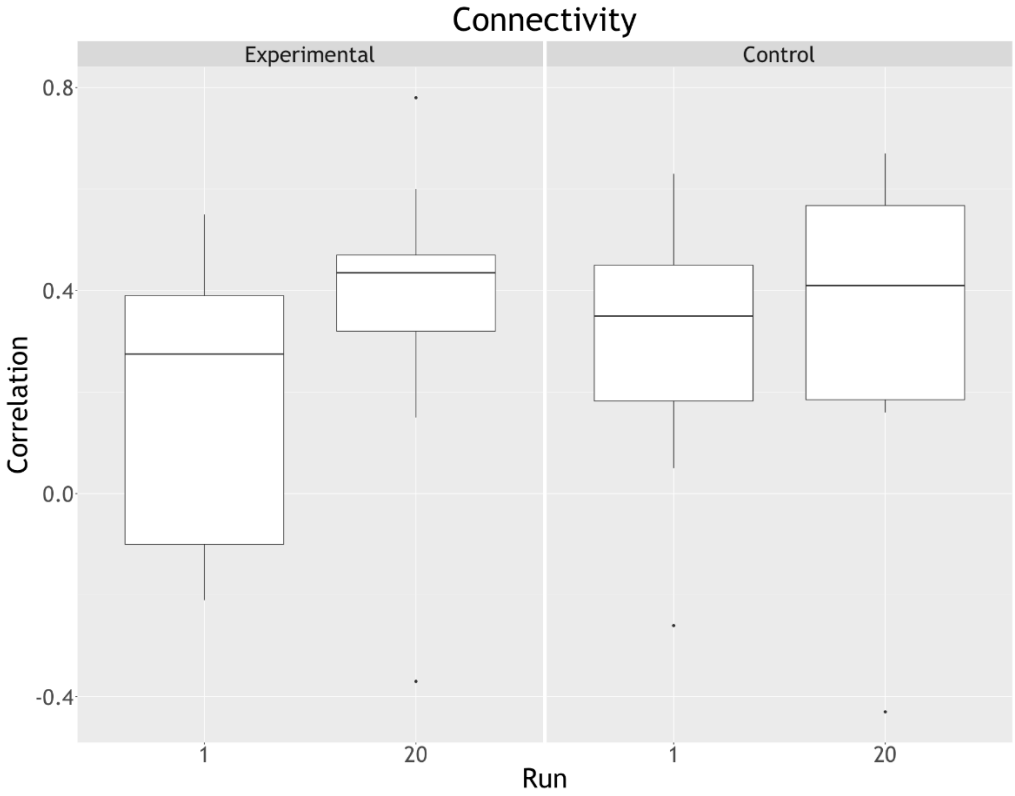

Figure 5.6 Box plot of run 1 and run 20 for the experimental and control groups. This plot demonstrates a significant change occurred for the experimental group when comparing the correlation at run 1 to run 20. No such effect occurred with the same runs for the control group.

Participants reported that they believed mental strategies such as playing music and engaging in sporting activities improved their ability to raise the thermometer bar during the training.

5.3.2 Whole brain analysis

A whole-brain RFX-GLM analysis was performed for both the NF and control groups, as illustrated in Figures 5.7, 5.8 and 5.9. For the NF group, activations were found in the right BA 6, thalamus, left BA 6 and left BA 40 in the left parietal lobe, as illustrated in Figure 5.8 and listed in Table 5. For the control group, the activations were seen at the right BA 21, the right BA 19, right BA 38, right BA 28, right BA 10 in the right superior frontal gyrus, left BA 38 and the left BA 19 in the left occipital lobe, as illustrated in Figure 5.9 and listed in Table 6.

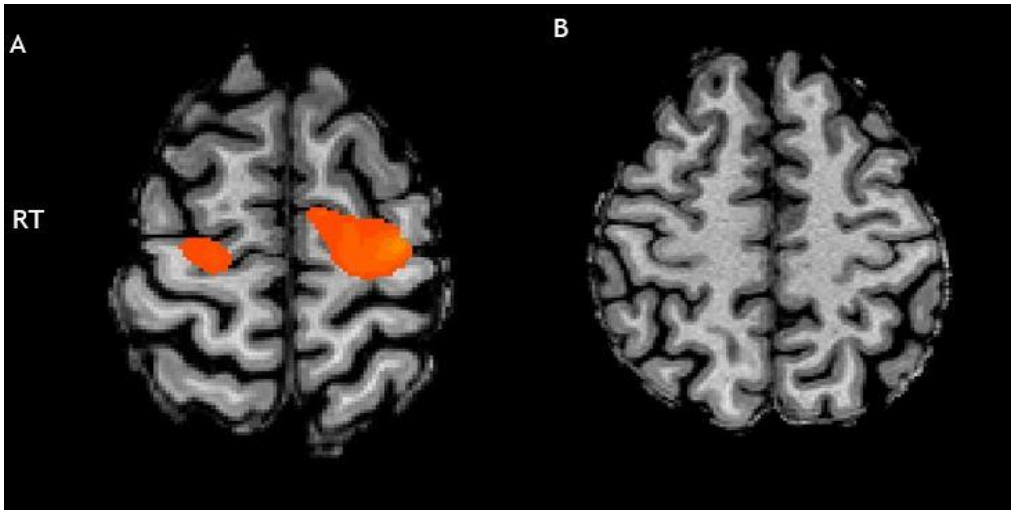

Figure 5.7 This figure reveals the results of the analysis of NF runs shown for the (A) NF group and (B) control group. There is activation seen at M1 in the experimental group, with such activation not seen at M1 in the control group.

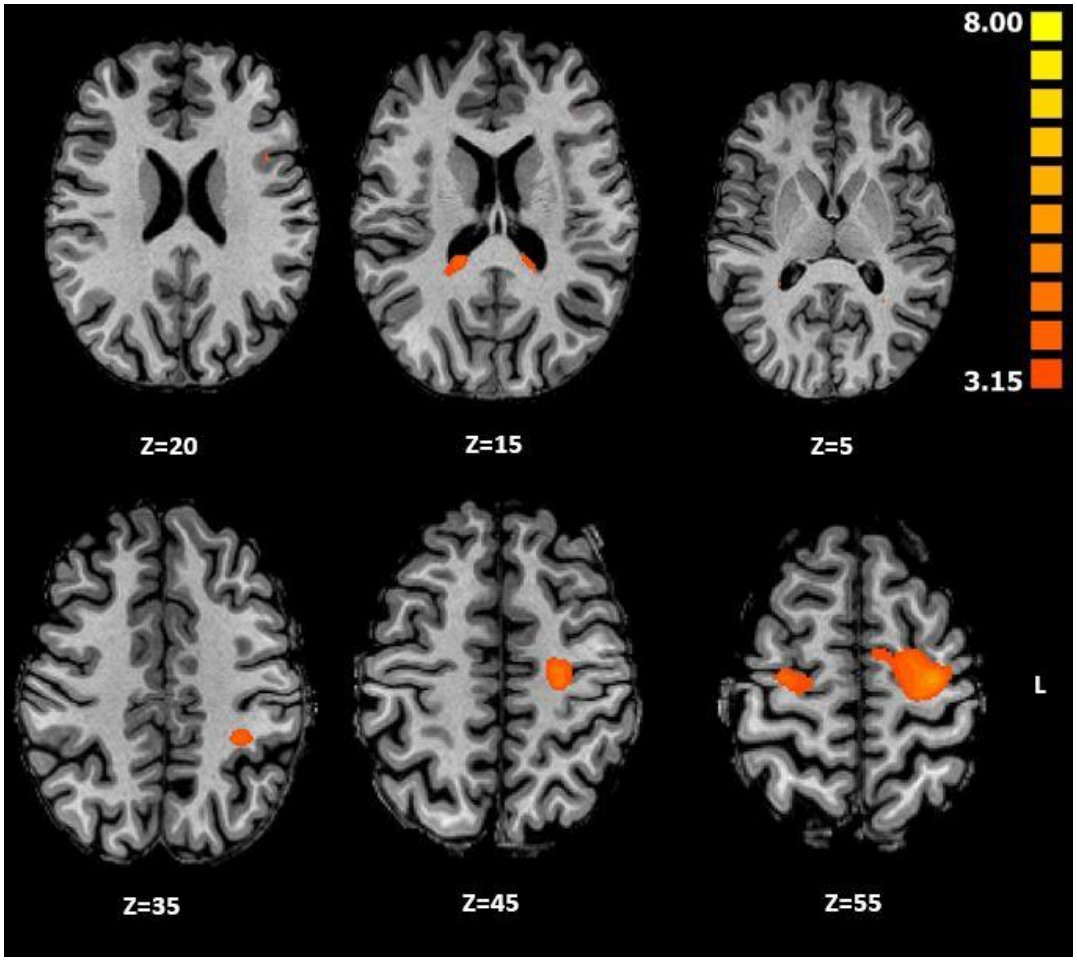

Figure 5.8 Results of the analysis of NF runs shown for the experimental group. These activations are significant at p<0.05 corrected.

Table 5 Clusters of brain activation during the NF in the experimental group

CORTEX	X	Y	Z	t	P value	Number of voxel
RT Precentral Gyrus, BA 6	27	-13	52	5.159	0.0006	1388
RT Thalamus	18	-34	13	5.03	0.00071	612
LT Precentral Gyrus, BA 6	-27	-13	55	5.79	0.00026	4864
LT Parietal lobe, BA 40	-30	-34	34	6.795	0.00008	407

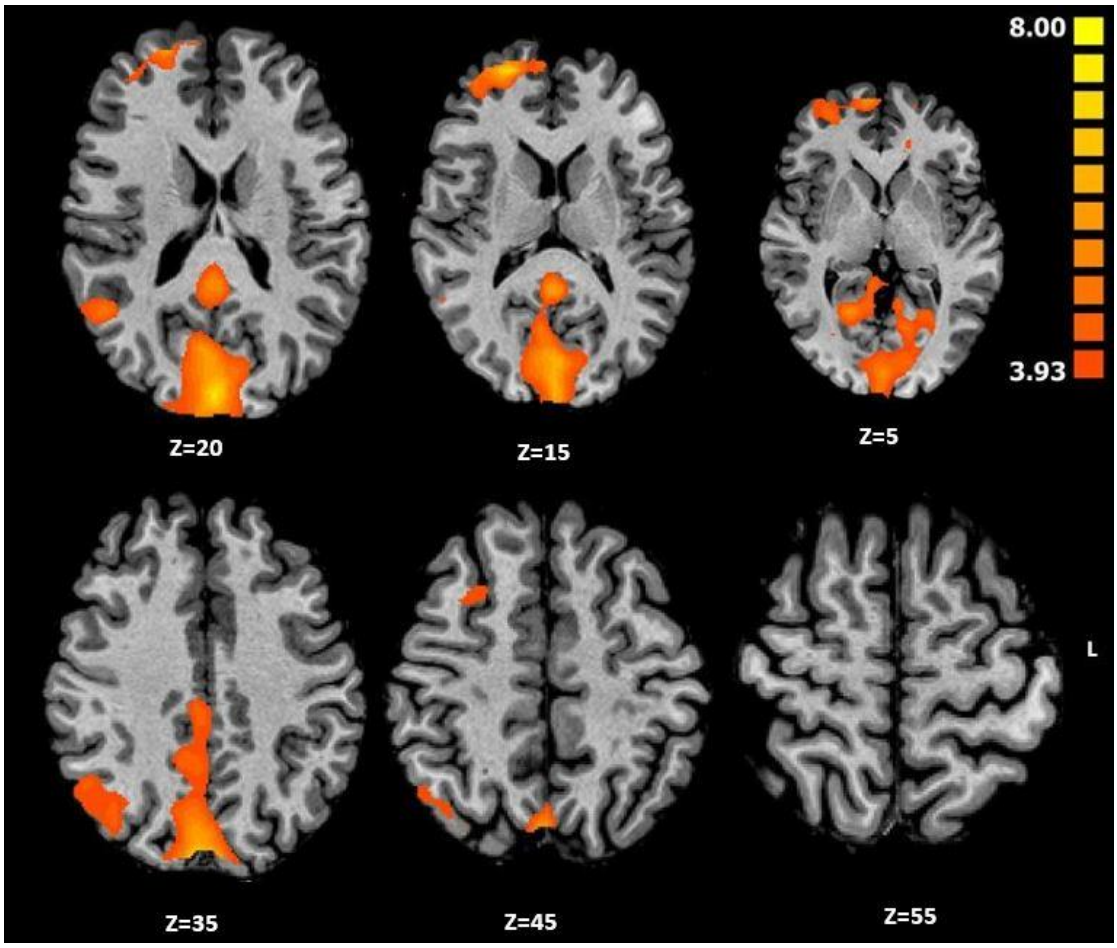

Figure 5.9 The resulting clusters of RFX-GLM analysis for the control group. Three clusters show significant activations at p< 0.05 uncorrected.

Table 6 Clusters of brain activation during the NF in the control group

CORTEX	X	Y	Z	t	P value	Number of voxel
RT Temporal Lobe, BA 21	66	-23	-8	5.364	0.00045	780
RT Temporal Lobe, BA 38	51	14	-24	5.618	0.00033	1464

RT Parietal Lobe, BA 19	31	-70	43	6.453	0.00012	4350
RT Superior Frontal Gyrus, BA 10	21	56	13	8.209	0.00002	5115
RT Frontal Lobe, BA 8	27	17	49	4.625	0.00125	478
RT Limbic Lobe, BA 28	24	-19	-5	6.953	0.000008	182
LT Occipital Lobe, BA 19	0	-86	31	9.022	0.000067	37316
LT Temporal Lobe, BA 38	-54	14	-20	5.484	0.00034	411

To assess whether activation in the NF group was significantly different from activation in the control group, a *t* map of M1-thalamus was compared to a t map of M1-SMA. The *t* test at p value =0.05 with FDR (Q<0.05) revealed no significant difference in activation between groups.

5.3.3 Behavioural results

5.3.3.1 Switching task

Inter-response times, as a function of position in the sequence of six taps, are shown in Figures 5.10 for the M1-thalamus group and Figures 5.12 for the M1-SMA group. The first interval indicates the reaction time following the onset of the double-letter instruction for initial responding. After the first tap, the two intertap intervals dropped greatly below the initial reaction time. The intertap interval then increased between taps 3 and 4, the point at which the sequence either repeats or is altered.

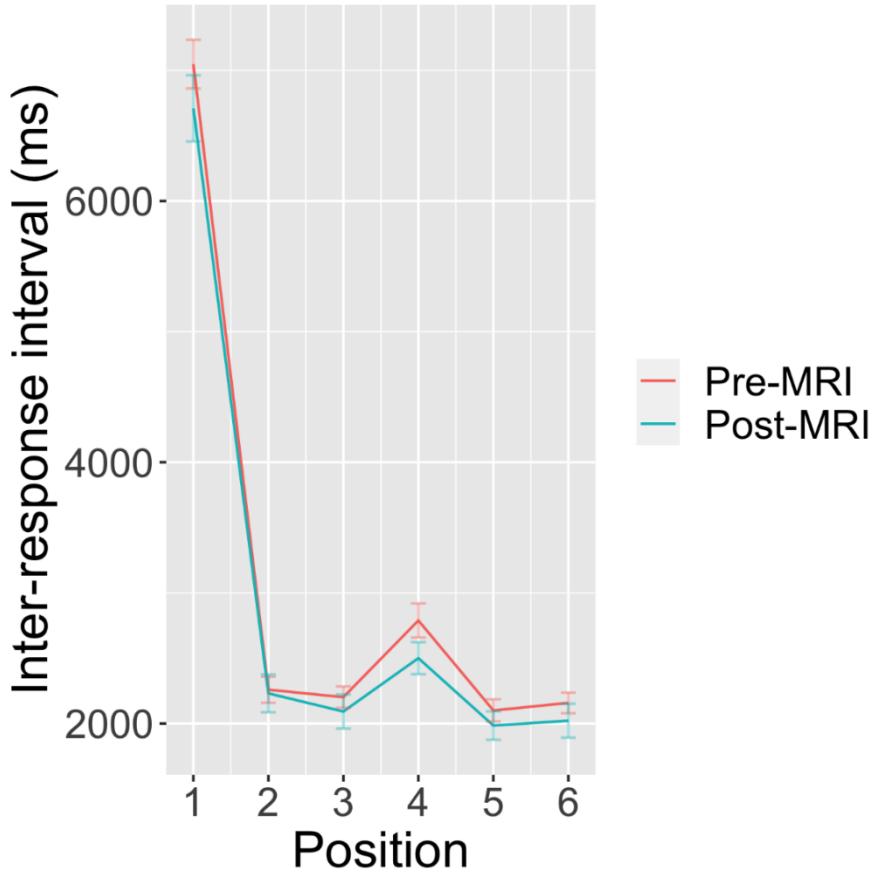

Figure 5.10 This figure shows the inter-response times between successive taps as a function of position in the sequence in the experimental group (M1-thalamus) before first MRI session (red) and after second MRI session (green) when the sequence altered (switching). The switching effect occurred at position 4.

Figures 5.10 shows the inter-response times in the experimental group for all sequential positions with position four being the point when switching occurs. The increase in time interval at that point is greater when the sequence changes. At the position of sequence four, the detected inter-response time at the post-second MRI session is greater compared with the pre-first MRI session (see Figures 5.10).

When ploting the effect at position 4 only, where the condition of switching or no switching occurred, the effect is greater in the case of switching while less effect is detected when no switching occurred, as seen in Figure 5.11. This effect was seen in the experiemental group (M1-thalamus).

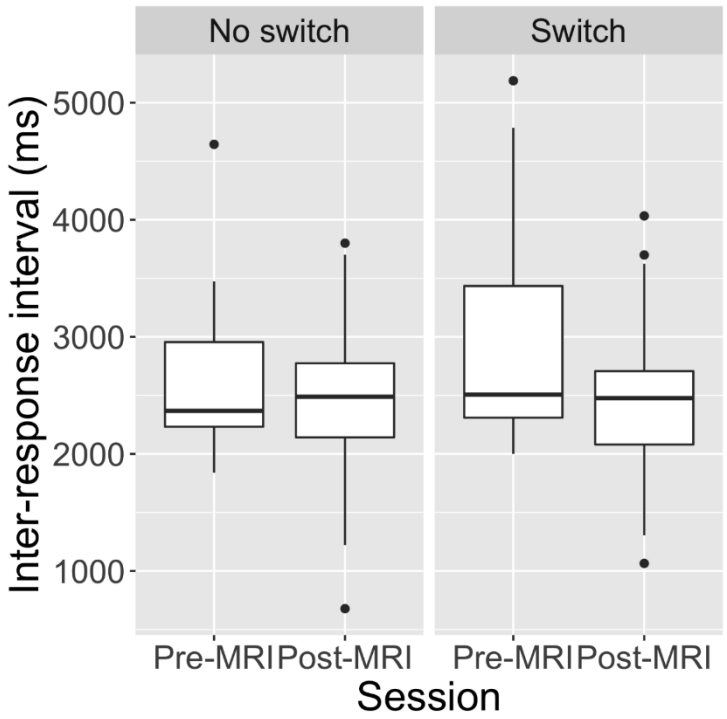

Figure 5.11 Box plot demonstrates the switching effect and no switching effect detected pre-first MRI session and post-second session at position 4 in the experimental group.

For the control group (M1-SMA), Figures 5.12 show the inter-response times at all subsequent positions. There is a slight increase in inter-response time detected at position four for the post-second MRI session compared with the pre-first MRI session.

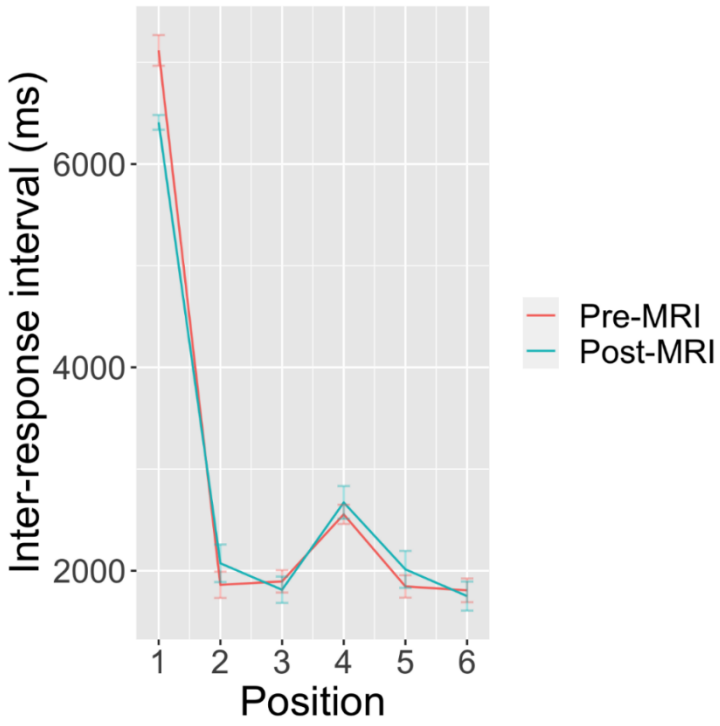

Figure 5.12 This figure shows the inter-response times between successive taps as a function of position in the sequence in the control group (M1-SMA) before the first MRI session (red) and after the second MRI session (green) the sequence altered (switching). The switching effect occurred at position 4.

When ploting the effect at position 4 only, where the conditions of switching or no switching occurred in the control group (M1-SMA), this effect is relatively increased in case of switching while less effect is detected when no switching is occurred as seen in Figure 5.13.

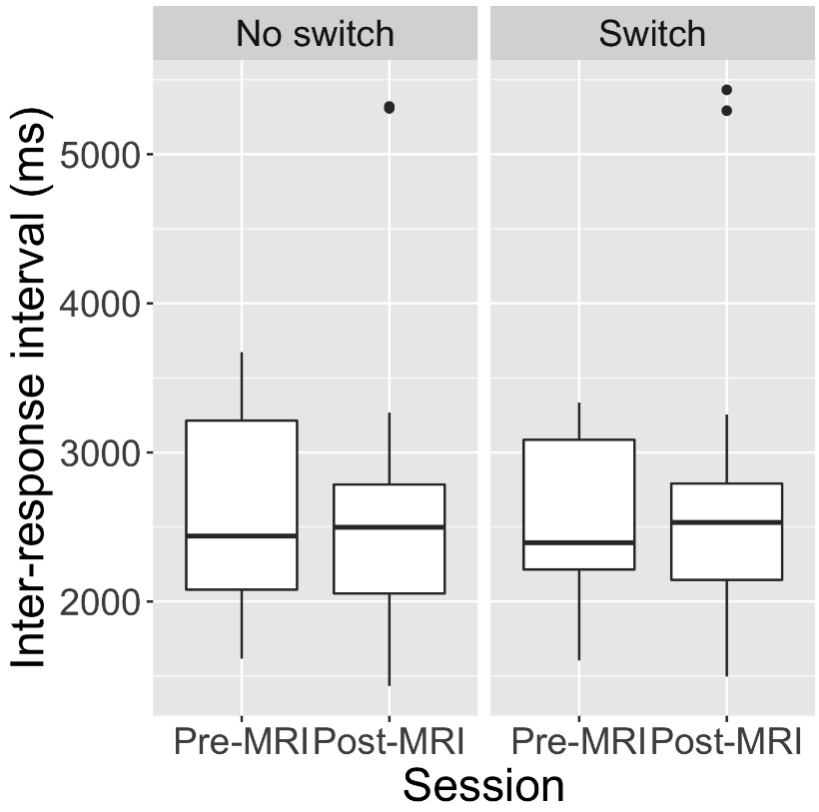

Figure 5.13 Box plot demonstrates the switching effect and no switching effect detected pre first MRI session and post second section at position 4 in the control group.

Figure 5.14 compares the switching effect to no switching effect between experimental group (M1-thalamus) and control group (M1-SMA) at pre first MRI session and post second MRI session.

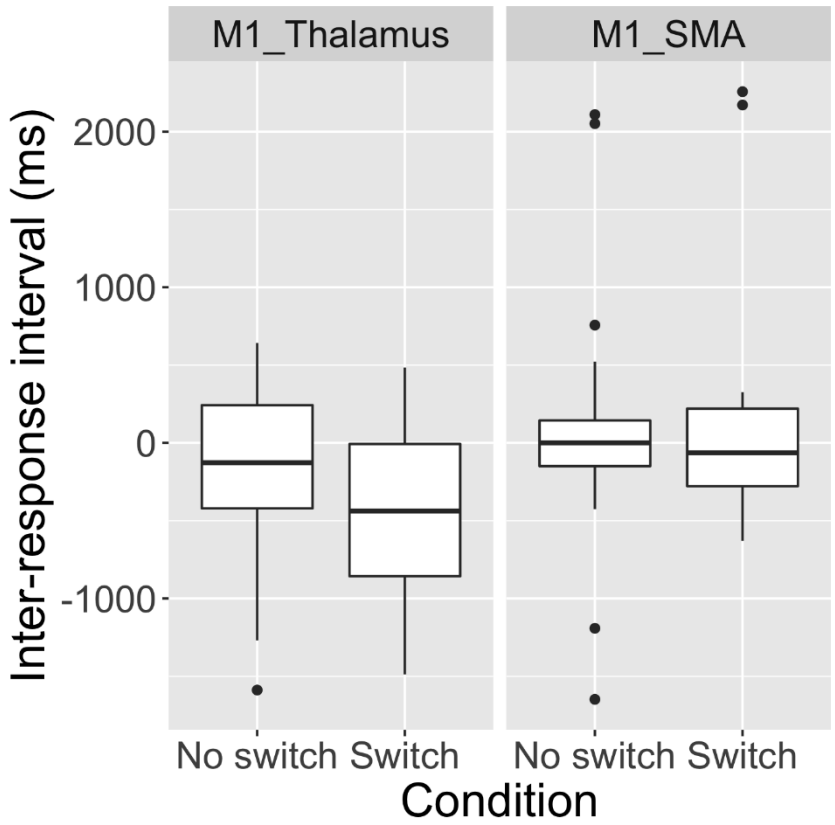

Figure 5.14 Boxplot compares the inter-response interval in experimental group versus control group detected when switching occurred at position 4 at pre first MRI session and post second MRI session.

The repeated measure ANOVA analysis showed significant effect at group × condition interaction (F=11.73, p<0.00082), no significant effect seen at group × session interaction (F=1.482, p<0.577) and condition × session (F=0.853, p<0.446).

A paired t test was used to compare the effect of the switching condition in the post-second MRI session to the pre-first MRI session. The results show a significant difference occurring in the M1-thalamus groups (p=0.042685) with no such effect being detected for the control group (p=0.58).

Furthermore, an unpaired t test was also used to compare the effect of switching to no switching at position four after the MR training session in both the M1-thalamus and M1-SMA groups. The results reveal a significant difference in the switching time (p=0.000349), with no such effect being detected for the control group (p=0.186).

5.3.3.2 Go/No Go task

Figures 5.15 shows the difference in reaction time of the two groups before and after the NF training. The reaction time reduced after performing NF training comparing with pre-NF training. These drops were clear in the M1-thalamus group and the M1-SMA group. However, the paired *t* test revealed that changes in reaction time between the post- and pre-MRI NF sessions were significant for the M1-SMA group (p = 0.0069) but not significant for the M1-thalamus group (p=0.247). Figure 5.16 shows the changes in reaction time between M1-SMA and M1-thalamus groups.

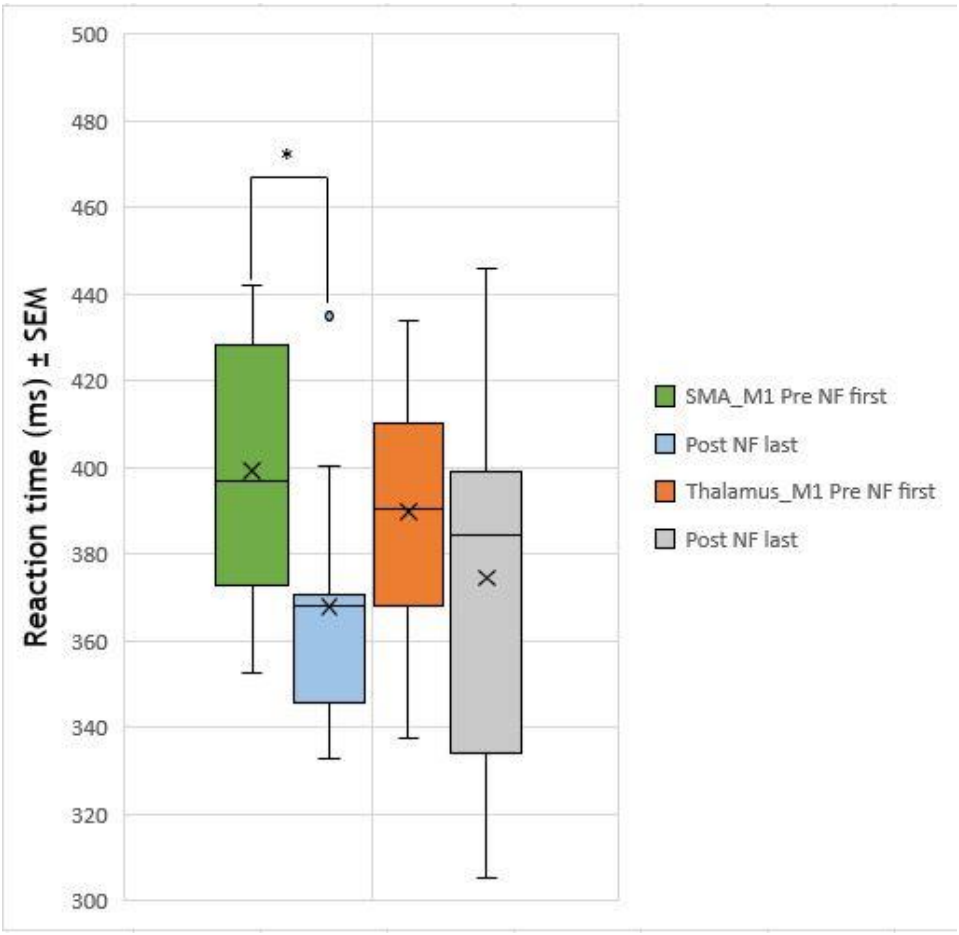

*Figure 5.15 This figure shows the reaction time (ms) difference at pre-first MRI session and post-second MRI session for the two groups. The errors bars represent the standard mean error (SEM) * p<0.05.*

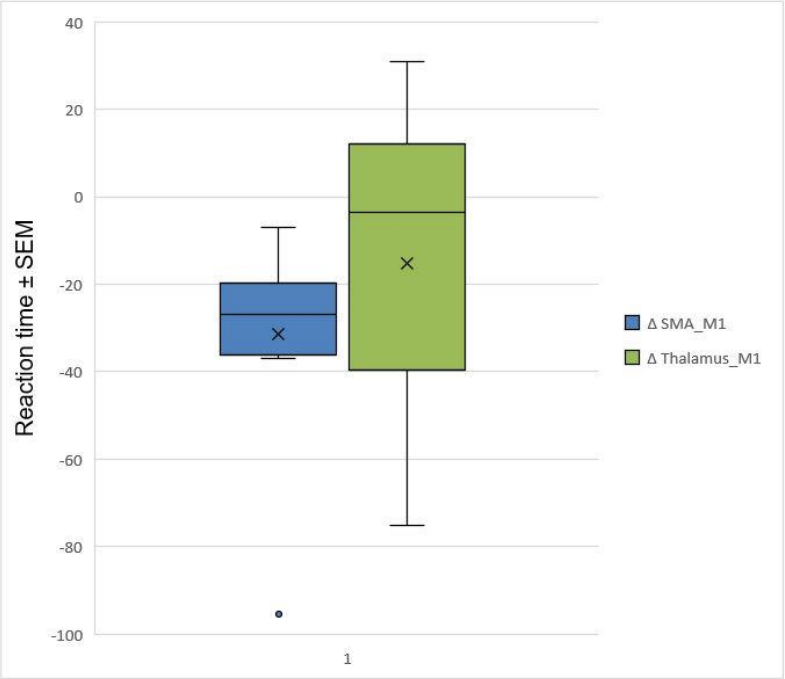

Figure 5.16 This box plot shows the difference in reaction time (post-NF and pre-NF) of both groups.

The unpaired *t* test was used to compare the difference in reaction time of the two groups, with the results yielding no significant changes in reaction time (*p*= 0.300073) (see Figure 5.20).

5.4 Discussion

In this research we investigated whether healthy participants could learn, in two sessions, to enhance the functional connectivity between M1 and the thalamus during a MI task of complex hand actions whilst receiving an intermittent feedback signal (displayed as the height of a thermometer bar) using rt-fMRI-NF. A significant enhancement in connectivity was identified in the experimental group. These results are consistent with Liew et al., (2016) who explored the connectivity between M1 and the thalamus in four stroke patients. Liew and colleagues used rt-fMRI neurofeedback to improve stroke-induced behavioural impairments and provided evidence that patients with stroke could modulate their neural activity in the brain regions which were implicated in the impaired functions. They learned to modulate functional connectivity between the

primary motor cortex and the thalamus in the ipsilesional hemisphere.

Three of them were able to maintain control over cortical-subcortical connectivity as they managed to increase the functional connectivity between M1 and the thalamus. However, that study was limited due to its small sample size, the conditions of participants involved that study and no control group being involved. The current research overcomes those limitations by recruiting a larger sample size than Liew and colleagues. In our research, twenty participants were recruited and divided into two groups, namely, experimental and control. The results of this research reinforce the capacity of rt-fMRI neurofeedback to manipulate functional connectivity. These results are consistent with those of Megumi et al. (2015) who demonstrated an improvement in the connectivity between M1 and the parietal cortex by using rt-fMRI neurofeedback.

The results of our research are also consistent with other studies (Hamilton et al., 2011; Lee et al., 2011; Rota et al., 2011) which found that neurofeedback training leads to specific changes in the connectivity of the target region, usually strengthening the relevant connections and suppressing others (Weiskopf, 2012).

In this research, young healthy participants were recruited. By contrast, Liew et al. (2016) recruited stroke patients. Their performance and ability to perform motor imagery was higher than that of the stroke patients. In general, older patients might have difficulties performing imagery tasks and have less tolerance compared with younger, healthy participants (Sulzer et al., 2013). However, patients could possess another factor, namely, motivation, that is often impacted by the disease. Motivation might decrease, as the compensation for disease-specific restrictions may require additional effort (Haugg et al., 2021). Nevertheless, the disease burden and the hope for improvement may also increase motivation and compliance by comparison with healthy participants who are partly motivated by financial incentives (Haugg et al., 2021).

Every participant performed the Vividness of Movement Imagery Questionnaire-2 (VMIQ-2) to measure their ability to perform motor imagery (MI) tasks (Callow and Roberts, 2010). This questionnaire aimed to reduce inhomogeneity between

the experimental and control groups' ability to perform motor imagery. The threshold for VMIQ-2 was 36 points, hence, any participant exceeding this threshold was excluded from this research due to the difficulty in their capacity to engage in motor imagery. However, if a participant exceeded the threshold in one element, for example, internal visual imagery (first-person perspective) and their score did not exceed the threshold in another element, such as external visual imagery (third-person perspective), then the participant is advised to carry out the experiment using the type of imagery that scores less than the threshold and avoid the use of motor imagery strategies with scores exceeding the threshold.

Before a participant took part in this research, the Vividness of Movement Imagery questionnaire was conducted to evaluate the participant's ability to perform motor imagery. The cutoff point for the questionnaire is 36 because exceeding this is associated with difficulty performing motor imagery tasks (see 5.4 for further information).
Participants who did not pass the questionnaire were not allowed to enter the study as they showed difficulties performing motor imagery. They were replaced by participants who had Vividness Questionnaire scores below the threshold, indicating they could perform motor imagery.
The included participants all met the inclusion criteria such as participant's age was less than 40 years old (young participant), the score of the Vividness of Movement Imagery was less than 36 points, the participant was right-handed based on the Edinburgh Handedness Inventory questionnaire.

The thermometer was a simple interface used in this research. This interface aimed to indicate the level of neural level activity changes, namely, how active was the target region during the training. This interface was thought to not distract the participant during the experiment (Lubianiker et al., 2019). However, it may produce fatigue which may affect participants' ability to perform motor tasks effectively (Paret et al., 2019).

The instructional strategy used in this research was an implicit strategy, in which participants are being asked to develop their own effective strategies to enhance their mental activity level during NF training. This strategy is popular in

most rt-fMRI-NF research (Paret et al., 2014). However, there is a recognised disadvantage of this strategy, namely, when participants identify an action that led to enhancement in their neural activity level, they stop exploring new mental actions which may provide more activation (Paret et al., 2019).

Motor imagery is a dynamic state in which participants imagine motor actions without apparent physical movement. This mental task has been used successfully and widely in real-time research to modulate single regions such as the sensorimotor cortex (Yoo et al., 2004), M1 (deCharms et al., 2004), and SMA (Al-Wasity et al., 2021). MI-based rt-fMRI has also been used successfully to modulate connectivity between two regions such as MI and the lateral parietal cortex (LP) (Yamashita et al., 2018) and M1 and the thalamus (Liew et al., 2016) as well as the prefrontal cortex (dlPFC) and the ventromedial prefrontal cortex (Spetter et al., 2017). The results of this research are consistent with the literature, as participants were able to successfully upregulate the connectivity between M1 and thalamus using MI-based rt-fMRI-NF.

During the debriefing after the scanning, participants reported that various imaging actions, namely, playing music, knocking doors, fist-clenching and boxing were the actions that they believed boosted the neural activity levels during NF training. They believed these MI strategies had positive effects on the thermometer bar height and the activity level dropped when they used other strategies. They reported that they were struggling to identify which MI action was suitable and most of them stated they tried not to change their strategy unless the activity level stopped increasing. These findings are consistent with other findings in the literature as the common documented strategies in successful modulation include MI of fist-clenching and pitching (Yoo et al., 2008; Chiew et al., 2012; Blefari et al., 2015) and sequential finger movements (Berman et al., 2012; Neyedli et al., 2018).

A paired *t* test was used as a post-hoc test to compare mean connectivity values of the first and the last runs in each group. Post hoc analysis showed that the M1-thalamus connectivity was significantly increased while no such effect was recorded in the control group. Post hoc analysis was used in previous research to compare the activation levels over runs (Al-Wasity et al., 2021; Liew at al.,

2016; Bray et al., 2007).

In a task-switching experiment, participants perform a task to measure time when switching between sequential operations. It was intended to compare the effect of switching from when it was performed before NF sessions to the same task when it was performed after the NF sessions were completed. The results showed a significant difference for the NF group (M1-thalmus) whereas there was no statistically significant difference for the control group. Moreover, the effect of switching to not switching was significant for the NF group. These results are consistent with the results of Hayes and colleagues (1998) who investigated the role of basal ganglia in switching. They found that patients with motor dysfunction, for example, Parkinson patients, showed a slow rate of switching (that involved sequences of finger movements) than not switching, compared with age-matched healthy participants. The basal ganglia have an indirect role in motor function as they are a part of a closed cortico-basal ganglia-thalamo-cortical loop and any lesion in basal ganglia may lead to motor deficits, for example, Parkinson disease. Since the basal ganglia play a role in switching and are part of the closed cortico-basal ganglia-thalamo-cortical loop, switching tasks are, theoretically, a useful behavioural task for any area in that loop, either cortical or sub-cortical. In this research, the detected significant change in switching results supports this theory. Therefore, a switching task is a valid behavioural test to measure the effect of modulation of the M1-thalamus using rt-fMRI-NF if it is conducted before and after the training sessions.

However, no such significant effect was detected in the control group (M1-SMA). These results are consistent with those of Braver and colleagues (2003) and Dosenbach and colleagues (2006) who state that SMA is not involved in a switching task. They highlight brain areas (not SMA) that showed transient activation in response to task switching. These areas are the dorsolateral prefrontal cortex (PFC), ventrolateral (vlPFC) and superior parietal cortex. They also stress that the ventral anterior cingulate cortex and the anterior PFC showed sustained activation as the result of a switching task.

SMA responds to conflict among current motor plans (Gazzaniga, 2009). Therefore, our results are consistent with the view that a switching task is not an appropriate behavioural task for studies that target SMA regulation. Another behavioural task used in this thesis is the Go/No-go task, which is a behavioural test used to measure the response rehibition to assess motor performance (Hershey et al., 2010). In this task, a response must be given in the "go" trials and inhibited in the "no-go" trials, providing a cognitively engaging scenario. In the Go/No-go task, participants were instructed to respond as quickly and accurately as possible and related decreases in reaction time between pre-test and post-test were found in both groups for the right hand. Importantly, this decrease was only significant in the control group. The reduction in reaction time in the NF group (M1-thalamus) was not significant. In the control group, we targeted the connectivity between M1 and SMA. The Go/No-go task involves planning and initiation of movements during the Go trials and inhibition of inappropriate actions during the No-go trials. These processes are likely mediated by the SMA (Nachev et al., 2008). The SMA has direct connections to M1, the ventrolateral thalamus and to the spinal cord via the corticospinal tract (Johansen-Berg et al., 2004; Nachev et al., 2008; Arai et al., 2012) and it has been shown that modulating SMA activity can increase the cortical excitability of M1 (Arai et al., 2012). These results of reduced motor reaction time following M1-SMA modulation are consistent with those of Al-Wasity and colleagues (2021) who stated that the Go/No Go task is a suitable behavioural task when modulating SMA. Therefore, the Go/No-go task is not a recommended behavioural task to test motor performance after the regulation of M1-thalamus connectivity using rt-fMRI neurofeedback, however, it is highly recommended for use as a behavioural test when modulating M1-SMA connectivity.

Whole-brain analysis reveals widespread brain activation in the M1-thalamus NF group rather than the targeted areas. For the NF group, activations were found in the right BA 6, thalamus and left BA 6 and left BA 40 in the left parietal lobe. It was expected that an activation in M1 and the thalamus would be found because these are areas where participants receive neurofeedback. Participants were instructed to imagine actions using two hands, which resulted in M1 activation since it is responsible for controlling voluntary motor movement on

the body's contralateral side (Banker and Tadi, 2019). This result is consistent with Mulder's results (2017) which found that motor imagery corresponds to activation of the neural correlates of motor representations and M1 will be activated in a similar manner to activation during actual motor execution.
The activation in the left parietal lobe could be due to using motor imagery (MI) because fMRI activation in the left parietal lobe was associated with MI and increased over time. This is because motor imagery recruits a fronto-parietal network and subcortical and cerebellar regions (Hétu et al., 2013; Lebon et al., 2018).
Comparison of brain activation between the experimental and the control groups showed significantly higher activations in the left M1, bilateral cerebellum and bilateral precentral gyrus of the M1-thalamus NF group, supporting our hypothesis that the experimental group would be able to increase the activation of M1-thalamus connectivity during NF training. These results are consistent with those of a study conducted by Al-Wasity and colleagues (2021), who found a significant difference between the experimental group and the control group in their study.

5.5 Conclusion

In this study, using a rt-fMRI connectivity neurofeedback method, we tested the hypothesis that connectivity neurofeedback can be used to train upregulation between M1 and the thalamus to improve motor performance. This capability would be especially beneficial to those known to have motor impairment, such as chronic stroke patients. Our results show that participants in the M1-thalamus NFB group learned to up-regulate and enhance their brain activity whilst receiving real-time feedback of the connectivity between M1 and the thalamus, compared with the control group who did not manage to upregulate activity. This suggests that up-regulation of connectivity neurofeedback between M1 and the thalamus can be achieved within two rt-fMRI neurofeedback sessions. Our results also reveal that a switching task is a suitable behavioural task that can be used when targeting the connectivity neurofeedback between M1 and the thalamus and that a Go/No-go task is a suitable behavioural task when investigating the connectivity neurofeedback between M1 and SMA.

6 Chapter six: M1-cerebellum connectivity modulation using real-time fMRI neurofeedback

Abstract

Real-time functional magnetic resonance imaging (rt-fMRI) neurofeedback is a tool used to obtain voluntary control over the activity of different regions of the brain including providing feedback regarding the connectivity between brain regions. Such connectivity neurofeedback can be a more effective feedback strategy than providing feedback from a single region. Enhancing connectivity between cortical and subcortical regions holds promise in improving motor function.

The cerebellum plays an important role in motor activity, especially for timing and precise movements. It is also involved in motor learning and in improved motor performance. The cerebral cortex and the cerebellum are spatially remote areas that are connected by complex circuits linking both primary and associative areas.

Using rt-fMRI neurofeedback in the present study, we aimed to investigate the effect of connectivity neurofeedback during motor imagery. The primary motor area (M1)-cerebellum connectivity was targeted as these regions play a role in performing motor actions.

Four right-handed participants were recruited for this research to test their ability to modulate the connectivity neurofeedback between the M1 and cerebellum. The results showed that there was enhancement in the connectivity neurofeedback between M1 and the cerebellum for each participant. However, this enhancement was not statistically significant.

6.1 Introduction

Research on cerebellar functions has increased tremendously during recent decades. The cerebellum plays an important role in motor functions, especially in timing and the precision of skilled movements (Bernard et al., 2012). Functional neuroimaging in humans also provides evidence that the cerebellum is involved in motor learning and performance. The right cerebellar hemisphere is connected to the left motor cortex and the left cerebellar hemisphere is connected the right motor cortex. This means any damage to the right side of the cerebellum affects the right side of the body and verse versa.

Functional magnetic resonance imaging (fMRI) studies demonstrate that the cerebellum is activated by many tasks including sensory and motor tasks, with fMRI able to identify any increases and decreases in activity for each task.

The role of the cerebellum is not limited to actual movement, it is involved in many mental aspects such as motor imagery (Kuhtz-Buschbeck et al., 2004). The cerebellum has been a target for many functional imaging studies. For example, Fox and colleagues (1985) conducted the first functional study of the cerebellum using a PET scan which showed that voluntary movement of fingers activated the bilateral lobule V of the cerebellum. Kuhtz-Buschbeck and colleagues (2003) conducted fMRI experiments that showed an activation in the anterior cerebellum, particularly in lobules IV and V, during a finger-tapping task.

Stoodley and Schmahmann (2009) demonstrated that the cerebellar areas subserving motor functions are distinct from those subserving cognitive functions and other non-motor functions. fMRI data has provided evidence that motor tasks are largely in the domain of the anterior cerebellum while cognitive tasks, such as working memory, are dominated by the posterior cerebellum (Stoodley et al., 2012).

The need to understand the connectivity between the cerebellum and cortical areas is imperative as it helps in understanding the mechanisms that play a role in the pathophysiology of motor disorders related to the cerebellum. Hoover and

Strick (1999) investigated the connection between the cerebellum and the primary motor cortex (M1) and found an indirect connection between the primary motor cortex (M1) and cerebellum. M1 is the target of both cerebellar and basal ganglia output, however, there are many cortical areas such as the premotor cortex and the prefrontal cortex that also receive input/messages from the cerebellum and basal ganglia (Hoover and Strick, 1999).

The effects of the cerebellum on motor functions are mediated as it influences the motor cortex and cortico-spinal outputs. Purkinje cells, which are the output of the cerebellar cortex, have inhibitory connections with the deep cerebellar nuclei (DCN), which have a dyspeptic excitatory pathway through the ventral thalamus to the motor cortex (Daskalakis et al., 2004).

FMRI studies have provided evidence to support the long-held belief that relatively intact cerebellar circuits may compensate for impaired functioning of the basal ganglia, resulting in a rise in cerebellar activity in patients with Parkinson's disease (Manto et al., 2012).

Many studies have been conducted to investigate the connection between the motor cortex and cerebellum for different purposes. For example, using fMRI, Anteraper et al. (2019) investigated resting-state functional-connectivity in young adults with high-functioning autism spectrum disorder (HF-ASD). They showed cerebellar functional connectivity disruptions in a cohort of HF-ASD subjects and stressed that the cerebellum is a potential target for therapeutic, diagnostic, predictive and prognostic developments in ASD.

Kaut et al., (2020) investigated the functional connectivity within the cerebellum in Parkinson's disease. They found significantly increased connectivity between the cerebellar cortex and the vermis of the cerebellum in Parkinson's disease patients compared with healthy participants. Furthermore, Ramos and colleagues (2019) explored the differences in intrinsic cortico-cerebellar functional connectivity between participants with autism spectrum disorder and participants with typical development using resting-state fMRI. Their results showed a reduction in the connectivity between the cerebellum and cognitive cortical areas such as the right fusiform gyrus, the right

postcentral gyrus, the right superior temporal gyrus, the right middle temporal gyrus and the left middle temporal gyrus.

Mostofsky and his colleagues (2009) investigated connectivity during sequential finger tapping in children with high-functioning autism (HFA) and typically developing children (TD). Their results showed activations in cortical and subcortical regions associated with motor execution such as the contralateral primary sensorimotor cortex, the contralateral thalamus, the ipsilateral cerebellum and the supplementary motor area (SMA). However, the TD group showed greater activation in the ipsilateral anterior cerebellum, while the HFA group showed greater activation in the SMA. They also showed that children with HFA demonstrated decreased connectivity between the anterior cerebellum (lobules IV/V) and motor cortical areas by comparison with control children (Mostofsky et al., 2009).

Motor imagery (MI) is a cognitive process in which people simulate actions or movements internally without the use of any apparent movement (Blefari et al., 2015). In motor imagery, participants imagine performing actions without any physical output (Jeannerod, 2001). There are two types of MI: visual imagery (VI) and kinaesthetic imagery (KI) (Guillot *et al.*, 2009). VI is to imagine action either from a first-person perspective (internal VI) or third-person perspective (external VI). During internal VI, people are asked to imagine observing actions and imagine themselves performing that in real-time, namely, from the imagined perspective of their own eyes. During external VI, participants are asked to imagine that there is a person is performing the action in front of them. KI is to imagine the observed actions including the feelings and sensations associated with those actions (Vogt *et al.*, 2013).

MI and motor execution (ME) engage similar neural networks (Jeannerod, 2001; Lotze et al., 2006). MI plays an essential role in motor learning tasks (Schuster *et al.*, 2011) as it is usually performed in motor learning skills (Mizuguchi et al., 2013). MI could be beneficial for athletics, skill acquisition and rehabilitation (Ietswaart *et al.*, 2011) as it can be used to improve motor performance over different time periods (Gentili *et al.*, 2010).

Imagining any motor action such as clenching or tapping without physical movement resulted in activation in the cerebellum (Mostofsky et al., 2009). Lotze and colleagues (2006) found that significant activation was detected in the cerebellum during ME, however, activation fell by 30% during MI (Lotze et al., 2006).

Neurofeedback can be defined as the measurement of neural activity in a participant that is represented to them as visual or auditory signals to enable self-regulation of neural activity (Mizuguchi *et al.*, 2013). Real-time fMRI (rt-fMRI) systems have been used for neurofeedback due to their speed and ability to provide feedback signals from the brain activity of deeper brain structures and with higher spatial resolution (Ruiz et al., 2014).

The present study described below aimed to investigate the ability of participants to modulate the connectivity neurofeedback between cerebellum and primary motor cortex (M1). Such modulation can provide information on the connection between cerebellum and motor cortex in healthy participants. Modulation of M1- cerebellum connectivity using fMRI has not previously been investigated in the literature. The ability to modulate M1-cerebellum connectivity would have the potential to improve motor functions and, hence, be beneficial in the therapy used for some diseases such as Parkinson's disease and motor deficits associated with autism (Dahlberg et al., 2020; Mostofsky et al., 2009).

6.2 Methods

6.2.1 Participants

Four participants (three males and one female) with normal or corrected-to-normal vision were recruited for this study. Each participant verified that their visual acuity was sufficient to resolve images and text presented on the screen without any correction. All participants were right-handed as determined by the Edinburgh Handedness Inventory (Oldfield, 1971). Participants were all proficient in written and spoken English. Their mean age was 36 years. Each participant undertook a Vividness of Movement Imagery Questionnaire-2 (VMIQ-2) (Callow and Roberts, 2010) to measure their ability to perform the motor

imagery tasks.

The VMIQ-2 is a revision of the Vividness of Movement Imagery Questionnaire (VMIQ: Isaac, Marks, and Russell, 1986) and comprises 12 items that evaluate the ability of an individual to imagine different movements. There are two ways to perform motor imagery: using internal visual imagery (first person perspective) and using external visual imagery (third person perspective), with ratings of vividness performed on a five-point Likert scale from 1 (perfectly clear and vivid) to 5 (cannot imagine at all). The VMIQ-2 has shown acceptable factorial validity, construct validity and concurrent validity as shown in table 7.

Table 7: Demographic features for participants in the NF and control groups

	M1-Cerebellum (Mean)
Number of participants	4
Age (years)	36
Handedness	92.5
MI vividness (third person perspective)	22.75
MI vividness (first person perspective)	21.5

This research was approved by the ethics committees of the College of Science and Engineering at the University of Glasgow. Consent was obtained from each participant for the experiment. The procedure of the whole experiment was explained to each participant prior to fMRI scanning. All participants completed an MRI safety checklist before undergoing the MRI scanning.

Imaging parameters and rt-fMRI neurofeedback platform

This prospective study was conducted between January 2019 and January 2020 using a 3T Siemens Tim Trio MRI scanner at the University of Glasgow Centre for Cognitive Neuroimaging (CCNi) with a 32-channel head coil. A T1-weighted high resolution anatomical scan was acquired at the beginning of the experiment (TR=2000ms, TE=2.52ms, 192 sagittal slices, 1 mm^3 isotropic voxels and image

resolution 256×256). T2*-weighted functional scans were collected with an Echo Planar Imaging (EPI) sequence (TR=2000ms, TE=30ms, whole brain coverage with 32 axial slices, 0.3 mm gap and 3 mm^3 isotropic voxels.

Participants in this study underwent a high-resolution anatomical scan (T1 weighted image), a functional localiser run and six NF runs.
For the NF runs, the data were sent volume by volume from the scanner to Turbo-BrainVoyager (TBV) software via a network connection. The functional data were then pre-processed in real time. Custom-made MATLAB code was used to estimate the connectivity between the two regions and this connectivity measure was shown as a thermometer bar on the monitor.

During the NF training, participants were instructed to increase the height of the thermometer bar by performing motor imagery of complex hand actions. No instructions were given on specific hand movements to be used during the motor imagery task. Participants were, therefore, free to explore which mental strategy and actions were useful in their situations to provide an enhancement of the thermometer bar. The height of the thermometer bar indicated connectivity between M1 and cerebellum as calculated using the Pearson correlation coefficient. An intermittent feedback paradigm that updated and displayed the thermometer bar level after each NF block was used.

6.2.2 Functional Localiser

The localiser run took approximately 5 minutes and was composed of 7 fixation blocks (16s) interspersed with 6 blocks of bimanual hand clenching (30s).
During the functional scanning (the localiser), participants were instructed to count either letters or numbers if “REST” appeared on the screen and to clench their fists if “Clench” appeared on the screen. The ‘Rest’ block lasts sixteen seconds and the ‘Clench’ block appears for thirty seconds.
The functional data were pre-processed and analysed online with an accumulative General Linear Model (GLM) embedded in Turbo-BrainVoyager and offline using BrainVoyager. The ROIs were defined in each participant in the native space.

6.2.3 Rt-fMRI neurofeedback

Every participant undertook NF training runs of 366s duration. Each NF training run consisted of 32s blocks. Each block comprised 14 seconds of rest (repeated twelve times during every run because every run started and ended with a rest block), 14 seconds when participants were asked to perform MI to modulate their brain activity (repeated eleven times), and 4 seconds when a thermometer bar was presented with the feedback signal (repeated eleven times) (Figure 6.1). During the NF blocks, participants were instructed to increase the activation of M1-cerebellum connectivity by imagining complex actions for 14 seconds. The thermometer bar was then displayed for 4 seconds after each NF block, representing the level of M1-cerebellum connectivity during the task. During the rest block, participants were instructed to count numbers or letters for 14 seconds, as a way of controlling the baseline activity (Hanakawa, 2011; Berman *et al.*, 2012).

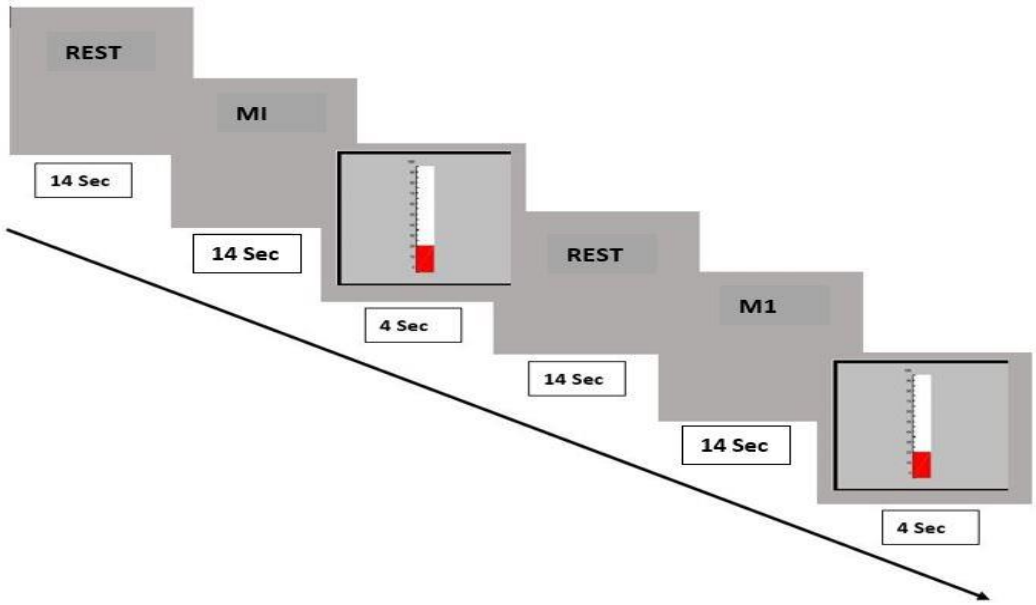

Figure 6-1 fMRI NF training paradigm design. A run lasted 366s and consisted of twelve 14s fixation (rest) blocks and eleven 14s NF blocks alternating with eleven segments when the thermometer bar was shown for 4 seconds.

6.2.4 Online data analysis

Turbo-BrainVoyager software and MATLAB were used to perform rt-fMRI data analysis and NF presentation. The data were sent, volume by volume, from the

scanner to Turbo-BrainVoyager via a network connection. The functional data were then pre-processed in real time.
The feedback signal consisted of an intermittent thermometer and was updated and displayed after each NF block based on the following equation:

$$\boldsymbol{bar\ height} = 50 * (Corr + 1) \qquad 6.1$$

Where scale is an arbitrary scale value to optimise visibility of the thermometer bar.

$$\mathbf{Corr}(\mathbf{x}, \mathbf{y}) = \frac{\sum_{i=1}^{n}(\boldsymbol{x_i} - \bar{\boldsymbol{x}})\ (\boldsymbol{y_i} - \bar{\boldsymbol{y}})}{\sqrt{\sum_{i=1}^{n}(\boldsymbol{x_i} - \bar{\boldsymbol{x}})^2}\sqrt{\sum_{i=1}^{n}(\boldsymbol{y_i} - \bar{\boldsymbol{y}})^2}} \qquad 6.2$$

Where **x** is a 14-s time course of M1, $\bar{\mathbf{x}}$ is the mean activation of M1 during a MI block, **y** is a 14-s time courses of the cerebellum and $\bar{\mathbf{y}}$ is the mean activation of cerebellum during a MI block.

6.2.5 Full brain analysis

The data were analysed offline using Brain Voyager QX 2.8.4 (Brain Innovation, Maastricht, the Netherlands) and custom-written MATLAB scripts (Version 8.2, The MathWorks Inc., Natick, MA, 2000). Anatomical T1 images were corrected for inhomogeneity and normalized to Talairach space. EPI data were slice-time corrected. Spatial alignment of all volumes to the first volume of the localiser was performed to correct for head motion. The fMRI data were co-registered to T1 images based on anatomical landmark points and co-registration was manually corrected if necessary.

The data were then normalised to Talairach space using rigid body transformation and scaling. Linear drifts were removed and a temporal high-pass filter (2 cycles) was used to eliminate non-linear drifts in the time series. Data were spatially smoothed using a Gaussian kernel with 6-mm full width at half maximum. All the pre-processed functional data of each subject were analysed using a General Linear Model (GLM) with two predictors (fist clenching and rest for analysis of the localiser; feedback and rest for analysis of NF), convolved with a hemodynamic response function and covariates derived from six head motion parameters (Johnston *et al.*, 2010; Dijk *et al.*, 2012).

Group data were evaluated based on a second level random effect analysis general linear model (RFX-GLM). The obtained statistical maps were first thresholded and these maps corrected for multiple comparisons using cluster-level thresholding (Goebel *et al.*, 2006).
Whole brain RFX-GLM analyses were then performed: all 6 NFB runs, comparing the NFB blocks with the baseline ($p<0.01$ uncorrected with cluster-level thresholding of $300mm^3$ for the NFB).

6.2.6 Statistical analysis

A *t*-test was used as a post-hoc test to compare the means of correlation in the first and the last runs. Furthermore, a linear regression of the average connectivity values over neurofeedback runs was used to examine the upregulation over runs.

6.3 Results

6.3.1 Connectivity Analysis

During the localiser, all participants showed activations in the cerebellum and M1 as a result of hand clenching, as seen in Figures 6.2 and 6.3.

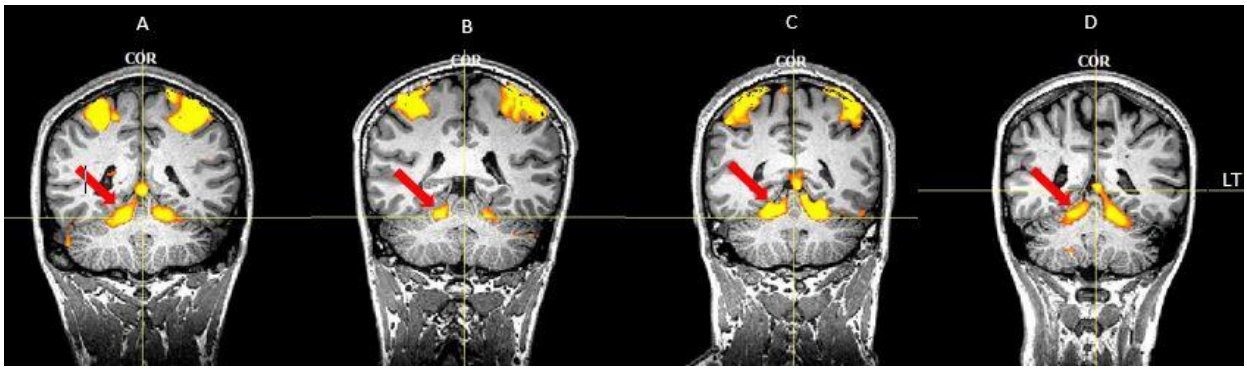

Figure 6-2 This figure shows activation in the bilateral cerebellum as a result of hand clenching. Panels A, B, C and D show coronal images of the first, second and third participants, respectively. Red arrows indicate activation in the right motor cerebellum.

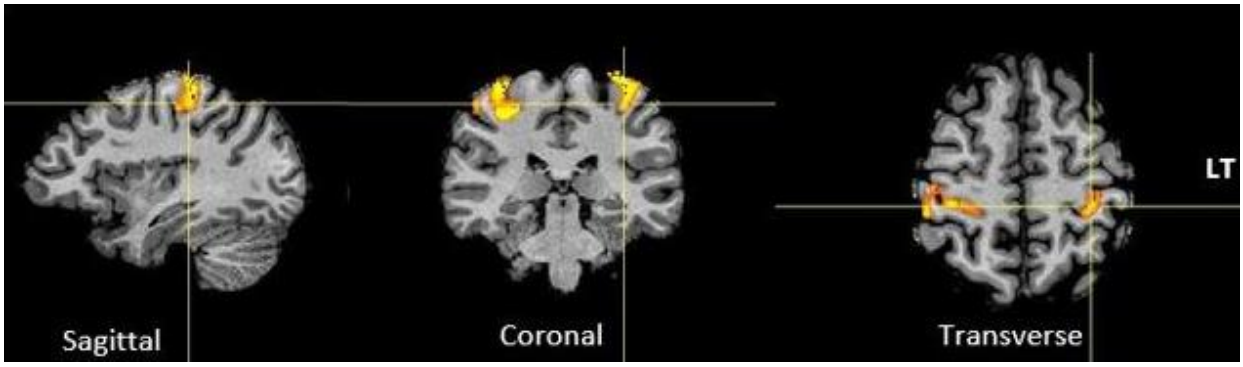

Figure 6-3 This figure shows activation in the bilateral M1 as a result of hand clenching.

Each participant successfully completed six runs. Figure 6.4 shows that participants appeared to upregulate the activation between M1-cerebellum at run 2 and 3 then drop at run 4, with the activation levels increasing again at run 6. Overall, participants showed a trend for successfully increasing the activations over runs, as seen as in Figure 6.4. However, the linear regression did not show an increase in the mean M1-cerebellum activity across runs in the NF group, which would indicate no learning effect (Intercept coefficient = -0.103, with R^2 =0.272, X variable coefficient =0.0087, p =0.0739).

These results suggesting successful upregulation are supported by the differences found in the activation levels from run 1 to run 6. Although there is an enhancement in the correlation seen at run 6 compared with run 1 (see Figure 6.5), the paired *t* test showed that the detected enhancement was not statistically significant (p= 0.287).

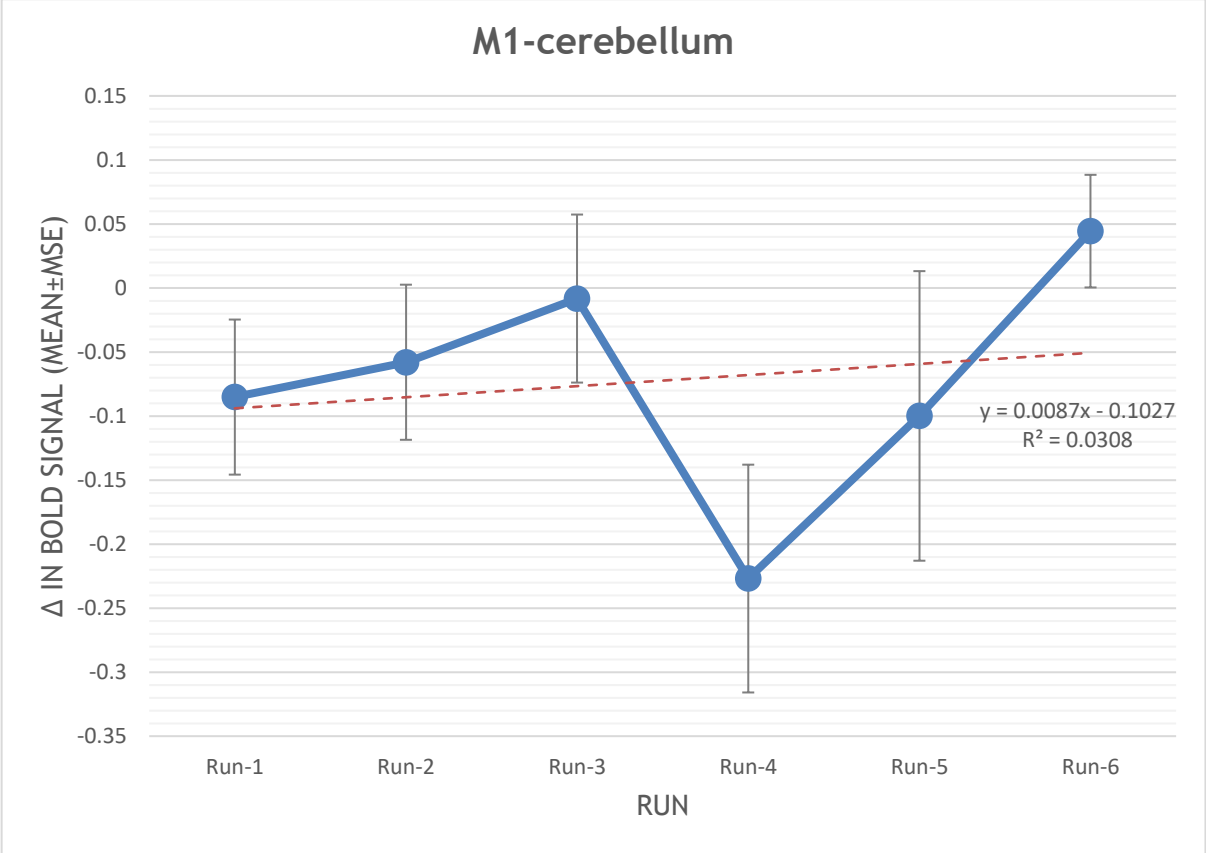

Figure 6-4 this figure shows the average BOLD signal change of M1-cerebellum connectivity when comparing the first and last runs. The error bars represent the standard error of the mean.

The results obtained from four participants indicated that they were not able to upregulate the connectivity neurofeedback between M1 and the cerebellum by using motor imagery and they did not show a learning effect.
In addition, participants reported that they believed that mental strategies such as imagining playing music, knocking on doors and lifting weights could be used to raise the level of the thermometer bar during the training.

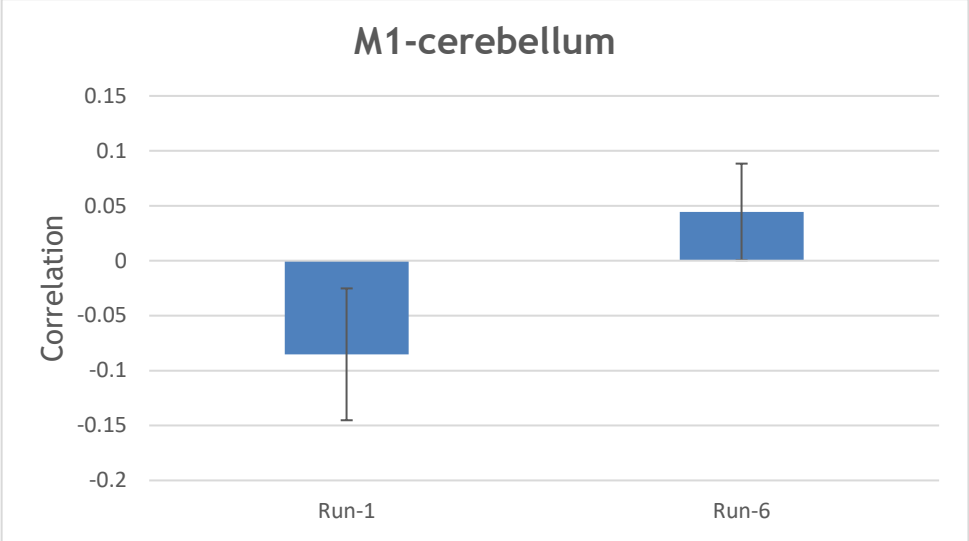

Figure 6-5 This figure shows the correlation between M1 and the cerebellum in the first run and last run. The error bars represent the standard error of the mean.

6.3.2 Whole brain analysis

A whole-brain RFX-GLM analysis was performed for NF runs (p<0.01 uncorrected) to investigate whether any brain regions were activated during the MI guided by the NF. The active regions of NF are listed in Table 8 and illustrated in Figures 6.6 and 6.7. The activation was seen at M1 and the cerebellum where the feedback was received. In addition, activation also seen at areas such as the bilateral parietal lobe, the bilateral insula and the caudate body.

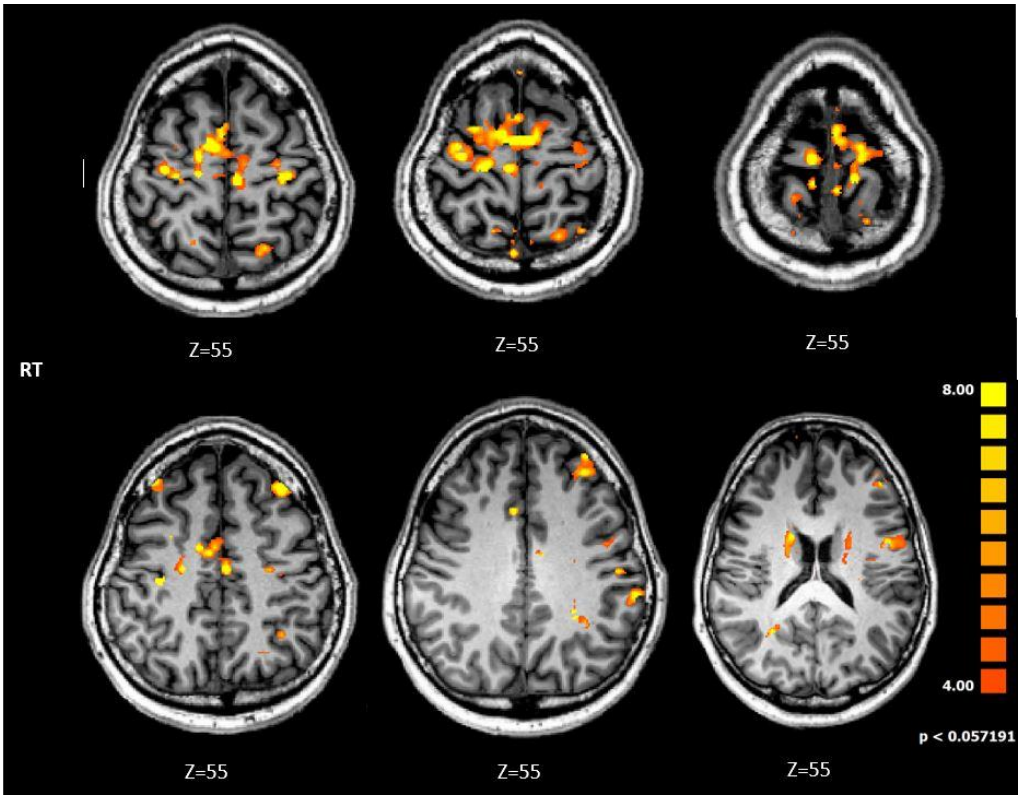

Figure 6-6 Results of the analysis of NF runs shown for the NF group (transverse images). These activations are significant at p<0.01 (uncorrected).

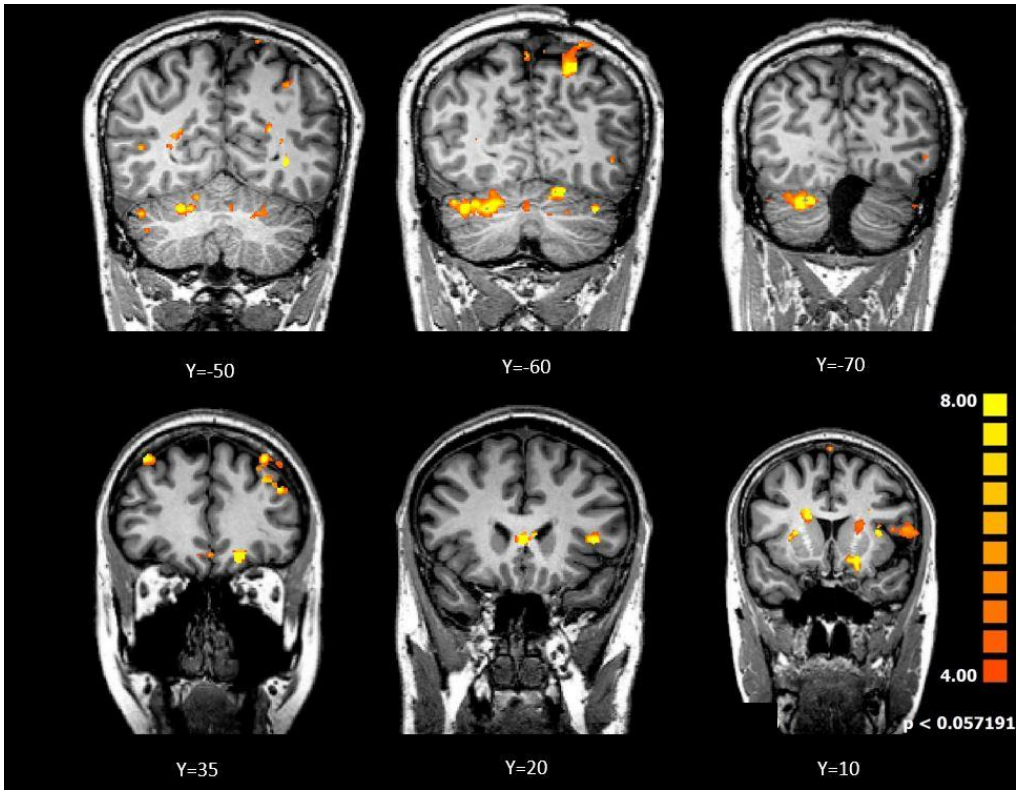

Figure 6-7 Results of the analysis of NF runs shown for the NF group (coronal images). These activations are significant at p<0.01 (uncorrected).

Table 8 Clusters of brain activation during the NF

CORTEX	X	Y	Z	t	P value	Number of voxels
RT Parietal Lobe, BA 7	21	-58	52	23.923	0.00174	5502
RT Insula, BA 13	32	-22	13	109.41	0.00008	14583
RT Caudate Body	12	7	25	52.201	0.00037	1470
LT Parietal Lobe, BA 7	-21	-58	34	54.443	0.000337	1278
LT Precentral Gyrus, BA 4	-33	-19	55	17.813	0.003137	257
LT Insula, BA 13	-33	8	10	92.853	0.000116	3903
LT Frontal Lobe, BA 9	-39	47	28	47.463	0.000444	2581
LT Cerebellum, Anterior lobe	-32	-58	-23	23.666	0.00178	646
RT Cerebellum, Posterior lobe	33	-64	-24	9.0189	0.002878	308
RT Medial Frontal Gyrus, BA 6	15	-7	56	24.706	0.000145	2221
LT Superior Frontal Gyrus, BA 6	-9	-1	63	7.4269	0.00505	603
RT Cerebellum, Anterior lobe	21	-59	-23	23.923	0.00174	5502
LT Cerebellum, Posterior lobe	-12	-59	-14	31.858	0.00098	520

6.4 Discussion

In this study we found preliminary evidence that healthy volunteers could learn, in a single session, to increase the activity in their functionally localised M1-cerebellum connectivity, during a MI task of complex body actions whilst receiving an intermittent feedback signal (displayed as the height of a thermometer bar). This feedback signal represented the activity of individuals localised in the correlation between left M1 and right cerebellum.

There is an absence in the literature regarding the correlation between motor areas and cerebellum using real-time fMRI. However, some research has investigated M1-cerebellum connectivity using resting-state fMRI (Daskalakis et al., 2004). The limited number of studies published to explore the correlation between motor areas and cerebellum, by using either resting-state fMRI or real-time fMRI NF, challenges any attempt to draw conclusions regarding the success of modulation in each subject (Tursic et al., 2020).
Every participant was able to modulate the connectivity neurofeedback between M1 and the cerebellum as the mean of the correlation at the last run was higher than that of the first run. However, the statistical analysis showed that the detected increase in the correlation was not significant.

A linear regression of the average connectivity values over neurofeedback runs was used to examine the upregulation over runs. A *t* test was carried out as an exploratory analysis to compare the correlation means between the first and last runs, with the difference between the first and last runs indicating the effect of training. However, neither of the two tests showed a statistically significant result. The possible reason could be the number of participants (four) recruited for this study. The size of the effect in this research is small and this influences the probability of finding a true effect since larger sample sizes lead to larger effects being observed and vice versa (Tursic et al., 2020).

Motor imagery (MI) occurs when a participant performs motor tasks mentally without any physical motor output. Many previous studies indicated that MI shares similar motor regions as those used when preparing for and performing actual motor actions (motor execution) (Cengiz and Baron, 2016). The mental

task of motor imagery has been used successfully and widely in real-time research to modulate brain activity in single regions such as the sensorimotor cortex (Yoo et al., 2008), M1 (deCharms et al., 2004), and SMA (Al-Wasity et al., 2021). Our results are consistent with those of (Lotze et al., 2006; Cengiz and Baron, 2016) who found that MI can activate the cerebellum since there were activations detected in the cerebellum and M1 as a result of motor imagery tasks.

The instruction strategy used in this research was an implicit strategy in which participants were asked to develop their own effective strategies to enhance their mental activity level during NF training. They reported that imagining playing music and lifting weights were associated with positive results on the thermometer bar. This implicit strategy is widely used in rt-fMRI NF research (Paret et al., 2014). However, a known disadvantage of this strategy is that when participants identify an action that leads to enhancement in their neural activity level, they stop exploring new mental action which could provide more activation (Paret et al., 2019).

Real-time fMRI allows for tracking of whole-brain activity to investigate the distributed learning processes in the brain. Most real-time fMRI studies showed that the training effects take place primarily in the neurofeedback target region (e.g., deCharms et al., 2004, 2005; Lee et al., 2011; Weiskopf et al., 2003). Recent studies have assessed the effects of self-regulation and learning of self-regulation on connectivity with effective connectivity analyses (Hamilton et al., 2011; Lee et al., 2011; Rota et al., 2011; Ruiz et al., 2014). The results of many real-time fMRI NF studies on connectivity indicate that neurofeedback training leads to specific changes in the connectivity of the target region, usually strengthening the relevant connections and suppressing others. Therefore, full-brain analysis provides information about target regions' activation and changes in connectivity. In this research, full-brain analysis was conducted to track the activation which occurred in the brain during the training.

The current results of a rise in correlation observed in individuals suggest that M1-cerebellum connectivity could be modulated using real-time fMRI NF. The activation seen at both M1 and the cerebellum in the full-brain analysis

supported this finding. Lindeman and colleagues (2021) demonstrated that M1 and the cerebellum can be modulated since they used a non-MRI technique to achieve that goal. They used whisker stimulation of Purkinje cells of the cerebellum to modulate the coherence between the primary somatosensory cortex (S1) and M1 and the cerebellum.

The previous resting-state fMRI research highlighted an indirect connection between M1 and the cerebellum (Daskalakis et al., 2004). Since our online and offline results reveal an effect on the targeted connectivity, we suggest undertaking further research with a larger sample size in the future.
During the NF training, full-brain analysis showed an activation of the bilateral parietal lobe. These areas were possibly activated due to the processing of visual stimuli. During the NF experiment, participants received visual feedback via a thermometer bar to indicate the activation levels of a motor imagery task. These feedback projections might be exploited to boost recruitment of parietal lobes by means of real-time neurofeedback (Andersson et al., 2019).

In addition, the activation in the left parietal lobe could be due to using motor imagery (MI), since fMRI activation in the left parietal lobe was associated with MI and increased over time since it is known to recruit a fronto-parietal network and subcortical and cerebellar regions (Hétu et al., 2013; Lebon et al., 2018). The activation shown in the insula during NF training could be because the insula plays an essential role in processing intentional movement and awareness (Tinaz et al., 2018).

Furthermore, activation in the insula during NF could be associated with the sense of self-agency during voluntary motor tasks (Farrer and Frith, 2002). Motor imagery evokes sensorimotor simulations of one's own body and recruits the sensorimotor-related brain regions including the insula (Lorey et al., 2009). Furthermore, Emmert et al., (2016) demonstrated that the insula is a key region in the brain as it consistently activated during self-regulation in real-time fMRI neurofeedback independent of the targeted region of interest.

6.5 Limitations and recommendations

This pilot study was conducted on only four participants and a small sample size is one of the primary reasons for underpowered studies (Algermissen and Mehler, 2018). Statistical power is the probability that an effect will be detected when it is actually present and it depends on the size of the effect and of the group sampled. Larger effects have a higher probability of being observed and larger groups increase the probability of finding a true effect (Tursic et al., 2020). Therefore, undertaking power analysis and recruiting more participants and to increase the sample size is recommended in future to increase the probability of finding a true effect, hence, a learning effect.

There was also no control group recruited in this research. Having a control group is important to be able to attribute effects to neurofeedback (Fede et al., 2020). Therefore, recruiting a control group for the neurofeedback experiment is necessary for comparison. This will demonstrate the importance of the feedback for learning self-regulation that occurs in the experimental group.

Based on our pilot data in chapter six (see 6.3 results) (N=4), comparing Run (first run, last run). The effect size (ES) in this study was 0.66, considered to be extremely large to medium using Cohen's (1988) criteria (Faul et al., 2007). With an alpha = .05 and power = 0.80, the projected sample size needed with this effect size (G*Power 3.1) is approximately N =16 for this simplest within group comparison. Thus, our proposed sample size of 16 participants in the experimental group would be more than adequate for the main objective of a future study. This would be a minimum and with more complex designs involving possible control conditions and control groups would increase.

Finally, this pilot study did not include any behavioural task to measure the behavioural changes that may occur as result of neurofeedback training, therefore, there was no measurement of regulation processes. Adding a valid behavioural task is recommended.

6.6 Conclusion

In conclusion, real-time functional magnetic resonance imaging (rt-fMRI) neurofeedback is a tool used to obtain voluntary control over the activity of different regions of the brain and includes providing feedback about the connectivity between brain regions. Such connectivity neurofeedback can be a more effective feedback strategy than providing feedback from a single region. Enhancing connectivity between cortical and subcortical regions holds promise for improving motor function.

The cerebellum plays an essential role in motor performance, especially in the timing and precision of skilled movement. M1 also plays a key role in planning and executing movements. The cerebral cortex and the cerebellum are connected by complex circuits that link both primary and associative areas, namely, cortico-cerebellar connections. This circuit is disturbed in many diseases such as Parkinson's disease and autism, therefore, the ability to enhance this connectivity may lead to positive results in developing therapies. Modulating the M1-cerebellum using real-time fMRI NF was shown to be a potentially useful tool to modulate M1-cerebellum connectivity.

We used this technique here and found an apparent enhancement in in the connectivity neurofeedback between M1 and the cerebellum in each participant. However, this enhancement was not statistically significant. Further investigation is required and recruiting more participants as well as adding a control group and behavioural task are recommended.

7 Chapter Seven: General discussion

7.1 General summary

The experimental studies in this thesis examined connectivity neurofeedback using motor imagery (MI) -based real-time fMRI neurofeedback. Several preliminary studies, such as defining motor localisers, were performed to refine the experimental method. In the first experiment, we targeted the connectivity neurofeedback between the primary motor cortex and the motor thalamus. In the second experiment, the connectivity neurofeedback between the primary motor cortex and the cerebellum was targeted. We investigated the participants' ability to upregulate the connectivity neurofeedback between the targeted regions in these studies.
In this general discussion, I will review the key findings and the implications of the experimental chapters and relate them to the aims of this thesis.

7.2 Neurofeedback

During neurofeedback experiments, the BOLD signal is processed and displayed to participants in real-time to enable self-regulation of brain activity. Previous fMRI neurofeedback (fMRI-NF) research has shown that it is possible to self-regulate the activity in brain regions or networks and, therefore, this regulation could impact behavioural variables (Emmert et al., 2016). Most of the rt-fMRI-NF research has been conducted with healthy subjects to investigate the neural substrates and possibilities of neurofeedback. Recently, rt-fMRI-NF research has shifted towards clinical applications due to the ability in patients suffering from psychiatric and neurological disorders to self-regulate brain activity (Gonzalez-Castillo et al., 2020).

In this thesis, a fMRI-NF system was established to modulate brain activity in healthy participants and also to investigate whether, as a consequence, fMRI-NF training can alter the behaviours of the targeted brain regions.
In the first and second experiments in the thesis, we used MI-based real-time neurofeedback to upregulate connectivity neurofeedback between M1 and the motor thalamus and M1 and the cerebellum. M1 plays a key role in the planning and execution of movements and has a large cortical representation for hand

and finger movements. The motor thalamus plays a role in the complex cognitive and proprioceptive control of movement (Middleton and Strick, 2000). It also plays a role in maintaining posture, general movement and motor learning (Bosch-Bouju et al., 2013). The ventral lateral nucleus of the thalamus (VL) serves as a central integrative centre for motor control, receiving inputs from the cerebellum, striatum and cortex and projects to the primary motor cortex (Bosch-Bouju et al., 2013).

Participants in the neurofeedback group of the M1-thalamus connectivity experiment (Chapter five) received an intermittent feedback signal in the form of a thermometer bar representing the percentage change of activation in the M1-thalamus connectivity. The results of modulation of the M1-thalamus connectivity study showed that participants were able to upregulate the connectivity neurofeedback. These results were consistent with those of Liew et al., (2016) who explored the connectivity between M1 and the thalamus in four stroke patients. In that study, three of the four participants successfully increased the connectivity between M1 and the thalamus.

The results of this research (Chapter five) are consistent with the results of Megumi and colleagues (2015) who found that rt-fMRI-NF is a tool capable of modulating functional connectivity. The results of Megumi et al. (2015) demonstrated an improvement in the connectivity between M1 and the parietal cortex by using rt-fMRI-NF. Also, our results are consistent with those of Hamilton et al. (2011), Lee et al. (2011) and Rota et al. (2011), who found that neurofeedback training leads to specific changes in connectivity of the target region, usually strengthening the relevant connections and suppressing others (Weiskopf, 2012).

The cerebellum plays an important role in motor functions, especially those related to timing and the precision of skilled movements. It is also involved in motor learning and performance (Cengiz and Boran, 2016). In the M1-cerebellum experiment (Chapter six), participants demonstrated enhanced connectivity neurofeedback between M1 and the cerebellum, however, this enhancement was not statistically significant.

The whole-brain GLM analysis of the neurofeedback group in both experiments revealed widespread cortical activation in the motor and motor-related regions (including the bilateral BA 6, thalamus, left BA 40, bilateral parietal lobe, bilateral insula and caudate body), areas that play an important role in planning, selecting, learning and preparation of movements. The activation detected in the left parietal lobe could be related to the use of MI. This activation is consistent with the findings of Hétu et al. (2013) and Lebon et al. (2018), who showed an activation in the left parietal lobe which was associated with MI and that activation increased over time, consistent with recruitment of a fronto-parietal network as well as subcortical and cerebellar regions. Consistent with the results of Emmert et al., (2016) and Farrer and Frith (2002), our results showed an activation at the insula, which is considered a key region in the brain for self-regulation, as it was consistently activated during rt-fMRI-NF independent of the targeted region of interest. The insula also plays an essential role in processing intentional movement and awareness and also in the sense of self-agency during voluntary motor tasks (Tinaz et al., 2018; Farrer and Frith, 2002).

In our experiments, we used Pearson's correlation coefficient to test the increase in connectivity during the M1-thalamus training in the first experiment and between M1 and the cerebellum in the second experiment. This technique has been used previously to modulate the connectivity using rt-fMRI (Megumi et al., 2015; Liew et al., 2016; Yamashita et al., 2018). Frassle and colleagues (2021) stated that Pearson's correlation coefficient between the respective BOLD signal time series is the simplest way to assess functional connectivity.

The connectivity between brain regions can be measured by different methods such as dynamic causal modelling (Frassle et al., 2021), partial correlation, coherence, mutual information, and independent component analysis and dynamic causal modelling (Karahanoglu and Van De Ville, 2017).
MI is a cognitive process in which people simulate actions or movements internally without use of any apparent movement (Blefari et al., 2015). MI can be used to enhance motor skills in healthy and clinical populations (Alkadhi et al., 2004) and it is usually performed in motor learning skills (Mizuguchi et al., 2013).

Most rt-fMRI-NF studies conducted that targeted modulation of motor areas were based on MI (Fede et al., 2020). However, there have been mixed results regarding the role of MI in modulation using rt-fMRI NF, for example, Berman and colleagues (2012) demonstrated that MI was not useful for M1 modulation while Mehler et al. (2019) found that MI-based neurofeedback was associated with an increase in SMA activation but a drop in M1 activation. Furthermore, Al-Wasity et al. (2021) demonstrated that MI is a useful motor task to upregulate SMA using rt-fMRI-NF.

Our results showed that participants were able to upregulate M1-thalamus and M1-cerebellum connectivity using MI based rt-fMRI-NF. These results are consistent with those of Liew et al. (2016), who showed that MI could be used to enhance the connectivity between cortical and subcortical regions.
Sharma et al. (2009) suggested that different types of MI might recruit different neural substrates. For example, kinesthetic MI recruits motor areas including the supplementary motor area (SMA), therefore, this type of imagery is of interest for motor rehabilitation (Guillot et al., 2009; Hetu et al., 2013).

In addition, MI-based rt-fMRI-NF can result in structural changes, with Papoutsi et al. (2018) suggesting that several sessions of rt-fMRI training of SMA leads to increased grey matter in the pre-SMA, therefore, areas receiving the training could result in plastic changes due to MI. In our research, we did not provide specific instruction about the MI task and we left it to participants to search for the best action to imagine which would increase the level of the thermometer bar.

In my research, described in this thesis, I used intermittent feedback because it has advantages over continuous feedback, such as no distraction during the performance of the MI task. Furthermore, intermittent feedback overcomes the haemodynamic delay that may occur during the use of continuous feedback, with the thermometer bar being displayed at the end of each feedback block in intermittent feedback (Fede et al., 2020). Our intermittent design was influenced by Megumi et al. (2015) and Yamashita et al. (2018) who used intermittent feedback in their designs to modulate connectivity neurofeedback

using rt-fMRI-NF.

In our experiments, every participant was informed about the purpose of the research, their initial strategy and the objectives of the training. An implicit strategy was used in our experiment as there was information given to focus on imagining actions using two hands to allow the subject to look for an applicable and effective mental approach. We asked participants to decide which MI action was suitable and which had a positive effect on the level of the thermometer bar (Sepulveda et al., 2016). This method is consistent with the strategy used by Al-Wasity et al. (2021).

An implicit strategy has advantages over an explicit strategy in the field of neurofeedback as it takes place independently of awareness (Amano et al., 2016; Birbaumer et al., 2013; Shibata et al., 2019). Therefore, an implicit strategy was used in this research. However, the explicit processes in motor skill learning occur faster, more time is required to unfold and they are sensitive to instruction (Muñoz-Moldes et al., 2020).

In the first experiment, two neurofeedback sessions were conducted with each group, with each session consisting of ten runs. This design was influenced by those of Kanel at al. (2019) and Al-Wasity et al. (2021) who conducted neurofeedback training over two sessions with each session involving ten runs. Fede and colleagues (2020) stated that the number of runs and sessions of neurofeedback training had better impact on neurofeedback and they stated that two sessions were considered ideal because the effect of neurofeedback changes to neural processes and symptomology is more credible when compared with one training session. However, the effects of the number of sessions and runs on neurofeedback training needs further investigation. In the second experiment we conducted only one session as it was a pilot study and, from those results, an increased number of sessions was recommended for future work.

The main objective of neurofeedback training is to identify behavioural effects occurring from learning to regulate brain activity. These effects are dependent on the function of the targeted regions. There are specific behavioural effects

associated with modulating particular brain regions, indicating the specificity of neurofeedback training. For example, reaction time changed with the modulation of motor areas (Weiskopf et al., 2004; Bray et al., 2007; Al-Wasity et al., 2021) and rating of emotional pictures changed during insula modulation (Caria et al., 2010). Since brain activation acts as an independent variable during neurofeedback learning, it allows causal references to be produced between brain activity and behaviour. The resulting behavioural changes from self-regulation of neural activation indicate that the physiological consequences of neurofeedback may be considered to be a form of endogenous neural stimulation (Sitaram et al., 2017).

In our first experiment, we conducted two behavioural tasks, namely, a switching task and Go/NoGo task. The results of the switching task were significant for the experimental group (M1-thalamus) but were not significant for the control group (M1-SMA). Our results were consistent with those of Hayes et al. (1998) who found that a switching task was significant with patients with Parkinson's disease. They suggested that this effect was because of the basal ganglia, which play a role in the switching effect. Since the basal ganglia play a role in switching and they are part of the closed cortico-basal ganglia-thalamo-cortical loop, a switching task can be used theoretically to assess behavioural changes resulting from neurofeedback training of the M1-thalamus. Our results supported this hypothesis as the switching task results showed a significant effect.

On the other hand, the results of Go/No Go task showed a significant decrease in the reaction time of the control group (M1-SMA), but no such effect was detected for the experimental group (M1-thalamus). These results are consistent with those of Al-Wasity et al. (2021) who state that the Go/No Go task showed a significant drop in the reaction time when modulating SMA using rt-fMRI-NF. Therefore, a Go/No Go task is a recommended behavioural task to test the motor performance after regulation of M1-SMA connectivity using rt-fMRI-NF.

7.3 Specific Limitations and Challenges in Conducting this Thesis Research

The first rt-fMRI experiment (Chapter five) was demanding, as it comprised two long sessions with participants reporting that each session was challenging since they required effort and concentration during ten runs, which took a long time. Many participants were unable to finish the procedure and they asked to stop the scanning due to fatigue or claustrophobia, while others did not attend the second session. Furthermore, many participants reported that they had fatigue during the scanning which had negative impacts on their performance and on the quality of the MI task in the last runs.

Another reason for excluding participants from completing the rt-fMRI experiments was excessive head motion during fMRI scanning. Head movement can also be related to the session length, as participants got uncomfortable after some time. These problems affected my progress in recruiting more participants. However, when designing the second experiment (Chapter six), reducing the length of the sessions and the number of runs was considered as a way of reducing fatigue and minimising head motion and loss of concentration.

Furthermore, in the first experiment (Chapter five) I had difficulty recruiting participants. For example, some participants were excluded from my research because they did not reach the minimum acceptable score on the Vividness of Movement Imagery Questionnaires-2 (VMIQ-2). Their scores indicated that they would have difficulty performing MI tasks. One of the criteria for participation in the first and second experiments was being right-handed. The Edinburgh Handedness Inventory questionnaire was used to confirm whether participants were right-handed or not. Two participants introduced themself as right-handed, however the Edinburgh Handedness Inventory demonstrated that they could use both hands equally well.

Finally, it is necessary to state that the coronavirus pandemic had extreme effects on this research as the college resources required to conduct advanced data analysis were not available and the CCNi MRI scanner used in this research was closed during the national lockdown. Therefore, because we were unable to

conduct any experiments or recruit participants, my research was suspended for more than one year.

Another issue arose at the CCNi research scanning facility that blocked my research progress. During the Coronavirus pandemic, the scanner was upgraded and the scanner was down for a week. Following this, issues with the upgrade were discovered. Various functionalities such as multiband sequences and real-time transfer, which were necessary to conduct my research, were no longer available and needed to be repaired. The issue with real-time transfer remained unsolved until late April, 2021.

The scanning facility then became available in May for my research and I did make progress during this time but, due to Covid social distancing restrictions and cleaning protocols, it was not possible to scan at full capacity. As restrictions became more relaxed in early July 2021 and I was poised to quickly complete this study, there was a flood in the MRI plant room due to a compressor problem. This meant that scanning could not be conducted from 11 July 2021 to 1 October 2021. Altogether, these unforeseen events have negatively affected my research progress in a way that could not have been predicted.

7.4 Conclusion

In conclusion, neurofeedback is one of only a few clinical neuroimaging tools that are being developed to modulate the connectivity between brain regions, namely, cortical-subcortical regions. The research conducted suggests that rt-fMRI-NF training shows promise as an upregulation tool in M1-thalamus connectivity. This could have positive impacts in clinical settings such as stroke recovery. In addition, this thesis investigated the ability to modulate M1-cerebellum connectivity using rt-fMRI-NF.

To our knowledge, no research has previously investigated cerebellum-cortical area connectivity for modulation using rt-fMRI-NF, therefore, our novel technique could be beneficial in clinical settings such as stroke recovery, Parkinson's disease and autism. Because our M1-cerebellum connectivity

experiment was limited due to the recruitment of only four participants, future research may include the scanning of more participants. If the results are promising, implementing this technique with patients would be our ultimate goal.

Other future works include modulating cerebellum activity as a single region only, using rt-fMRI-NF. This technique will help to upregulate the activation in the cerebellum and may be a useful therapeutic tool for diseases such as autism and Parkinson disease. A final possible avenue for future research is to simultaneously combine action observation with MI (AOMI) and use this as part of a rt-fMRI-NF paradigm to modulate activation in motor areas such as SMA and PMC.

Finally, rt-fMRI-NF increases the robustness of using neurofeedback training to modulate brain areas, especially deeper regions such as the thalamus. The recent increase in research in rt-fMRI boosts the credibility of the field. My goal is to conduct more research in this field so that this technique can become a routine therapeutic tool for many diseases such as stroke rehabilitation.

List of References

ALGERMISSEN, J. and MEHLER, D.M., 2018. May the power be with you: are there highly powered studies in neuroscience, and how can we get more of them? *Journal of neurophysiology,* **119**(6), pp. 2114-2117.

ALKADHI, H., BRUGGER, P., BOENDERMAKER, S.H., CRELIER, G., CURT, A., HEPP-REYMOND, M. and KOLLIAS, S.S., 2004. What disconnection tells about motor imagery: evidence from paraplegic patients. *Cerebral cortex,* **15**(2), pp. 131-140.

AL-WASITY, S., VOGT, S., VUCKOVIC, A. and POLLICK, F.E., 2021. Upregulation of Supplementary Motor Area Activation with fMRI Neurofeedback during Motor Imagery. *eNeuro,* **8**(1), pp. 10.1523/ENEURO.0377-18.2020. Print 2021 Jan-Feb.

AMANO, K., SHIBATA, K., KAWATO, M., SASAKI, Y. and WATANABE, T., 2016. Learning to associate orientation with color in early visual areas by associative decoded fMRI neurofeedback. *Current Biology,* **26**(14), pp. 1861-1866.

ANDERSSON, P., RAGNI, F. and LINGNAU, A., 2019. Visual imagery during real-time fMRI neurofeedback from occipital and superior parietal cortex. *NeuroImage,* **200**, pp. 332-343.

ARAI, N., LU, M., UGAWA, Y. and ZIEMANN, U., 2012. Effective connectivity between human supplementary motor area and primary motor cortex: a paired-coil TMS study. *Experimental brain research,* **220**(1), pp. 79-87.

ARNOLD ANTERAPER, S., GUELL, X., D'MELLO, A., JOSHI, N., WHITFIELD-GABRIELI, S. and JOSHI, G., 2019. Disrupted cerebrocerebellar intrinsic functional connectivity in young adults with high-functioning autism spectrum disorder: a data-driven, whole-brain, high-temporal resolution functional magnetic resonance imaging study. *Brain connectivity,* **9**(1), pp. 48-59.

ARNS, M., BATAIL, J., BIOULAC, S., CONGEDO, M., DAUDET, C., DRAPIER, D., FOVET, T., JARDRI, R., LE-VAN-QUYEN, M. and LOTTE, F., 2017. Neurofeedback: One of today's techniques in psychiatry? *L'Encephale,* **43**(2), pp. 135-145.

AUER, T., SCHWEIZER, R. and FRAHM, J., 2015. Training efficiency and transfer success in an extended real-time functional MRI neurofeedback training of the somatomotor cortex of healthy subjects. *Frontiers in human neuroscience,* **9**, pp. 547.

BANCA, P., SOUSA, T., DUARTE, I.C. and CASTELO-BRANCO, M., 2015. Visual motion imagery neurofeedback based on the hMT /V5 complex: evidence for a feedback-specific neural circuit involving neocortical and cerebellar regions. *Journal of neural engineering,* **12**(6), pp. 066003.

BANKER, L. and TADI, P., 2021. Neuroanatomy, Precentral Gyrus. *StatPearls*. Treasure Island (FL): StatPearls Publishing LLC, .

BARCH, D.M., BURGESS, G.C., HARMS, M.P., PETERSEN, S.E., SCHLAGGAR, B.L., CORBETTA, M., GLASSER, M.F., CURTISS, S., DIXIT, S. and FELDT, C., 2013. Function in the human connectome: task-fMRI and individual differences in behavior. *NeuroImage,* **80**, pp. 169-189.

BASKIN, S.M., KIRK, L.P., LEHRER, P.M., LUBAR, J.F., LAVAQUE, T., MOSS, D. and KIRK, L., 2004. Evidence-based practice in biofeedback and neurofeedback.

BEARDEN, T.S., CASSISI, J.E. and PINEDA, M., 2003. Neurofeedback training for a patient with thalamic and cortical infarctions. *Applied Psychophysiology and Biofeedback,* **28**(3), pp. 241-253.

BEKINSCHTEIN, T.A., PEETERS, M., SHALOM, D. and SIGMAN, M., 2011. Sea slugs, subliminal pictures, and vegetative state patients: boundaries of consciousness in classical conditioning. *Frontiers in psychology,* **2**, pp. 337.

BENJAMINI, Y. and HOCHBERG, Y., 1995. Controlling the false discovery rate: a practical and powerful approach to multiple testing. *Journal of the Royal statistical society: series B (Methodological),* **57**(1), pp. 289-300.

BERMAN, B.D., HOROVITZ, S.G., VENKATARAMAN, G. and HALLETT, M., 2012. Self-modulation of primary motor cortex activity with motor and motor imagery tasks using real-time fMRI-based neurofeedback. *NeuroImage,* **59**(2), pp. 917-925.

BERNARD, J.A., SEIDLER, R.D., HASSEVOORT, K.M., BENSON, B.L., WELSH, R.C., WIGGINS, J.L., JAEGGI, S.M., BUSCHKUEHL, M., MONK, C.S. and JONIDES, J., 2012. Resting state cortico-cerebellar functional connectivity networks: a comparison of anatomical and self-organizing map approaches. *Frontiers in neuroanatomy,* **6**, pp. 31.

BIRBAUMER, N., RUIZ, S. and SITARAM, R., 2013. Learned regulation of brain metabolism. *Trends in cognitive sciences,* **17**(6), pp. 295-302.

BLEFARI, M.L., SULZER, J., HEPP-REYMOND, M., KOLLIAS, S. and GASSERT, R., 2015. Improvement in precision grip force control with self-modulation of primary motor cortex during motor imagery. *Frontiers in behavioral neuroscience,* **9**, pp. 18.

BLOCK, H., BASTIAN, A. and CELNIK, P., 2013. Virtual lesion of angular gyrus disrupts the relationship between visuoproprioceptive weighting and realignment. *Journal of cognitive neuroscience,* **25**(4), pp. 636-648.

BOSCH-BOUJU, C., HYLAND, B.I. and PARR-BROWNLIE, L.C., 2013. Motor thalamus integration of cortical, cerebellar and basal ganglia information: implications for normal and parkinsonian conditions. *Frontiers in computational neuroscience,* **7**, pp. 163.

BOSCHKER, M.S., BAKKER, F.C. and MICHAELS, C.F., 2002. Effect of mental imagery on realizing affordances. *The Quarterly Journal of Experimental Psychology: Section A,* **55**(3), pp. 775-792.

BRAVER, T.S., REYNOLDS, J.R. and DONALDSON, D.I., 2003. Neural mechanisms of transient and sustained cognitive control during task switching. *Neuron,* **39**(4), pp. 713-726.

BRAY, S., SHIMOJO, S. and O'DOHERTY, J.P., 2007. Direct instrumental conditioning of neural activity using functional magnetic resonance imaging-derived reward feedback. *The Journal of neuroscience : the official journal of the Society for Neuroscience,* **27**(28), pp. 7498-7507.

BRETT, M., JOHNSRUDE, I.S. and OWEN, A.M., 2002. The problem of functional localization in the human brain. *Nature reviews neuroscience,* **3**(3), pp. 243-249.

BROYD, S.J., DEMANUELE, C., DEBENER, S., HELPS, S.K., JAMES, C.J. and SONUGA-BARKE, E.J., 2009. Default-mode brain dysfunction in mental disorders: a systematic review. *Neuroscience & biobehavioral reviews,* **33**(3), pp. 279-296.

BRÜHL, A.B., SCHERPIET, S., SULZER, J., STÄMPFLI, P., SEIFRITZ, E. and HERWIG, U., 2014. Real-time neurofeedback using functional MRI could improve down-regulation of amygdala activity during emotional stimulation: a proof-of-concept study. *Brain topography,* **27**(1), pp. 138-148.

BUCCINO, G., BINKOFSKI, F., FINK, G.R., FADIGA, L., FOGASSI, L., GALLESE, V., SEITZ, R.J., ZILLES, K., RIZZOLATTI, G. and FREUND, H., 2001. Action observation activates premotor and parietal areas in a somatotopic manner: an fMRI study. *European journal of neuroscience,* **13**(2), pp. 400-404.

BUCH, E.R., MODIR SHANECHI, A., FOURKAS, A.D., WEBER, C., BIRBAUMER, N. and COHEN, L.G., 2012. Parietofrontal integrity determines neural modulation associated with grasping imagery after stroke. *Brain,* **135**(2), pp. 596-614.

BUXTON, R.B., 2009. *Introduction to functional magnetic resonance imaging: principles and techniques.* Cambridge university press.

BUYUKTURKOGLU, K., RANA, M., RUIZ, S., HACKLEY, S.A., SOEKADAR, S.R., BIRBAUMER, N. and SITARAM, R., 2013. Volitional regulation of the supplementary motor area with fMRI-BCI neurofeedback in Parkinson's disease: A pilot study, *2013 6th International IEEE/EMBS Conference on Neural Engineering (NER)* 2013, IEEE, pp. 677-681.

CALLOW, N. and ROBERTS, R., 2010. Imagery research: An investigation of three issues. *Psychology of Sport and Exercise,* **11**(4), pp. 325-329.

CARIA, A., SITARAM, R., VEIT, R., BEGLIOMINI, C. and BIRBAUMER, N., 2010. Volitional control of anterior insula activity modulates the response to aversive stimuli. A real-time functional magnetic resonance imaging study. *Biological psychiatry,* **68**(5), pp. 425-432.

CARIA, A., VEIT, R., SITARAM, R., LOTZE, M., WEISKOPF, N., GRODD, W. and BIRBAUMER, N., 2007. Regulation of anterior insular cortex activity using real-time fMRI. *NeuroImage,* **35**(3), pp. 1238-1246.

CARTER, A.R., PATEL, K.R., ASTAFIEV, S.V., SNYDER, A.Z., RENGACHARY, J., STRUBE, M.J., POPE, A., SHIMONY, J.S., LANG, C.E. and SHULMAN, G.L., 2012. Upstream dysfunction of somatomotor functional connectivity after corticospinal damage in stroke. *Neurorehabilitation and neural repair,* **26**(1), pp. 7-19.

CARTONI, E., BALLEINE, B. and BALDASSARRE, G., 2016. Appetitive Pavlovian-instrumental transfer: a review. *Neuroscience & Biobehavioral Reviews,* **71**, pp. 829-848.

CASPERS, S., ZILLES, K., LAIRD, A.R. and EICKHOFF, S.B., 2010. ALE meta-analysis of action observation and imitation in the human brain. *NeuroImage,* **50**(3), pp. 1148-1167.

CENGIZ, B. and BORAN, H.E., 2016. The role of the cerebellum in motor imagery. *Neuroscience letters,* **617**, pp. 156-159.

CHAVHAN, G.B., BABYN, P.S., THOMAS, B., SHROFF, M.M. and HAACKE, E.M., 2009. Principles, techniques, and applications of T2*-based MR imaging and its special applications. *Radiographics,* **29**(5), pp. 1433-1449.

CHIEW, M., LACONTE, S.M. and GRAHAM, S.J., 2012. Investigation of fMRI neurofeedback of differential primary motor cortex activity using kinesthetic motor imagery. *NeuroImage,* **61**(1), pp. 21-31.

CHRISTOPHER DECHARMS, R., CHRISTOFF, K., GLOVER, G.H., PAULY, J.M., WHITFIELD, S. and GABRIELI, J.D., 2004. Learned regulation of spatially localized brain activation using real-time fMRI. *NeuroImage,* **21**(1), pp. 436-443.

CLEEREMANS, A., ACHOUI, D., BEAUNY, A., KEUNINCKX, L., MARTIN, J., MUÑOZ-MOLDES, S., VUILLAUME, L. and DE HEERING, A., 2020. Learning to be conscious. *Trends in cognitive sciences,* **24**(2), pp. 112-123.

COOKE, D.F., TAYLOR, C.S., MOORE, T. and GRAZIANO, M.S., 2003. Complex movements evoked by microstimulation of the ventral intraparietal area. *Proceedings of the National Academy of Sciences of the United States of America,* **100**(10), pp. 6163-6168.

CORDES, J.S., MATHIAK, K.A., DYCK, M., ALAWI, E.M., GABER, T.J., ZEPF, F.D., KLASEN, M., ZVYAGINTSEV, M., GUR, R.C. and MATHIAK, K., 2015. Cognitive and neural strategies during control of the anterior cingulate cortex by fMRI neurofeedback in patients with schizophrenia. *Frontiers in behavioral neuroscience,* **9**, pp. 169.

DASKALAKIS, Z.J., PARADISO, G.O., CHRISTENSEN, B.K., FITZGERALD, P.B., GUNRAJ, C. and CHEN, R., 2004. Exploring the connectivity between the cerebellum and motor cortex in humans. *The Journal of physiology,* **557**(2), pp. 689-700.

DAVARE, M., MONTAGUE, K., OLIVIER, E., ROTHWELL, J.C. and LEMON, R.N., 2009. Ventral premotor to primary motor cortical interactions during object-driven grasp in humans. *Cortex,* **45**(9), pp. 1050-1057.

DEBETTENCOURT, M.T. and NORMAN, K.A., 2016. Neuroscience: incepting associations. *Current Biology,* **26**(14), pp. R673-R675.

DECETY, J., PERANI, D., JEANNEROD, M., BETTINARDI, V., TADARY, B., WOODS, R., MAZZIOTTA, J.C. and FAZIO, F., 1994. Mapping motor representations with positron emission tomography. *Nature,* **371**(6498), pp. 600-602.

DECHARMS, R.C., 2008. Applications of real-time fMRI. *Nature Reviews Neuroscience,* **9**(9), pp. 720-729.

DECHARMS, R.C., MAEDA, F., GLOVER, G.H., LUDLOW, D., PAULY, J.M., SONEJI, D., GABRIELI, J.D. and MACKEY, S.C., 2005. Control over brain activation and pain learned by using real-time functional MRI. *Proceedings of the National Academy of Sciences of the United States of America,* **102**(51), pp. 18626-18631.

DESSEILLES, M., SCHWARTZ, S., DANG-VU, T.T., STERPENICH, V., ANSSEAU, M., MAQUET, P. and PHILLIPS, C., 2011. Depression alters “top-down” visual attention: a dynamic causal modeling comparison between depressed and healthy subjects. *NeuroImage,* **54**(2), pp. 1662-1668.

DIENES, Z. and PERNER, J., 2007. Executive control without conscious awareness: The cold control theory of hypnosis. *Hypnosis and conscious states: The cognitive neuroscience perspective,* , pp. 293-314.

DIMITROVA, A., ZELJKO, D., SCHWARZE, F., MASCHKE, M., GERWIG, M., FRINGS, M., BECK, A., AURICH, V., FORSTING, M. and TIMMANN, D., 2006. Probabilistic 3D MRI atlas of the human cerebellar dentate/interposed nuclei. *NeuroImage,* **30**(1), pp. 12-25.

DOSENBACH, N.U., VISSCHER, K.M., PALMER, E.D., MIEZIN, F.M., WENGER, K.K., KANG, H.C., BURGUND, E.D., GRIMES, A.L., SCHLAGGAR, B.L. and PETERSEN, S.E., 2006. A core system for the implementation of task sets. *Neuron,* **50**(5), pp. 799-812.

DUM, R.P. and STRICK, P.L., 2005. Frontal lobe inputs to the digit representations of the motor areas on the lateral surface of the hemisphere. *The Journal of neuroscience : the official journal of the Society for Neuroscience,* **25**(6), pp. 1375-1386.

DUNCAN, K.J., PATTAMADILOK, C., KNIERIM, I. and DEVLIN, J.T., 2009. Consistency and variability in functional localisers. *NeuroImage,* **46**(4), pp. 1018-1026.

EAVES, D.L., RIACH, M., HOLMES, P.S. and WRIGHT, D.J., 2016. Motor imagery during action observation: a brief review of evidence, theory and future research opportunities. *Frontiers in neuroscience,* **10**, pp. 514.

EDMONDS, W.A. and TENENBAUM, G., 2011. *Case studies in applied psychophysiology: Neurofeedback and biofeedback treatments for advances in human performance*. John Wiley & Sons.

EKLUND, A., 2010. *Signal Processing for Robust and Real-Time fMRI With Application to Brain Computer Interfaces,* .

EMMERT, K., 2016. *Improvement of real-time fMRI neurofeedback for clinical applications,* .

ERTELT, D., SMALL, S., SOLODKIN, A., DETTMERS, C., MCNAMARA, A., BINKOFSKI, F. and BUCCINO, G., 2007. Action observation has a positive impact on rehabilitation of motor deficits after stroke. *NeuroImage,* **36**, pp. T164-T173.

FANG, P., STEPNIEWSKA, I. and KAAS, J.H., 2006. The thalamic connections of motor, premotor, and prefrontal areas of cortex in a prosimian primate (Otolemur garnetti). *Neuroscience,* **143**(4), pp. 987-1020.

FARRER, C. and FRITH, C.D., 2002. Experiencing oneself vs another person as being the cause of an action: the neural correlates of the experience of agency. *NeuroImage,* **15**(3), pp. 596-603.

FAUL, F., ERDFELDER, E., LANG, A. and BUCHNER, A., 2007. G* Power 3: A flexible statistical power analysis program for the social, behavioral, and biomedical sciences. *Behavior research methods,* **39**(2), pp. 175-191.

FEDE, S.J., DEAN, S.F., MANUWEERA, T. and MOMENAN, R., 2020. A guide to literature informed decisions in the design of real time fMRI neurofeedback studies: a systematic review. *Frontiers in human neuroscience,* **14**, pp. 60.

FETZ, E.E., 1969. Operant conditioning of cortical unit activity. *Science (New York, N.Y.),* **163**(3870), pp. 955-958.

FILLMORE, M.T., RUSH, C.R. and HAYS, L., 2006. Acute effects of cocaine in two models of inhibitory control: implications of non-linear dose effects. *Addiction,* **101**(9), pp. 1323-1332.

FOGASSI, L., FERRARI, P.F., GESIERICH, B., ROZZI, S., CHERSI, F. and RIZZOLATTI, G., 2005. Parietal lobe: from action organization to intention understanding. *Science (New York, N.Y.),* **308**(5722), pp. 662-667.

FORMISANO, E., DI SALLE, F. and GOEBEL, R., 2006. Fundamentals of data analysis methods in fMRI. *Signal processing and communication,* (27),.

FORNITO, A., ZALESKY, A. and BREAKSPEAR, M., 2015. The connectomics of brain disorders. *Nature Reviews Neuroscience,* **16**(3), pp. 159-172.

FOX, P.T., RAICHLE, M.E. and THACH, W.T., 1985. Functional mapping of the human cerebellum with positron emission tomography. *Proceedings of the*

National Academy of Sciences of the United States of America, **82**(21), pp. 7462-7466.

FRIESEN, C.L., BARDOUILLE, T., NEYEDLI, H.F. and BOE, S.G., 2017. Combined action observation and motor imagery neurofeedback for modulation of brain activity. *Frontiers in human neuroscience,* **10**, pp. 692.

FRISTON, K.J., ASHBURNER, J., FRITH, C.D., POLINE, J., HEATHER, J.D. and FRACKOWIAK, R.S., 1995. Spatial registration and normalization of images. *Human brain mapping,* **3**(3), pp. 165-189.

FRISTON, K.J., ROTSHTEIN, P., GENG, J.J., STERZER, P. and HENSON, R.N., 2006. A critique of functional localisers. *NeuroImage,* **30**(4), pp. 1077-1087.

GALDO-ÁLVAREZ, S. and CARRILLO-DE-LA-PEÑA, M.T., 2004. ERP evidence of MI activation without motor response execution. *Neuroreport,* **15**(13), pp. 2067-2070.

GATTI, R., TETTAMANTI, A., GOUGH, P., RIBOLDI, E., MARINONI, L. and BUCCINO, G., 2013. Action observation versus motor imagery in learning a complex motor task: a short review of literature and a kinematics study. *Neuroscience letters,* **540**, pp. 37-42.

GAUME, A., VIALATTE, A., MORA-SÁNCHEZ, A., RAMDANI, C. and VIALATTE, F., 2016. A psychoengineering paradigm for the neurocognitive mechanisms of biofeedback and neurofeedback. *Neuroscience & Biobehavioral Reviews,* **68**, pp. 891-910.

GAZZANIGA, M.S., 2009. *The cognitive neurosciences.* MIT press.

GENTILI, R., PAPAXANTHIS, C. and POZZO, T., 2006. Improvement and generalization of arm motor performance through motor imagery practice. *Neuroscience,* **137**(3), pp. 761-772.

GENTILI, R., HAN, C.E., SCHWEIGHOFER, N. and PAPAXANTHIS, C., 2010. Motor learning without doing: trial-by-trial improvement in motor performance during mental training. *Journal of neurophysiology,* **104**(2), pp. 774-783.

GERIN, M.I., FICHTENHOLTZ, H., ROY, A., WALSH, C.J., KRYSTAL, J.H., SOUTHWICK, S. and HAMPSON, M., 2016. Real-time fMRI neurofeedback with war veterans with chronic PTSD: A feasibility study. *Frontiers in Psychiatry,* **7**, pp. 111.

GLOVER, G.H. and KRÜGER, G., 2002. Optimum voxel size in BOLD fMRI, *Proc Intl Soc Magn Reson Med* 2002, pp. 1395.

GOEBEL, R., ESPOSITO, F. and FORMISANO, E., 2006. Analysis of functional image analysis contest (FIAC) data with brainvoyager QX: From single-subject to cortically aligned group general linear model analysis and self-organizing group independent component analysis. *Human brain mapping,* **27**(5), pp. 392-401.

GOEBEL, R., SORGER, B., KAISER, J., BIRBAUMER, N. and WEISKOPF, N., 2004. BOLD brain pong: self-regulation of local brain activity during synchronously scanned, interacting subjects, *34th Annual Meeting of the Society for Neuroscience* 2004.

GONZALEZ-CASTILLO, J., RAMOT, M. and MOMENAN, R., 2020. Editorial: Towards Expanded Utility of Real Time fMRI Neurofeedback in Clinical Applications. *Frontiers in human neuroscience,* **14**, pp. 606868.

GRAFTON, S.T., ARBIB, M.A., FADIGA, L. and RIZZOLATTI, G., 1996. Localization of grasp representations in humans by positron emission tomography. *Experimental brain research,* **112**(1), pp. 103-111.

GRUZELIER, J.H., 2014. EEG-neurofeedback for optimising performance. I: a review of cognitive and affective outcome in healthy participants. *Neuroscience & Biobehavioral Reviews,* **44**, pp. 124-141.

GUILLOT, A. and COLLET, C., 2005. Duration of mentally simulated movement: a review. *Journal of motor behavior,* **37**(1), pp. 10-20.

GUILLOT, A., COLLET, C., NGUYEN, V.A., MALOUIN, F., RICHARDS, C. and DOYON, J., 2009. Brain activity during visual versus kinesthetic imagery: an fMRI study. *Human brain mapping,* **30**(7), pp. 2157-2172.

HABES, I., RUSHTON, S., JOHNSTON, S., SOKUNBI, M., BARAWI, K., BROSNAN, M., DALY, T., IHSSEN, N. and LINDEN, D.E., 2016. fMRI neurofeedback of higher visual areas and perceptual biases. *Neuropsychologia,* **85**, pp. 208-215.

HAMILTON, J.P., GLOVER, G.H., HSU, J., JOHNSON, R.F. and GOTLIB, I.H., 2011. Modulation of subgenual anterior cingulate cortex activity with real-time neurofeedback. *Human brain mapping,* **32**(1), pp. 22-31.

HAMPSON, M., SCHEINOST, D., QIU, M., BHAWNANI, J., LACADIE, C.M., LECKMAN, J.F., CONSTABLE, R.T. and PAPADEMETRIS, X., 2011. Biofeedback of real-time functional magnetic resonance imaging data from the supplementary motor area reduces functional connectivity to subcortical regions. *Brain connectivity,* **1**(1), pp. 91-98.

HAMPSON, M., STOICA, T., SAKSA, J., SCHEINOST, D., QIU, M., BHAWNANI, J., PITTENGER, C., PAPADEMETRIS, X. and CONSTABLE, T., 2012. Real-time fMRI biofeedback targeting the orbitofrontal cortex for contamination anxiety. *JoVE (Journal of Visualized Experiments),* (59), pp. e3535.

HANAKAWA, T., 2011. Rostral premotor cortex as a gateway between motor and cognitive networks. *Neuroscience research,* **70**(2), pp. 144-154.

HANAKAWA, T., IMMISCH, I., TOMA, K., DIMYAN, M.A., VAN GELDEREN, P. and HALLETT, M., 2003. Functional properties of brain areas associated with motor execution and imagery. *Journal of neurophysiology,* **89**(2), pp. 989-1002.

HARDWICK, R.M., CASPERS, S., EICKHOFF, S.B. and SWINNEN, S.P., 2017. Neural Correlates of Motor Imagery, Action Observation, and Movement Execution: A Comparison Across Quantitative Meta-Analyses. *bioRxiv,* , pp. 198432.

HARMELECH, T., PREMINGER, S., WERTMAN, E. and MALACH, R., 2013. The day-after effect: long term, Hebbian-like restructuring of resting-state fMRI patterns induced by a single epoch of cortical activation. *The Journal of neuroscience : the official journal of the Society for Neuroscience,* **33**(22), pp. 9488-9497.

HARTWELL, K.J., HANLON, C.A., LI, X., BORCKARDT, J.J., CANTERBERRY, M., PRISCIANDARO, J.J., MORAN-SANTA MARIA, M.M., LEMATTY, T., GEORGE, M.S. and BRADY, K.T., 2016. Individualized real-time fMRI neurofeedback to

attenuate craving in nicotine-dependent smokers. *Journal of psychiatry & neuroscience : JPN,* **41**(1), pp. 48-55.

HAUGG, A., RENZ, F.M., NICHOLSON, A.A., LOR, C., GÖTZENDORFER, S.J., SLADKY, R., SKOURAS, S., MCDONALD, A., CRADDOCK, C. and HELLRUNG, L., 2021. Predictors of real-time fMRI neurofeedback performance and improvement–A machine learning mega-analysis. *NeuroImage,* , pp. 118207.

HAYES, A.E., DAVIDSON, M.C., KEELE, S.W. and RAFAL, R.D., 1998. Toward a functional analysis of the basal ganglia. *Journal of cognitive neuroscience,* **10**(2), pp. 178-198.

HE, B. and LIU, Z., 2008. Multimodal functional neuroimaging: integrating functional MRI and EEG/MEG. *IEEE reviews in biomedical engineering,* **1**, pp. 23-40.

HELLRUNG, L., DIETRICH, A., HOLLMANN, M., PLEGER, B., KALBERLAH, C., ROGGENHOFER, E., VILLRINGER, A. and HORSTMANN, A., 2018. Intermittent compared to continuous real-time fMRI neurofeedback boosts control over amygdala activation. *NeuroImage,* **166**, pp. 198-208.

HENSON, R., 2007. Efficient experimental design for fMRI. *Statistical parametric mapping: The analysis of functional brain images,* , pp. 193-210.

HERBEC, A., KAUPPI, J., JOLA, C., TOHKA, J. and POLLICK, F.E., 2015. Differences in fMRI intersubject correlation while viewing unedited and edited videos of dance performance. *Cortex,* **71**, pp. 341-348.

HERSHEY, T., CAMPBELL, M.C., VIDEEN, T.O., LUGAR, H.M., WEAVER, P.M., HARTLEIN, J., KARIMI, M., TABBAL, S.D. and PERLMUTTER, J.S., 2010. Mapping Go–No-Go performance within the subthalamic nucleus region. *Brain,* **133**(12), pp. 3625-3634.

HÉTU, S., GRÉGOIRE, M., SAIMPONT, A., COLL, M., EUGÈNE, F., MICHON, P. and JACKSON, P.L., 2013. The neural network of motor imagery: an ALE meta-analysis. *Neuroscience & Biobehavioral Reviews,* **37**(5), pp. 930-949.

HEYES, C., 2012. Simple minds: a qualified defence of associative learning. *Philosophical Transactions of the Royal Society B: Biological Sciences,* **367**(1603), pp. 2695-2703.

HIRANO, Y., STEFANOVIC, B. and SILVA, A.C., 2011. Spatiotemporal evolution of the functional magnetic resonance imaging response to ultrashort stimuli. *The Journal of neuroscience : the official journal of the Society for Neuroscience,* **31**(4), pp. 1440-1447.

HOHENFELD, C., NELLESSEN, N., DOGAN, I., KUHN, H., MÜLLER, C., PAPA, F., KETTELER, S., GOEBEL, R., HEINECKE, A. and SHAH, N.J., 2017. Cognitive improvement and brain changes after real-time functional MRI neurofeedback training in healthy elderly and prodromal Alzheimer's disease. *Frontiers in neurology,* **8**, pp. 384.

HOOVER, J.E. and STRICK, P.L., 1999. The organization of cerebellar and basal ganglia outputs to primary motor cortex as revealed by retrograde transneuronal transport of herpes simplex virus type 1. *The Journal of neuroscience : the official journal of the Society for Neuroscience,* **19**(4), pp. 1446-1463.

HOSHI, E. and TANJI, J., 2007. Distinctions between dorsal and ventral premotor areas: anatomical connectivity and functional properties. *Current opinion in neurobiology,* **17**(2), pp. 234-242.

HOU, B.L., BHATIA, S. and CARPENTER, J.S., 2016. Quantitative comparisons on hand motor functional areas determined by resting state and task BOLD fMRI and anatomical MRI for pre-surgical planning of patients with brain tumors. *NeuroImage: Clinical,* **11**, pp. 378-387.

HUBERDEAU, D.M., KRAKAUER, J.W. and HAITH, A.M., 2015. Dual-process decomposition in human sensorimotor adaptation. *Current opinion in neurobiology,* **33**, pp. 71-77.

HUETTEL, S.A., SONG, A.W. and MCCARTHY, G., 2004. *Functional magnetic resonance imaging*. Sinauer Associates Sunderland, MA.

HUI, M., ZHANG, H., GE, R., YAO, L. and LONG, Z., 2014. Modulation of functional network with real-time fMRI feedback training of right premotor cortex activity. *Neuropsychologia,* **62**, pp. 111-123.

HULL, C.L., 1943. Principles of behavior: An introduction to behavior theory. .

IETSWAART, M., JOHNSTON, M., DIJKERMAN, H.C., JOICE, S., SCOTT, C.L., MACWALTER, R.S. and HAMILTON, S.J., 2011. Mental practice with motor imagery in stroke recovery: randomized controlled trial of efficacy. *Brain,* **134**(5), pp. 1373-1386.

INUGGI, A., FILIPPI, M., CHIEFFO, R., AGOSTA, F., ROCCA, M.A., GONZÁLEZ-ROSA, J.J., CURSI, M., COMI, G. and LEOCANI, L., 2010. Motor area localization using fMRI-constrained cortical current density reconstruction of movement-related cortical potentials, a comparison with fMRI and TMS mapping. *Brain research,* **1308**, pp. 68-78.

ISAAC, A., MARKS, D.F. and RUSSELL, D.G., 1986. An instrument for assessing imagery of movement: The Vividness of Movement Imagery Questionnaire (VMIQ). *Journal of mental Imagery,* .

JANG, S.H., KWON, Y.H., LEE, M.Y., LEE, D.Y. and HONG, J.H., 2012. Difference of neural connectivity for motor function in chronic hemiparetic stroke patients with intracerebral hemorrhage. *Neuroscience letters,* **531**(2), pp. 80-85.

JEANNEROD, M., 2006. *Motor cognition: What actions tell the self*. Oxford University Press.

JEANNEROD, M., 2001. Neural simulation of action: a unifying mechanism for motor cognition. *NeuroImage,* **14**(1), pp. S103-S109.

JEZZARD, P., MATTHEWS, P.M. and SMITH, S.M., 2001. *Functional MRI: an introduction to methods*. Oxford university press Oxford.

JOHNSON, K.A., HARTWELL, K., LEMATTY, T., BORCKARDT, J., MORGAN, P.S., GOVINDARAJAN, K., BRADY, K. and GEORGE, M.S., 2012. Intermittent "Real-time" fMRI feedback is superior to continuous presentation for a motor imagery task: a pilot study. *Journal of Neuroimaging,* **22**(1), pp. 58-66.

JOHNSTON, S.J., BOEHM, S.G., HEALY, D., GOEBEL, R. and LINDEN, D.E., 2010. Neurofeedback: a promising tool for the self-regulation of emotion networks. *NeuroImage,* **49**(1), pp. 1066-1072.

KANEL, D., AL-WASITY, S., STEFANOV, K. and POLLICK, F.E., 2019. Empathy to emotional voices and the use of real-time fMRI to enhance activation of the anterior insula. *NeuroImage,* **198**, pp. 53-62.

KANG, L., ZHANG, A., SUN, N., LIU, P., YANG, C., LI, G., LIU, Z., WANG, Y. and ZHANG, K., 2018. Functional connectivity between the thalamus and the primary somatosensory cortex in major depressive disorder: a resting-state fMRI study. *BMC psychiatry,* **18**(1), pp. 1-8.

KARCH, S., KEESER, D., HÜMMER, S., PAOLINI, M., KIRSCH, V., KARALI, T., KUPKA, M., RAUCHMANN, B., CHROBOK, A. and BLAUTZIK, J., 2015. Modulation of craving related brain responses using real-time fMRI in patients with alcohol use disorder. *PLoS One,* **10**(7), pp. e0133034.

KAUT, O., MIELACHER, C., HURLEMANN, R. and WÜLLNER, U., 2020. Resting-state fMRI reveals increased functional connectivity in the cerebellum but decreased functional connectivity of the caudate nucleus in Parkinson's disease. *Neurological research,* **42**(1), pp. 62-67.

KEYNAN, J.N., MEIR-HASSON, Y., GILAM, G., COHEN, A., JACKONT, G., KINREICH, S., IKAR, L., OR-BORICHEV, A., ETKIN, A. and GYURAK, A., 2016. Limbic activity modulation guided by functional magnetic resonance imaging–inspired electroencephalography improves implicit emotion regulation. *Biological psychiatry,* **80**(6), pp. 490-496.

KEYSERS, C. and GAZZOLA, V., 2009. Expanding the mirror: vicarious activity for actions, emotions, and sensations. *Current opinion in neurobiology,* **19**(6), pp. 666-671.

KIM, J., LEE, J., JO, H.J., KIM, S.H., LEE, J.H., KIM, S.T., SEO, S.W., COX, R.W., NA, D.L. and KIM, S.I., 2010. Defining functional SMA and pre-SMA subregions in human MFC using resting state fMRI: functional connectivity-based parcellation method. *NeuroImage,* **49**(3), pp. 2375-2386.

KIRSCHNER, M., SLADKY, R., HAUGG, A., STÄMPFLI, P., JEHLI, E., HODEL, M., ENGELI, E., HÖSLI, S., BAUMGARTNER, M.R. and SULZER, J., 2018. Self-regulation of the dopaminergic reward circuit in cocaine users with mental imagery and neurofeedback. *EBioMedicine,* **37**, pp. 489-498.

KLANN, J., BINKOFSKI, F. and CASPERS, S., 2015. On the neuroanatomical parcellation and multiple functions of the inferior parietal lobule. *Comparative Neuropsychology and Brain Imaging,* , pp. 75-84.

KOBER, S.E., WITTE, M., NINAUS, M., NEUPER, C. and WOOD, G., 2013. Learning to modulate one's own brain activity: the effect of spontaneous mental strategies. *Frontiers in human neuroscience,* **7**, pp. 695.

KOIZUMI, A., AMANO, K., CORTESE, A., SHIBATA, K., YOSHIDA, W., SEYMOUR, B., KAWATO, M. and LAU, H., 2016. Fear reduction without fear through reinforcement of neural activity that bypasses conscious exposure. *Nature human behaviour,* **1**(1), pp. 1-7.

KORALEK, A.C., COSTA, R.M. and CARMENA, J.M., 2013. Temporally precise cell-specific coherence develops in corticostriatal networks during learning. *Neuron,* **79**(5), pp. 865-872.

KORALEK, A.C., JIN, X., LONG II, J.D., COSTA, R.M. and CARMENA, J.M., 2012. Corticostriatal plasticity is necessary for learning intentional neuroprosthetic skills. *Nature,* **483**(7389), pp. 331-335.

KOUSH, Y., ROSA, M.J., ROBINEAU, F., HEINEN, K., RIEGER, S.W., WEISKOPF, N., VUILLEUMIER, P., VAN DE VILLE, D. and SCHARNOWSKI, F., 2013. Connectivity-based neurofeedback: dynamic causal modeling for real-time fMRI. *NeuroImage,* **81**, pp. 422-430.

KRAKAUER, J.W., HADJIOSIF, A.M., XU, J., WONG, A.L. and HAITH, A.M., 2019. Motor learning. *Compr Physiol,* **9**(2), pp. 613-663.

KÜBLER, A., KOTCHOUBEY, B., KAISER, J., WOLPAW, J.R. and BIRBAUMER, N., 2001. Brain–computer communication: Unlocking the locked in. *Psychological bulletin,* **127**(3), pp. 358.

KUHTZ-BUSCHBECK, J.P., MAHNKOPF, C., HOLZKNECHT, C., SIEBNER, H., ULMER, S. and JANSEN, O., 2003. Effector-independent representations of simple and complex imagined finger movements: A combined fMRI and TMS study. *European Journal of Neuroscience,* **18**(12), pp. 3375-3387.

KWONG, K.K., BELLIVEAU, J.W., CHESLER, D.A., GOLDBERG, I.E., WEISSKOFF, R.M., PONCELET, B.P., KENNEDY, D.N., HOPPEL, B.E., COHEN, M.S. and TURNER, R., 1992. Dynamic magnetic resonance imaging of human brain activity during primary sensory stimulation. *Proceedings of the National Academy of Sciences of the United States of America,* **89**(12), pp. 5675-5679.

LACOURSE, M.G., ORR, E.L., CRAMER, S.C. and COHEN, M.J., 2005. Brain activation during execution and motor imagery of novel and skilled sequential hand movements. *NeuroImage,* **27**(3), pp. 505-519.

LACROIX, J.M. and ROBERTS, L.E., 1978. A comparison of the mechanisms and some properties of instructed sudomotor and cardiac control. *Biofeedback and self-regulation,* **3**(2), pp. 105-132.

LANCASTER, J.L., WOLDORFF, M.G., PARSONS, L.M., LIOTTI, M., FREITAS, C.S., RAINEY, L., KOCHUNOV, P.V., NICKERSON, D., MIKITEN, S.A. and FOX, P.T., 2000. Automated Talairach atlas labels for functional brain mapping. *Human brain mapping,* **10**(3), pp. 120-131.

LEBON, F., HORN, U., DOMIN, M. and LOTZE, M., 2018. Motor imagery training: Kinesthetic imagery strategy and inferior parietal f MRI activation. *Human brain mapping,* **39**(4), pp. 1805-1813.

LEE, S., RUIZ, S., CARIA, A., VEIT, R., BIRBAUMER, N. and SITARAM, R., 2011. Detection of cerebral reorganization induced by real-time fMRI feedback training of insula activation: a multivariate investigation. *Neurorehabilitation and neural repair,* **25**(3), pp. 259-267.

LI, X., HARTWELL, K.J., BORCKARDT, J., PRISCIANDARO, J.J., SALADIN, M.E., MORGAN, P.S., JOHNSON, K.A., LEMATTY, T., BRADY, K.T. and GEORGE, M.S., 2013. Volitional reduction of anterior cingulate cortex activity produces decreased cue craving in smoking cessation: A preliminary real-time fMRI study. *Addiction Biology,* **18**(4), pp. 739-748.

LIEW, S., RANA, M., CORNELSEN, S., FORTUNATO DE BARROS FILHO, MARCOS, BIRBAUMER, N., SITARAM, R., COHEN, L.G. and SOEKADAR, S.R., 2016. Improving motor corticothalamic communication after stroke using real-time fMRI connectivity-based neurofeedback. *Neurorehabilitation and neural repair,* **30**(7), pp. 671-675.

LINDEMAN, S., HONG, S., KROS, L., MEJIAS, J.F., ROMANO, V., OOSTENVELD, R., NEGRELLO, M., BOSMAN, L.W. and DE ZEEUW, C.I., 2021. Cerebellar Purkinje cells can differentially modulate coherence between sensory and motor cortex depending on region and behavior. *Proceedings of the National Academy of Sciences,* **118**(2),.

LINDEN, D.E., HABES, I., JOHNSTON, S.J., LINDEN, S., TATINENI, R., SUBRAMANIAN, L., SORGER, B., HEALY, D. and GOEBEL, R., 2012. Real-time self-regulation of emotion networks in patients with depression. *PloS one,* **7**(6), pp. e38115.

LINDQUIST, M.A., 2008. The statistical analysis of fMRI data. *Statistical science,* , pp. 439-464.

LOREY, B., BISCHOFF, M., PILGRAMM, S., STARK, R., MUNZERT, J. and ZENTGRAF, K., 2009. The embodied nature of motor imagery: the influence of posture and perspective. *Experimental brain research,* **194**(2), pp. 233-243.

LOTZE, M. and HALSBAND, U., 2006. Motor imagery. *Journal of Physiology-paris,* **99**(4-6), pp. 386-395.

LOVIBOND, P.F. and SHANKS, D.R., 2002. The role of awareness in Pavlovian conditioning: empirical evidence and theoretical implications. *Journal of Experimental Psychology: Animal Behavior Processes,* **28**(1), pp. 3.

LU, Z., PHUA, K.S., HUANG, W., HONG, X., NASRALLAH, F.A., CHUANG, K. and GUAN, C., 2015. Combining EPI and motion correction for fMRI human brain images with big motion, *2015 37th Annual International Conference of the IEEE Engineering in Medicine and Biology Society (EMBC)* 2015, IEEE, pp. 5449-5452.

LUBIANIKER, N., GOLDWAY, N., FRUCHTMAN-STEINBOK, T., PARET, C., KEYNAN, J.N., SINGER, N., COHEN, A., KADOSH, K.C., LINDEN, D.E. and HENDLER, T.,

2019. Process-based framework for precise neuromodulation. *Nature human behaviour,* **3**(5), pp. 436-445.

LUI, F., BUCCINO, G., DUZZI, D., BENUZZI, F., CRISI, G., BARALDI, P., NICHELLI, P., PORRO, C.A. and RIZZOLATTI, G., 2008. Neural substrates for observing and imagining non-object-directed actions. *Social neuroscience,* **3**(3-4), pp. 261-275.

MACPHAIL, E.M., 1982. *Brain and intelligence in vertebrates.* Oxford University Press, USA.

MANTO, M., BOWER, J.M., CONFORTO, A.B., DELGADO-GARCÍA, J.M., DA GUARDA, SUZETE NASCIMENTO FARIAS, GERWIG, M., HABAS, C., HAGURA, N., IVRY, R.B. and MARIËN, P., 2012. Consensus paper: roles of the cerebellum in motor control—the diversity of ideas on cerebellar involvement in movement. *The Cerebellum,* **11**(2), pp. 457-487.

MARINS, T.F., RODRIGUES, E.C., ENGEL, A., HOEFLE, S., BASÍLIO, R., LENT, R., MOLL, J. and TOVAR-MOLL, F., 2015. Enhancing motor network activity using real-time functional MRI neurofeedback of left premotor cortex. *Frontiers in behavioral neuroscience,* **9**, pp. 341.

MARTIN, K.A., MORITZ, S.E. and HALL, C.R., 1999. Imagery use in sport: A literature review and applied model. *The sport psychologist,* **13**(3), pp. 245-268.

MARZBANI, H., MARATEB, H.R. and MANSOURIAN, M., 2016. Neurofeedback: A Comprehensive Review on System Design, Methodology and Clinical Applications. *Basic and clinical neuroscience,* **7**(2), pp. 143-158.

MATHIAK, K.A., KOUSH, Y., DYCK, M., GABER, T.J., ALAWI, E., ZEPF, F.D., ZVYAGINTSEV, M. and MATHIAK, K., 2010. Social reinforcement can regulate localized brain activity. *European archives of psychiatry and clinical neuroscience,* **260**(2), pp. 132-136.

MEGAN, T.D., COHEN, J.D., LEE, R.F., NORMAN, K.A. and TURK-BROWNE, N.B., 2015. Closed-loop training of attention with real-time brain imaging. *Nature neuroscience,* **18**(3), pp. 470-475.

MEGUMI, F., YAMASHITA, A., KAWATO, M. and IMAMIZU, H., 2015. Functional MRI neurofeedback training on connectivity between two regions induces long-lasting changes in intrinsic functional network. *Frontiers in human neuroscience,* **9**, pp. 160.

MEHLER, D., 2018. *Clinical applications of real-time FMRI neurofeedback training–premises, promises, and pitfalls,* .

MENDELSOHN, A., PINE, A. and SCHILLER, D., 2014. Between thoughts and actions: motivationally salient cues invigorate mental action in the human brain. *Neuron,* **81**(1), pp. 207-217.

MIDDLETON, F.A. and STRICK, P.L., 2000. Basal ganglia and cerebellar loops: motor and cognitive circuits. *Brain Research Reviews,* **31**(2-3), pp. 236-250.

MIZUGUCHI, N., NAKATA, H., HAYASHI, T., SAKAMOTO, M., MURAOKA, T., UCHIDA, Y. and KANOSUE, K., 2013. Brain activity during motor imagery of an action with an object: a functional magnetic resonance imaging study. *Neuroscience research,* **76**(3), pp. 150-155.

MOSS, D. and KIRK, L., 2004. Evidence-based practice in biofeedback and neurofeedback. Foreword to C. Yucha & C. Gilbert. *Evidence-based practice for biofeedback assisted behavioral therapy,* .

MOSTOFSKY, S.H., POWELL, S.K., SIMMONDS, D.J., GOLDBERG, M.C., CAFFO, B. and PEKAR, J.J., 2009. Decreased connectivity and cerebellar activity in autism during motor task performance. *Brain,* **132**(9), pp. 2413-2425.

MUCKLI, L. and PETRO, L.S., 2017. The significance of memory in sensory cortex. *Trends in neurosciences,* **40**(5), pp. 255-256.

MULDER, T., ZIJLSTRA, S., ZIJLSTRA, W. and HOCHSTENBACH, J., 2004. The role of motor imagery in learning a totally novel movement. *Experimental brain research,* **154**(2), pp. 211-217.

MUÑOZ-MOLDES, S. and CLEEREMANS, A., 2020. Delineating implicit and explicit processes in neurofeedback learning. *Neuroscience & Biobehavioral Reviews,* .

MURPHY, K., BIRN, R.M. and BANDETTINI, P.A., 2013. Resting-state fMRI confounds and cleanup. *NeuroImage,* **80**, pp. 349-359.

NACHEV, P., KENNARD, C. and HUSAIN, M., 2008. Functional role of the supplementary and pre-supplementary motor areas. *Nature Reviews Neuroscience,* **9**(11), pp. 856-869.

NAN, W., DIAS, A.P.B. and ROSA, A.C., 2019. Neurofeedback training for cognitive and motor function rehabilitation in chronic stroke: Two case reports. *Frontiers in neurology,* **10**, pp. 800.

NEDELKO, V., HASSA, T., HAMZEI, F., SCHOENFELD, M.A. and DETTMERS, C., 2012. Action imagery combined with action observation activates more corticomotor regions than action observation alone. *Journal of Neurologic Physical Therapy,* **36**(4), pp. 182-188.

NEUMAN, B. and GRAY, R., 2013. A direct comparison of the effects of imagery and action observation on hitting performance. *Movement & Sport Sciences-Science & Motricité,* (79), pp. 11-21.

NEUMANN, N., KÜBLER, A., KAISER, J., HINTERBERGER, T. and BIRBAUMER, N., 2003. Conscious perception of brain states: mental strategies for brain–computer communication. *Neuropsychologia,* **41**(8), pp. 1028-1036.

NEYEDLI, H.F., SAMPAIO-BAPTISTA, C., KIRKMAN, M.A., HAVARD, D., LÜHRS, M., RAMSDEN, K., FLITNEY, D.D., CLARE, S., GOEBEL, R. and JOHANSEN-BERG, H., 2018. Increasing lateralized motor activity in younger and older adults using real-time fMRI during executed movements. *Neuroscience,* **378**, pp. 165-174.

NEYEDLI, H.F., SAMPAIO-BAPTISTA, C., KIRKMAN, M.A., HAVARD, D., LÜHRS, M., RAMSDEN, K., FLITNEY, D.D., CLARE, S., GOEBEL, R. and JOHANSEN-BERG, H., 2018. Increasing lateralized motor activity in younger and older adults using real-time fMRI during executed movements. *Neuroscience,* **378**, pp. 165-174.

NIKOLAOU, F., ORPHANIDOU, C., PAPAKYRIAKOU, P., MURPHY, K., WISE, R.G. and MITSIS, G.D., 2016. Spontaneous physiological variability modulates dynamic functional connectivity in resting-state functional magnetic resonance

imaging. *Philosophical Transactions of the Royal Society A: Mathematical, Physical and Engineering Sciences,* **374**(2067), pp. 20150183.

NINAUS, M., KOBER, S.E., WITTE, M., KOSCHUTNIG, K., STANGL, M., NEUPER, C. and WOOD, G., 2013. Neural substrates of cognitive control under the belief of getting neurofeedback training. *Frontiers in human neuroscience,* **7**, pp. 914.

NYBERG, L., ERIKSSON, J., LARSSON, A. and MARKLUND, P., 2006. Learning by doing versus learning by thinking: an fMRI study of motor and mental training. *Neuropsychologia,* **44**(5), pp. 711-717.

OGAWA, S., TANK, D.W., MENON, R., ELLERMANN, J.M., KIM, S.G., MERKLE, H. and UGURBIL, K., 1992. Intrinsic signal changes accompanying sensory stimulation: functional brain mapping with magnetic resonance imaging. *Proceedings of the National Academy of Sciences of the United States of America,* **89**(13), pp. 5951-5955.

OLDFIELD, R.C., 1971. The assessment and analysis of handedness: the Edinburgh inventory. *Neuropsychologia,* **9**(1), pp. 97-113.

PAPOUTSI, M., WEISKOPF, N., LANGBEHN, D., REILMANN, R., REES, G. and TABRIZI, S.J., 2018. Stimulating neural plasticity with real-time f MRI neurofeedback in H untington's disease: A proof of concept study. *Human brain mapping,* **39**(3), pp. 1339-1353.

PARET, C., GOLDWAY, N., ZICH, C., KEYNAN, J.N., HENDLER, T., LINDEN, D. and KADOSH, K.C., 2019. Current progress in real-time functional magnetic resonance-based neurofeedback: methodological challenges and achievements. *NeuroImage,* **202**, pp. 116107.

PARET, C., RUF, M., GERCHEN, M.F., KLUETSCH, R., DEMIRAKCA, T., JUNGKUNZ, M., BERTSCH, K., SCHMAHL, C. and ENDE, G., 2016. fMRI neurofeedback of amygdala response to aversive stimuli enhances prefrontal–limbic brain connectivity. *NeuroImage,* **125**, pp. 182-188.

PASCUAL-LEONE, A., NGUYET, D., COHEN, L.G., BRASIL-NETO, J.P., CAMMAROTA, A. and HALLETT, M., 1995. Modulation of muscle responses evoked

by transcranial magnetic stimulation during the acquisition of new fine motor skills. *Journal of neurophysiology,* **74**(3), pp. 1037-1045.

PASCUAL-LEONE, A., NGUYET, D., COHEN, L.G., BRASIL-NETO, J.P., CAMMAROTA, A. and HALLETT, M., 1995. Modulation of muscle responses evoked by transcranial magnetic stimulation during the acquisition of new fine motor skills. *Journal of neurophysiology,* **74**(3), pp. 1037-1045.

PASSOW, S., SPECHT, K., ADAMSEN, T.C., BIERMANN, M., BREKKE, N., CRAVEN, A.R., ERSLAND, L., GRÜNER, R., KLEVEN-MADSEN, N. and KVERNENES, O., 2015. Default-mode network functional connectivity is closely related to metabolic activity. *Human brain mapping,* **36**(6), pp. 2027-2038.

PEREIRA, J., DIREITO, B., SAYAL, A., FERREIRA, C. and CASTELO-BRANCO, M., 2019. Self-modulation of premotor cortex interhemispheric connectivity in a real-time functional magnetic resonance imaging neurofeedback study using an adaptive approach. *Brain connectivity,* **9**(9), pp. 662-672.

PERRONNET, L., LÉCUYER, A., MANO, M., BANNIER, E., LOTTE, F., CLERC, M. and BARILLOT, C., 2017. Unimodal versus bimodal EEG-fMRI neurofeedback of a motor imagery task. *Frontiers in Human Neuroscience,* **11**, pp. 193.

PETERSEN, S.E. and DUBIS, J.W., 2012. The mixed block/event-related design. *NeuroImage,* **62**(2), pp. 1177-1184.

POSSE, S., FITZGERALD, D., GAO, K., HABEL, U., ROSENBERG, D., MOORE, G.J. and SCHNEIDER, F., 2003. Real-time fMRI of temporolimbic regions detects amygdala activation during single-trial self-induced sadness. *NeuroImage,* **18**(3), pp. 760-768.

POUSTCHI-AMIN, M., MIROWITZ, S.A., BROWN, J.J., MCKINSTRY, R.C. and LI, T., 2001. Principles and applications of echo-planar imaging: a review for the general radiologist. *Radiographics,* **21**(3), pp. 767-779.

RAM, N., RIGGS, S., SKALING, S., LANDERS, D. and MCCULLAGH, P., 2007. A comparison of modelling and imagery in the acquisition and retention of motor skills. *Journal of sports sciences,* **25**(5), pp. 587-597.

RAMOS, T.C., BALARDIN, J.B., SATO, J.R. and FUJITA, A., 2018. Abnormal Cortico-Cerebellar Functional Connectivity in Autism Spectrum Disorder. *Frontiers in systems neuroscience,* **12**, pp. 74.

RAMOT, M., GROSSMAN, S., FRIEDMAN, D. and MALACH, R., 2016. Covert neurofeedback without awareness shapes cortical network spontaneous connectivity. *Proceedings of the National Academy of Sciences of the United States of America,* **113**(17), pp. E2413-20.

RESCORLA, R.A., 1988. Pavlovian conditioning: It's not what you think it is. *American psychologist,* **43**(3), pp. 151.

RICHARDSON, A., 1967. Mental practice: a review and discussion part I. *Research Quarterly.American Association for Health, Physical Education and Recreation,* **38**(1), pp. 95-107.

RIZZOLATTI, G., FADIGA, L., MATELLI, M., BETTINARDI, V., PAULESU, E., PERANI, D. and FAZIO, F., 1996. Localization of grasp representations in humans by PET: 1. Observation versus execution. *Experimental brain research,* **111**(2), pp. 246-252.

ROBINEAU, F., MESKALDJI, D.E., KOUSH, Y., RIEGER, S.W., MERMOUD, C., MORGENTHALER, S., VAN DE VILLE, D., VUILLEUMIER, P. and SCHARNOWSKI, F., 2017. Maintenance of voluntary self-regulation learned through real-time fMRI neurofeedback. *Frontiers in Human Neuroscience,* **11**, pp. 131.

ROBINEAU, F., RIEGER, S.W., MERMOUD, C., PICHON, S., KOUSH, Y., VAN DE VILLE, D., VUILLEUMIER, P. and SCHARNOWSKI, F., 2014. Self-regulation of inter-hemispheric visual cortex balance through real-time fMRI neurofeedback training. *NeuroImage,* **100**, pp. 1-14.

RODRÍGUEZ-FORNELLS, A., CUNILLERA, T., MESTRES-MISSÉ, A. and DE DIEGO-BALAGUER, R., 2009. Neurophysiological mechanisms involved in language learning in adults. *Philosophical Transactions of the Royal Society B: Biological Sciences,* **364**(1536), pp. 3711-3735.

ROMANO-SMITH, S., WOOD, G., WRIGHT, D. and WAKEFIELD, C., 2018. Simultaneous and alternate action observation and motor imagery combinations improve aiming performance. *Psychology of Sport and Exercise,* **38**, pp. 100-106.

ROS, T., J BAARS, B., LANIUS, R.A. and VUILLEUMIER, P., 2014. Tuning pathological brain oscillations with neurofeedback: a systems neuroscience framework. *Frontiers in human neuroscience,* **8**, pp. 1008.

ROTA, G., HANDJARAS, G., SITARAM, R., BIRBAUMER, N. and DOGIL, G., 2011. Reorganization of functional and effective connectivity during real-time fMRI-BCI modulation of prosody processing. *Brain and language,* **117**(3), pp. 123-132.

ROTA, G., SITARAM, R., VEIT, R., ERB, M., WEISKOPF, N., DOGIL, G. and BIRBAUMER, N., 2009. Self-regulation of regional cortical activity using real-time fMRI: The right inferior frontal gyrus and linguistic processing. *Human brain mapping,* **30**(5), pp. 1605-1614.

ROZZI, S., FERRARI, P.F., BONINI, L., RIZZOLATTI, G. and FOGASSI, L., 2008. Functional organization of inferior parietal lobule convexity in the macaque monkey: electrophysiological characterization of motor, sensory and mirror responses and their correlation with cytoarchitectonic areas. *European Journal of Neuroscience,* **28**(8), pp. 1569-1588.

RUIZ, S., BUYUKTURKOGLU, K., RANA, M., BIRBAUMER, N. and SITARAM, R., 2014. Real-time fMRI brain computer interfaces: self-regulation of single brain regions to networks. *Biological psychology,* **95**, pp. 4-20.

SCHARNOWSKI, F., VEIT, R., ZOPF, R., STUDER, P., BOCK, S., DIEDRICHSEN, J., GOEBEL, R., MATHIAK, K., BIRBAUMER, N. and WEISKOPF, N., 2015. Manipulating motor performance and memory through real-time fMRI neurofeedback. *Biological psychology,* **108**, pp. 85-97.

SCHARNOWSKI, F., VEIT, R., ZOPF, R., STUDER, P., BOCK, S., DIEDRICHSEN, J., GOEBEL, R., MATHIAK, K., BIRBAUMER, N. and WEISKOPF, N., 2015. Manipulating motor performance and memory through real-time fMRI neurofeedback. *Biological psychology,* **108**, pp. 85-97.

SCHARNOWSKI, F., HUTTON, C., JOSEPHS, O., WEISKOPF, N. and REES, G., 2012. Improving visual perception through neurofeedback. *The Journal of neuroscience : the official journal of the Society for Neuroscience,* **32**(49), pp. 17830-17841.

SCHEINOST, D., STOICA, T., SAKSA, J., PAPADEMETRIS, X., CONSTABLE, R., PITTENGER, C. and HAMPSON, M., 2013. Orbitofrontal cortex neurofeedback produces lasting changes in contamination anxiety and resting-state connectivity. *Translational psychiatry,* **3**(4), pp. e250-e250.

SCHLERF, J.E., VERSTYNEN, T.D., IVRY, R.B. and SPENCER, R.M., 2010. Evidence of a novel somatopic map in the human neocerebellum during complex actions. *Journal of neurophysiology,* **103**(6), pp. 3330-3336.

SCHUSTER, C., HILFIKER, R., AMFT, O., SCHEIDHAUER, A., ANDREWS, B., BUTLER, J., KISCHKA, U. and ETTLIN, T., 2011. Best practice for motor imagery: a systematic literature review on motor imagery training elements in five different disciplines. *BMC medicine,* **9**(1), pp. 1-35.

SCHWEEN, R., TAUBE, W., GOLLHOFER, A. and LEUKEL, C., 2014. Online and post-trial feedback differentially affect implicit adaptation to a visuomotor rotation. *Experimental brain research,* **232**(9), pp. 3007-3013.

SCOTT, M., TAYLOR, S., CHESTERTON, P., VOGT, S. and EAVES, D.L., 2018. Motor imagery during action observation increases eccentric hamstring force: an acute non-physical intervention. *Disability and rehabilitation,* **40**(12), pp. 1443-1451.

SEPULVEDA, P., SITARAM, R., RANA, M., MONTALBA, C., TEJOS, C. and RUIZ, S., 2016. How feedback, motor imagery, and reward influence brain self-regulation using real-time fMRI. *Human brain mapping,* **37**(9), pp. 3153-3171.

SHARMA, N. and BARON, J., 2013. Does motor imagery share neural networks with executed movement: a multivariate fMRI analysis. *Frontiers in human neuroscience,* **7**, pp. 564.

SHERWOOD, M.S., KANE, J.H., WEISEND, M.P. and PARKER, J.G., 2016. Enhanced control of dorsolateral prefrontal cortex neurophysiology with real-time

functional magnetic resonance imaging (rt-fMRI) neurofeedback training and working memory practice. *NeuroImage,* **124**, pp. 214-223.

SHIBATA, K., LISI, G., CORTESE, A., WATANABE, T., SASAKI, Y. and KAWATO, M., 2019. Toward a comprehensive understanding of the neural mechanisms of decoded neurofeedback. *NeuroImage,* **188**, pp. 539-556.

SHIBATA, K., WATANABE, T., SASAKI, Y. and KAWATO, M., 2011. Perceptual learning incepted by decoded fMRI neurofeedback without stimulus presentation. *Science (New York, N.Y.),* **334**(6061), pp. 1413-1415.

SITARAM, R., ROS, T., STOECKEL, L., HALLER, S., SCHARNOWSKI, F., LEWIS-PEACOCK, J., WEISKOPF, N., BLEFARI, M.L., RANA, M. and OBLAK, E., 2017. Closed-loop brain training: the science of neurofeedback. *Nature Reviews Neuroscience,* **18**(2), pp. 86-100.

SITARAM, R., VEIT, R., STEVENS, B., CARIA, A., GERLOFF, C., BIRBAUMER, N. and HUMMEL, F., 2012. Acquired control of ventral premotor cortex activity by feedback training: an exploratory real-time FMRI and TMS study. *Neurorehabilitation and neural repair,* **26**(3), pp. 256-265.

SITARAM, R., VEIT, R., STEVENS, B., CARIA, A., GERLOFF, C., BIRBAUMER, N. and HUMMEL, F., 2012. Acquired control of ventral premotor cortex activity by feedback training: an exploratory real-time FMRI and TMS study. *Neurorehabilitation and neural repair,* **26**(3), pp. 256-265.

SITARAM, R., VEIT, R., STEVENS, B., CARIA, A., GERLOFF, C., BIRBAUMER, N. and HUMMEL, F., 2012. Acquired control of ventral premotor cortex activity by feedback training: an exploratory real-time FMRI and TMS study. *Neurorehabilitation and neural repair,* **26**(3), pp. 256-265.

SMITH, D. and HOLMES, P., 2004. The effect of imagery modality on golf putting performance. *Journal of Sport and Exercise Psychology,* **26**(3), pp. 385-395.

SOKHADZE, T.M., CANNON, R.L. and TRUDEAU, D.L., 2008. EEG biofeedback as a treatment for substance use disorders: review, rating of efficacy, and recommendations for further research. *Applied Psychophysiology and Biofeedback,* **33**(1), pp. 1-28.

SOKUNBI, M.O., LINDEN, D.E., HABES, I., JOHNSTON, S. and IHSSEN, N., 2014. Real-time fMRI brain-computer interface: development of a “motivational feedback” subsystem for the regulation of visual cue reactivity. *Frontiers in behavioral neuroscience,* **8**, pp. 392.

SOLSTRAND DAHLBERG, L., LUNGU, O. and DOYON, J., 2020. Cerebellar contribution to motor and non-motor functions in Parkinson's disease: a meta-analysis of fMRI findings. *Frontiers in neurology,* **11**, pp. 127.

SPETTER, M.S., MALEKSHAHI, R., BIRBAUMER, N., LÜHRS, M., VAN DER VEER, ALBERT H, SCHEFFLER, K., SPUCKTI, S., PREISSL, H., VEIT, R. and HALLSCHMID, M., 2017. Volitional regulation of brain responses to food stimuli in overweight and obese subjects: A real-time fMRI feedback study. *Appetite,* **112**, pp. 188-195.

STAM, C.J., 2014. Modern network science of neurological disorders. *Nature Reviews Neuroscience,* **15**(10), pp. 683-695.

STANLEY, J. and KRAKAUER, J.W., 2013. Motor skill depends on knowledge of facts. *Frontiers in human neuroscience,* **7**, pp. 503.

STINEAR, C.M., PETOE, M.A. and BYBLOW, W.D., 2015. Primary motor cortex excitability during recovery after stroke: implications for neuromodulation. *Brain stimulation,* **8**(6), pp. 1183-1190.

STOODLEY, C.J. and SCHMAHMANN, J.D., 2009. Functional topography in the human cerebellum: a meta-analysis of neuroimaging studies. *NeuroImage,* **44**(2), pp. 489-501.

STOODLEY, C.J., VALERA, E.M. and SCHMAHMANN, J.D., 2012. Functional topography of the cerebellum for motor and cognitive tasks: an fMRI study. *NeuroImage,* **59**(2), pp. 1560-1570.

SUBRAMANIAN, L., MORRIS, M.B., BROSNAN, M., TURNER, D.L., MORRIS, H.R. and LINDEN, D.E., 2016. Functional magnetic resonance imaging neurofeedback-guided motor imagery training and motor training for Parkinson’s disease: randomized trial. *Frontiers in behavioral neuroscience,* **10**, pp. 111.

SULZER, J., HALLER, S., SCHARNOWSKI, F., WEISKOPF, N., BIRBAUMER, N., BLEFARI, M.L., BRUEHL, A.B., COHEN, L.G., DECHARMS, R.C. and GASSERT, R., 2013. Real-time fMRI neurofeedback: progress and challenges. *NeuroImage*, **76**, pp. 386-399.

SUN, Y., WEI, W., LUO, Z., GAN, H. and HU, X., 2016. Improving motor imagery practice with synchronous action observation in stroke patients. *Topics in stroke rehabilitation,* **23**(4), pp. 245-253.

TALAIRACH, J., 1988. Co-planar stereotaxic atlas of the human brain-3-dimensional proportional system. *An approach to cerebral imaging,* .

TAUBE, W., MOUTHON, M., LEUKEL, C., HOOGEWOUD, H., ANNONI, J. and KELLER, M., 2015. Brain activity during observation and motor imagery of different balance tasks: an fMRI study. *cortex,* **64**, pp. 102-114.

TAYLOR, J.A., KRAKAUER, J.W. and IVRY, R.B., 2014. Explicit and implicit contributions to learning in a sensorimotor adaptation task. *The Journal of neuroscience : the official journal of the Society for Neuroscience,* **34**(8), pp. 3023-3032.

THIBAULT, R.T., LIFSHITZ, M. and RAZ, A., 2016. The self-regulating brain and neurofeedback: experimental science and clinical promise. *cortex,* **74**, pp. 247-261.

THIBAULT, R.T., LIFSHITZ, M. and RAZ, A., 2016. The self-regulating brain and neurofeedback: experimental science and clinical promise. *cortex,* **74**, pp. 247-261.

THIBAULT, R.T., MACPHERSON, A., LIFSHITZ, M., ROTH, R.R. and RAZ, A., 2018. Neurofeedback with fMRI: A critical systematic review. *NeuroImage,* **172**, pp. 786-807.

THIBAULT, R.T., LIFSHITZ, M., BIRBAUMER, N. and RAZ, A., 2015. Neurofeedback, Self-Regulation, and Brain Imaging: Clinical Science and Fad in the Service of Mental Disorders. *Psychotherapy and psychosomatics,* **84**(4), pp. 193-207.

THOMPSON, G.J., MAGNUSON, M.E., MERRITT, M.D., SCHWARB, H., PAN, W., MCKINLEY, A., TRIPP, L.D., SCHUMACHER, E.H. and KEILHOLZ, S.D., 2013. Short-time windows of correlation between large-scale functional brain networks predict vigilance intraindividually and interindividually. *Human brain mapping,* **34**(12), pp. 3280-3298.

TINAZ, S., PARA, K., VIVES-RODRIGUEZ, A., MARTINEZ-KAIGI, V., NALAMADA, K., SEZGIN, M., SCHEINOST, D., HAMPSON, M., LOUIS, E.D. and CONSTABLE, R.T., 2018. Insula as the interface between body awareness and movement: a neurofeedback-guided kinesthetic motor imagery study in Parkinson's disease. *Frontiers in human neuroscience,* **12**, pp. 496.

TURSIC, A., ECK, J., LÜHRS, M., LINDEN, D.E. and GOEBEL, R., 2020. A systematic review of fMRI neurofeedback reporting and effects in clinical populations. *NeuroImage: Clinical,* , pp. 102496.

UMILTA, M.A., KOHLER, E., GALLESE, V., FOGASSI, L., FADIGA, L., KEYSERS, C. and RIZZOLATTI, G., 2001. I know what you are doing: A neurophysiological study. *Neuron,* **31**(1), pp. 155-165.

VAN DEN HEUVEL, MARTIJN P and POL, H.E.H., 2010. Exploring the brain network: a review on resting-state fMRI functional connectivity. *European neuropsychopharmacology,* **20**(8), pp. 519-534.

VAN DIJK, K.R., SABUNCU, M.R. and BUCKNER, R.L., 2012. The influence of head motion on intrinsic functional connectivity MRI. *NeuroImage,* **59**(1), pp. 431-438.

VILLIGER, M., ESTÉVEZ, N., HEPP-REYMOND, M., KIPER, D., KOLLIAS, S.S., ENG, K. and HOTZ-BOENDERMAKER, S., 2013. Enhanced activation of motor execution networks using action observation combined with imagination of lower limb movements. *PloS one,* **8**(8), pp. e72403.

VOGT, S., DI RIENZO, F., COLLET, C., COLLINS, A. and GUILLOT, A., 2013. Multiple roles of motor imagery during action observation. *Frontiers in human neuroscience,* **7**, pp. 807.

VOOGD, J. and GLICKSTEIN, M., 1998. The anatomy of the cerebellum. *Trends in cognitive sciences,* **2**(9), pp. 307-313.

VOVK, U., PERNUS, F. and LIKAR, B., 2007. A review of methods for correction of intensity inhomogeneity in MRI. *IEEE Transactions on Medical Imaging,* **26**(3), pp. 405-421.

WAGNER, M., FUCHS, M. and KASTNER, J., 2000. fMRI-constrained dipole fits and current density reconstructions, *Proc 12th Intl Conf Biomag* 2000, pp. 785-788.

WANG, T., MANTINI, D. and GILLEBERT, C.R., 2018. The potential of real-time fMRI neurofeedback for stroke rehabilitation: a systematic review. *cortex,* **107**, pp. 148-165.

WARD, N.S. and COHEN, L.G., 2004. Mechanisms underlying recovery of motor function after stroke. *Archives of Neurology,* **61**(12), pp. 1844-1848.

WATANABE, T., SASAKI, Y., SHIBATA, K. and KAWATO, M., 2017. Advances in fMRI real-time neurofeedback. *Trends in cognitive sciences,* **21**(12), pp. 997-1010.

WEISKOPF, N., 2012. Real-time fMRI and its application to neurofeedback. *NeuroImage,* **62**(2), pp. 682-692.

WEISKOPF, N., MATHIAK, K., BOCK, S.W., SCHARNOWSKI, F., VEIT, R., GRODD, W., GOEBEL, R. and BIRBAUMER, N., 2004. Principles of a brain-computer interface (BCI) based on real-time functional magnetic resonance imaging (fMRI). *IEEE transactions on biomedical engineering,* **51**(6), pp. 966-970.

WEISKOPF, N., VEIT, R., ERB, M., MATHIAK, K., GRODD, W., GOEBEL, R. and BIRBAUMER, N., 2003. Physiological self-regulation of regional brain activity using real-time functional magnetic resonance imaging (fMRI): methodology and exemplary data. *NeuroImage,* **19**(3), pp. 577-586.

WEISKOPF, N., VEIT, R., ERB, M., MATHIAK, K., GRODD, W., GOEBEL, R. and BIRBAUMER, N., 2003. Physiological self-regulation of regional brain activity using real-time functional magnetic resonance imaging (fMRI): methodology and exemplary data. *NeuroImage,* **19**(3), pp. 577-586.

XIE, F., XU, L., LONG, Z., YAO, L. and WU, X., 2015. Functional connectivity alteration after real-time fMRI motor imagery training through self-regulation of activities of the right premotor cortex. *BMC neuroscience,* **16**(1), pp. 1-11.

YAMASHITA, A., HAYASAKA, S., KAWATO, M. and IMAMIZU, H., 2017. Connectivity neurofeedback training can differentially change functional connectivity and cognitive performance. *Cerebral Cortex,* **27**(10), pp. 4960-4970.

YEŞILYURT, B., UĞURBIL, K. and ULUDAĞ, K., 2008. Dynamics and nonlinearities of the BOLD response at very short stimulus durations. *Magnetic resonance imaging,* **26**(7), pp. 853-862.

YIN, H.H. and KNOWLTON, B.J., 2006. Addiction and learning in the brain. *Handbook of implicit cognition and addiction,* , pp. 167-183.

YOO, S. and JOLESZ, F.A., 2002. Functional MRI for neurofeedback: feasibility studyon a hand motor task. *Neuroreport,* **13**(11), pp. 1377-1381.

YOO, S., LEE, J., O'LEARY, H., PANYCH, L.P. and JOLESZ, F.A., 2008. Neurofeedback fMRI-mediated learning and consolidation of regional brain activation during motor imagery. *International Journal of Imaging Systems and Technology,* **18**(1), pp. 69-78.

YOO, S., O'LEARY, H.M., FAIRNENY, T., CHEN, N., PANYCH, L.P., PARK, H. and JOLESZ, F.A., 2006. Increasing cortical activity in auditory areas through neurofeedback functional magnetic resonance imaging. *Neuroreport,* **17**(12), pp. 1273-1278.

YOUNG, K.D., ZOTEV, V., PHILLIPS, R., MISAKI, M., YUAN, H., DREVETS, W.C. and BODURKA, J., 2014. Real-time FMRI neurofeedback training of amygdala activity in patients with major depressive disorder. *PloS one,* **9**(2), pp. e88785.

YOUSRY, T.A., SCHMID, U.D., ALKADHI, H., SCHMIDT, D., PERAUD, A., BUETTNER, A. and WINKLER, P., 1997. Localization of the motor hand area to a knob on the precentral gyrus. A new landmark. *Brain : a journal of neurology,* **120 (Pt 1)**(Pt 1), pp. 141-157.

YUCHA, C. and MONTGOMERY, D., 2008. *Evidence-based practice in biofeedback and neurofeedback*. AAPB Wheat Ridge, CO.

YUCHA, P. and GILBERT, P.C., 2004. Evidence-Based Practice in Biofeedback and Neurofeedback. *Overview of Biofeedback,* , pp. 1-2.

ZENKE, F. and GERSTNER, W., 2017. Hebbian plasticity requires compensatory processes on multiple timescales. *Philosophical Transactions of the Royal Society B: Biological Sciences,* **372**(1715), pp. 20160259.

ZHAO, X., SONG, S., YE, Q., GUO, J. and YAO, L., 2013. Causal interaction following the alteration of target region activation during motor imagery training using real-time fMRI. *Frontiers in Human Neuroscience,* **7**, pp. 866.

ZILVERSTAND, A., SORGER, B., SARKHEIL, P. and GOEBEL, R., 2015. fMRI neurofeedback facilitates anxiety regulation in females with spider phobia. *Frontiers in behavioral neuroscience,* **9**, pp. 148.

ZOTEV, V., KRUEGER, F., PHILLIPS, R., ALVAREZ, R.P., SIMMONS, W.K., BELLGOWAN, P., DREVETS, W.C. and BODURKA, J., 2011. Self-regulation of amygdala activation using real-time fMRI neurofeedback. *PloS one,* **6**(9), pp. e24522.